RAPID ROTATIONAL FOAM MOLDING OF INTEGRAL SKIN POLYPROPYLENE CELLULAR COMPOSITES

by

Emad Samy Abdalla

A Thesis Submitted in Partial Fulfillment
of the Requirements for the Degree of

Master of Applied Science

in

The Faculty of Engineering and Applied Science

Department of Mechanical Engineering

University of Ontario Institute of Technology

May 2009

Canada

RAPID ROTATIONAL FOAM MOLDING OF INTEGRAL SKIN POLYPROPYLENE CELLULAR COMPOSITES

Emad Samy Abdalla
Degree of Master of Applied Science, 2009
Mechanical Engineering, Faculty of Engineering and Applied Science
University of Ontario Institute of Technology

ABSTRACT

Rapid Rotational Foam Molding (RRFM) is a novel patent-pending process that was designed and developed to maximize the synergistic effects resulting from the deliberate combination of extrusion and rotational foam molding and thereby serve as a time-and-energy efficient technology for the manufacture of integral-skin rotationally molded foams of high quality. This thesis presents a thorough study of the scientific and engineering aspects related to the evolution of the RRFM process and its feasibility. This innovative processing technology was assessed and verified through a battery of planned experimental trials conducted utilizing an in-house custom-built industrial-grade lab-scale experimental setup. The experimental trials involved a variety of polypropylene (PP)-based foamable formulations with a chemical blowing agent (CBA) that were compounded and processed by utilizing an extruder and then foamed and injected as a foamed core, instantly, into the cavity of a suitable non-chilled rotationally molded hollow shell made of non-foamed pulverized PP grades. The investigated mold shapes included a cylindrical shaped mold and a rectangular flat shaped mold. The obtained moldings were examined for the quality of the skin surface, the skin-foam interface, and the achieved foam morphologies that were characterized in terms of foam density, average cell size, and average cell density. Optimal processing parameters were successfully determined for three different PP skin-foam formulation combinations. The accomplished reduction in processing time and energy consumption by implementing RRFM were substantial. A variety of processing impediments that hindered the efficiency of the single-charge conventional rotational foam molding practice were resolved by implementing RRFM; these include: the foam/skin invasion into the skin/foam layer of the manufactured article and the premature decomposition of CBA during compounding or subsequent rotational foam molding processing steps.

DEDICATIONS

To my beloved family,

My parents, *Samy* and *Manal*

My siblings, *Ayman* and *Mariam*

ACKNOWLEDGEMENTS

TABLE OF CONTENTS

CHAPTER 3: DESIGN AND DEVELOPMENT OF A NOVEL TECHNOLOGY AND ITS RESPECTIVE EXPERIMENTAL SETUP 65

LIST OF TABLES

LIST OF FIGURES

LIST OF SYMBOLS

V_{mold} – Mold volume in [cm^3]

r_{mold} – Radius of the mold in [cm]

H_{mold} – Height of the mold in [cm]

t_{skin} – Skin thickness in [cm]

r_{cavity} – Radius of the mold less the skin thickness factor in [cm]

H_{cavity} – Height of the mold less the skin thickness factor in [cm]

V_{cavity} – Volume of the mold less the skin layer in [cm^3]

V_{skin} – Volume occupied by the solid skin portion in [cm^3]

$m_{polymer}$ – Mass of a polymer in [g]

ρ_{resin} – Density of a polymer resin in [g/cm^3]

$V_{initial}$ – Initial volume occupied by a plastic resin before foaming in [cm^3]

V_{gas} – Volume occupied by the blowing gas in a foaming process [cm^3]

m_{CBA} – Mass of the used CBA in [g]

$\% CBA$ – Amount of CBA as a percentage of the polymer to be foamed

ϕ – Gas yield factor of a CBA in [cm^3/g]

VER – Volume expansion ratio

ϕ_{STP} – Gas yield factor of a CBA at standard temperature (298 [^{o}C]) and
        Pressure (1 [atm]) in [cm^3/g]

V_C – Volume at the crystallization temperature in [cm^3]

V_{room} – Volume at room temperature in [cm^3]

T_C – Crystallization temperature of a polymer [K]

T_{room} – Room temperature in [K]

T_m – Polymer's melt temperature in [^{o}C]

T_g – Polymer's glass transition temperature in [^{o}C]

T_c – Polymer's crystallization temperature in [^{o}C]

$\Delta H_{melting}$ – Latent heat of melting in [J.K/g.s]

$\Delta H_{crystallization}$ – Latent heat of crystallization in [J.K/g.s]

$\Delta H_{melting}{}^{*}$ – Heat absorbed by one gram of material during melting in [J.K/g.s]

M_w – Average molecular weight in [g/mol]

MFI – Melt flow index of a polymer in [g/10 min]

M_w – the weight of a polymeric chain at a given molecular weight distribution [g/mol]

M_n – the number average molecular weight [g/mol]

$T_{decomposition}$ – Decomposition temperature of a CBA in [^{o}C]

T_{BZ1} – Extruder barrel zone 1 temperature in [^{o}C]

T_{BZ2} – Extruder barrel zone 2 temperature in [^{o}C]

T_{BZ3} – Extruder barrel zone 3 temperature in [^{o}C]

T_{DZ} – Extruder die zone temperature in [^{o}C]

$RPM_{extruder}$ – Extruder screw RPM [RPM]

RPM_{mold} – Mold RPM [RPM]

RPM_{Arm} – Arm RPM [RPM]

Chapter 1: Introduction

1.1 Preamble

The nature of the rapid development and expansion that took place in the world during the past century has forced mankind to search for means to achieve optimal levels of energy, materials, and environment usage in order to preserve precious resources and attain sustainability. This rationale had an immense effect on the characteristics of the solutions devised to treat problems facing humanity. Leading minds are recently more oriented towards the sustainable development of societies. Adverse phenomena, like the increased green house emissions, the depletion of the ozone layer, the exhaustion of the resources of the planet, and the elevated levels of pollution, triggered the motivation of innovators to introduce green alternatives. Examples of engineered solutions that are based on this perspective are countless. In the field of power generation for instance, fossil fuels are currently being replaced by environmentally conservative technologies such as nuclear, hydro, wind, geothermal, tidal, and solar power. The use of toxic substances in various industrial processes has been strictly regulated by governments and global agreements. Manufacturing industries endured fundamental changes in their strategies; replacing non-green fabrication methods and materials with more ecologically aware alternatives of equal function.

Plastics industries experienced a great deal of advancements to comply with the pertinent global market changes. At present, plastics in their different types and forms are of preference to designers due to factors such as weight, flexibility, toughness, corrosion resistance, transparency, ease to color, and ease to process [1-3]. Available studies

projected that the global investments in plastics processing machinery will increase by approximately 31% to reach $25 billion in the year 2012 as opposed to $19 billion in the year 2007 [4]. This growth percentage conforms with the increased market demand to use plastics in the automotive, building and construction, electronics, packaging, and aviation industries, along with others. Plastics processing technologies such as extrusion, injection molding, blow molding, rotational molding, and compression molding are now directly and extensively involved in manufacturing many of the articles that people interact with on a daily basis. Plastics and plastics-based composite materials have replaced conventionally less-green constituents in applied efforts to conserve energy and resources throughout various applications and ventures.

1.1 Plastics

1.1.1 Introduction

Plastics are a member of a larger family named polymers. The word "polymer" is of Greek nature, as "poly" stands for many and "meros" stands for part [1]. The name of this family of materials is directly related to their molecular structure, as they exhibit identical structural units arranged in long chains by means of chemical bonds [1-3]. This type of structure is found naturally in substances like silk, rubber, and cellulose. During the 19th century, Alexander Parkes was the first successful inventor of a synthetic polymer-based material; he named it Parkesine. Parkesine was used later to derive Celluloid; a material that was useful in preventing the exhaustion of analogous natural substances like ivory, replacing it in a variety of applications. Commercially, polymers grew in importance during the time of the Second World War. Polymers such as nylon, polyethylene, and

acrylic were developed as an economical substitute to more expensive materials used in manufacturing military equipment and in other applications [1].

1.1.2 Classification of Polymers

There are two general classes of polymers: thermosetting polymers or thermosets and thermoplastic polymers or thermoplastics [2]. Thermosets are three-dimensional organic structures that, after processing into final products, are substantially infusible and insoluble; moreover, they cannot be re-softened once cured. The reuse of thermosets is confined to granulation and inclusion as fillers when required in the plastics industries. Thermoplastics, on the other hand, are plastics that can be reprocessed, i.e., they repeatedly melt or soften when heated and harden when cooled without undergoing any change in their chemical state [2]. Further classifications exist under each of these general polymer categories.

The processing methodologies and the various theories presented throughout this thesis serve the scope of thermoplastics and specifically the family of polyolefins. The fundamental structure of materials within this family is based on the monomers named olefins. Olefins, for example, include ethylene and propylene, which are the base constituents of the polymeric materials polyethylene (PE) and polypropylene (PP).

Brief emphasis on thermosets will be presented within the conducted literature survey for purposes of elucidating the fundamental chemical and physical differences between thermoplastics and thermosets.

1.2 Plastic Foams

1.2.1 Introduction

Polymeric foams, cellular plastics, plastic foams, or expanded plastics are terminologies of equal meaning that can be used to represent structures consisting of at least two phases, one of which is a solid polymer matrix and the other a gaseous phase generated by utilizing a foaming or blowing agent [5]. Naturally occurring polymeric foams such as sponges and cork have been recognized for a long time. Synthetic polymeric foams on the other hand have only been introduced to the market approximately fifty years ago, in a manner such that the development of a new polymer was shortly followed by the foam or expanded form of the same [6].

Foamed structures can be obtained from almost all polymers upon utilizing the appropriate processing methods. A variety of advantages, depending on the respective end-use applications, can be exploited when utilizing polymeric foams. These include enhancements of: the mechanical properties, strength-to-weight ratio, stiffness, thermal and acoustic insulation ability, cushioning, and the improved economics of end-products due to less materials usage [5,6].

1.2.2 Processing Polymeric Foams

Most polymeric foams are formed by a process involving the dispersion of gas bubbles generated using a foaming/blowing agent in a liquid polymeric matrix. Blowing agents are selected to conform to the processing technology used, and can either be Chemical Blowing Agents (CBAs), which are pure chemicals that react within certain temperature ranges to produce gas, or Physical Blowing Agents (PBAs), which are soluble substances

(liquids or gases) introduced directly under pressure into the polymer melt. Any foaming process can be explained in at least three distinct steps: cell nucleation, cell growth, and cell stabilization [5-7].

1.2.3 Classification and Applications of Foams

It is common practice to categorize cellular plastics based on their apparent densities, cell sizes and/or cell populations [5-9]; such quantities present an indication of the relative proportions between the solid and gaseous phases and greatly determine the physical properties (i.e. strength, thermal, and electrical properties) of a foamed polymeric structure. Polymeric foams can also be classified based on their pertinent cellular morphologies, which are divided into closed-cell or open-cell foam systems [8,9].

Currently achievable apparent foam densities range from 2 [kg/m^3] to 960 [kg/m^3] [9]. Based on these values, plastic foams can be classified into one of three classes:

1. *Low Density Foams:* foams having an apparent density value between 2 [kg/m^3] and 50 [kg/m^3].

2. *Medium Density Foams:* foams having an apparent density value between 50 [kg/m^3] and 350 [kg/m^3].

3. *High Density Foams:* foams having an apparent density value between 350 [kg/m^3] and 960 [kg/m^3].

In terms of cell size and cell density, plastic foams can be classified into one of three categories [10]:

1. *Conventional foams:* foam structures with an average cell size greater than 300 [μm] and a cell density less than 10^6 [cells/cm^3].

2. ***Fine celled foams***: foam structures with an average cell size between 10 and 300 [μm] and a cell density between 10^6 and 10^9 [cells/cm^3].

3. ***Microcellular foams:*** foam structures with an average cell size less than 10 [μm] and a cell density greater than 10^9 [cells/cm^3].

Lower density plastic foams, i.e., up to ≈300 [kg/cm^3], are used in a variety of applications; these include: comfort cushioning (automotive, transportation, and furniture); floatation (in-place floatation for small vessels, marine life vests, pool accessories, child toys); shock mitigation (food packaging, construction and transportation crash barriers); and thermal shielding (industrial coolants, appliances, insulative packaging) [11].

Higher density plastic foams, i.e., above ≈300 [kg/cm^3], in opposition, are used to serve the following applications: furniture (frames, tables); materials handling (pallets, milk and soda cases, containers); industrial (battery cases, trash containers, electrical housings); automotive (decorative paneling, glove box door, instrument panels, fender liners, vehicle crash barriers); and marine (seats, fish boxes, cabin structures) [11].

1.2.4 PP Foams

Cellular plastics often exhibit the properties of their base materials [2]. The most commonly used thermoplastic material in processing foamed articles is polyethylene (PE); this is due to its excellent economics, good temperature stability, exceptional processability, and chemical resistance. The melting temperature of PE is around 120 [^{o}C], which makes it employable in applications requiring end products to endure temperatures close to this limit. The most invaluable attribute of PE, however, is its low stiffness, which when foamed, directly affects the load bearing capacity of the resulting

structure. This is evident when magnifying the fact that the flexural modulus of PE averages only about 210 [MPa] [12].

The investigation of alternative polymers for foaming applications became viable due to the end-use limitations imposed by the physical properties of PE. This promoted PP foams to grow in importance. PP like PE, offers excellent economics, good processing stability, and outstanding chemical resistance. Additionally, PP has a higher melting temperature ($\approx$165 [^{o}C]), good impact properties, and superior stiffness resembled by about 1.50 [GPa] of flexural modulus. Such attributes are due to the steric interaction of the pendant methyl groups forming the various PP structural arrangements. The properties of PP grades allow them to serve versatile applications in the realm of expanded plastics, with potential applications including packaging, automotive industry, and as insulation material (thermal and acoustic) [12].

Despite their numerous advantageous properties, PP foams have not yet received the anticipated consideration in terms of research and industrial applications. The reasons lie in the difficulty to foam PP due to its weak melt strength and melt elasticity, which limits the global material processing window [13-16]. The melt strength and melt elasticity values influence the ability of foam bubbles to retain their cell walls during processing, causing poor cell density, poor cell population, and coarse cell size.

1.3 Rotational Foam Molding

1.3.1 Background

The manufacturing of plastic foams extends to most plastics processing technologies [17]. Foams can be processed in extrusion, injection molding, blow molding, coating, calendaring, rotational molding, etc.

Conventional rotational molding, or rotomolding, is a plastics fabrication technology that is advantageously utilized to manufacture single-piece, hollow or double-walled, large-sized, complex-shaped, seamless, stress-free plastic articles. Rotomolding is best implemented in manufacturing environments that practice medium to low production runs of large parts; this is due to the intrinsically lengthy cycle time of the process, as it is required to elevate the temperature of a mold, while rotating it bi-axially, from room temperature to beyond the melting temperature of the plastic to allow shaping, and then cool it back to room temperature for part removal [18-23]. The relatively long cycle duration of rotomolding is evident when observing Table 1-1, which compares it, based on various criteria, to blow molding and thermoforming; two plastics molding technologies that are used to manufacture parts of comparative attributes [2,8,9,10].

Table 1-1: Characteristics of rotational molding compared to blow molding and thermoforming

Comparison Criteria	Rotational Molding	Blow Molding	Thermoforming
Plastic form during processing	Powder, usually exhibiting a particle diameter of 500 mm or less	Pellets	Extruded plastic sheets
Plastic melting and shaping method	Melting occurs inside the mold. The mold is heated, thereby heating the air inside it, and hence raising the temperature of the plastic to beyond its melting temperature for shaping. Mold rotation during heating is required	Plastic is first melted/softened using an extrusion-based apparatus and then introduced to the mold under elevated pressures	Plastic is heated and formed into or over a mold. Uses vacuum, air pressure, and/or mechanical forming to move the heated sheet over the mold
Mold/tooling cost	Low, due to the atmospheric nature of the process	High, due to the need to preserve a pressure profile in the mold during the process	Low initial setup cost, fast setup time
Possible Characteristics of end-use products	Seamless large sized relatively complex parts with undercuts, can have foam cores (e.g., tanks, storage bins, mannequins)	Medium to small sized parts of average complexity (e.g., parsons, fluids bottles/containers, seats) A seam or parting line is typically present in end-parts	Medium to large shallow parts with low undercuts and precise dimensional control of one side (e.g., large panels, housings, enclosures, tubs, cabinets)
Manufacturing cycle duration	Long, due to the atmospheric nature of the process and since the plastic is heated indirectly through the mold	Short, plastic is instantly melted and introduced to the mold for shaping	Average, the forming process is short. However, a secondary cutting operation is required which generates scrap
Production Volumes	Medium to low, due to the lengthy cycle times	Mass production, due to the short cycle times	Medium to mass production

For end-use applications that require buoyancy, enhanced mechanical and/or insulative properties, and improved strength-to-weight ratio, the cavities of hollow rotationally molded articles are partially or completely filled with foam for purposes of reinforcement. Preliminary foam filling mechanisms entailed introducing polyurethane or polystyrene foams in predetermined amounts within the cores of such articles in a secondary processing operation. The drawbacks of this procedure include the reduced process efficiency due to the implementation of at least two processing cycles, as well as the almost certain incompatibility of adjacent skin and foam layers within a part, which causes them to act as discrete structures, thus demoting the overall properties of the end-product.

1.3.2 Process Evolution and Description

In the 1970s, addressing the aforesaid drawbacks through various research ventures led to the modification of the conventional rotational molding process to perform as a single-cycle plastic foams fabrication technology. The redesigned process became commonly known as rotational foam molding. This process allowed the manufacture of high quality single parts with or without an integral distinct non-foamed solid-skin encapsulating a partially or completely foamed inner core. Typical procedures used to achieve such articles involve a continuous (single shot) practice, where a mold, that is part of a rotational molding apparatus, is charged with predetermined quantities of non-foamable and foamable plastic resins all together at the beginning of the rotational molding processing cycle, or an interruptive (multiple shot) practice, by using designated drop boxes or plastic bags to introduce the foamable resin to the mold at an intermediate stage within the identical cycle [18-21].

1.3.3 Advantages and Disadvantages

The rotational foam molding technology provided remedial solutions to a range of problems endured when implementing the preliminary practice. The manufacturing time was reduced due to the elimination of the secondary foam filling cycles. The use of compatible plastic resins for respective skin and foam layers provided a strong integral bond between them, typically allowing the manufactured articles to act as one body that exhibited enhanced physical properties. Moreover, the overall cost of the manufacturing practice was reduced, since rotational foam molding involves less time, labor, tooling, and energy [17-19].

However, the rotational foam molding technology continued to inherit one of the greatest unresolved disadvantages from the conventional rotational molding technology; its length cycle times. The cycle times are long due to the need to elevate the temperature of the mold and the plastic resin beyond the melting temperature of the plastic and the decomposition temperature of the CBA for foaming, and then cooling the mold back to room temperature. In rotational foam molding this disadvantage is even complicated further due to the negative insulative effects of the foam during the heating and cooling processing segments; which prevents the real-time control over the foam processing parameters, resulting in a courser and less uniform cell size than desired [18-21]. Additionally, the unpredictable foaming behavior and/or the premature decomposition of the CBA at times results in poor skin thickness uniformity, foam invasion into the skin, and the presence of a weak and non-uniform skin-foam interface.

1.4 Solution Fundamentals

The shortcomings of the rotational foam molding technology resulted in reducing its economic feasibility and narrowing its applications, materials, and processing window. Accordingly, the need exists to introduce a processing technology that is able to concurrently manufacture parts with equivalent, if not improved, attributes and quality.

Previously conducted research work illustrated the presence of a strong relation between the duration of the heating cycle and the properties of the obtained polyolefin foamed morphologies in rotational foam molding [24]. These studies implicitly indicated that the morphologies of these cellular structures might be dramatically improved if the processing cycle was shortened. In this context, a processing strategy that will utilize synergistically and concurrently the advantages of both the melt extrusion and rotational foam molding technologies has been conceived. By adopting this conclusion, this thesis focuses on deliberately superimposing two technologies; rotational molding with its aforementioned advantages, and melt extrusion, which is considered as the most efficient method for continuous melting and mixing of plastics, in order to accomplish a primarily significant reduction in processing cycle time as well as energy consumption.

1.5 Thesis Objectives

This thesis is an integral portion of a prominent project under the name Rapid Rotational Foam Molding (RRFM) that is intended to achieve the successful and beneficial combination between the extrusion and the rotational molding plastic processing technologies [25,26]. The main goals of this project entail the design, development, analysis, construction, and testing of a reliable, efficient, and robust processing

technology and approach by which the drawbacks of the conventional rotational foam molding process can be successfully reduced or eliminated. The designed solution is intended to allow the manufacture of high quality seamless plastic parts exhibiting a solid integral-skin enclosing a partially or completely foamed core. The desired solution should include the following simultaneous processing benefits: (i) significantly reduce the processing time and cost needed to achieve such articles without compromising quality, (ii) scale up the process and achieve an industry-desired level of repeatability, durability, and reliability, and (iii) provide the opportunity to extend and expand the currently achieved frame of materials and applications [25,26].

The specific and fundamental goals of this thesis involve: (i) presenting the design procedure and the evolution of the RRFM technology, (ii) assessing and experimentally verifying the feasibility of processing multiple-shaped integral-skin foamed core PP-based rotomolded articles using this technology, and (iii) developing the engineering basis for accomplishing an optimal processing control designated to manufacture high-quality fine-celled integral skin foamed core PP foams utilizing RRFM.

1.6 Thesis Scope and Relevance

This thesis presents the novel RRFM technology and the respective systematic approach for producing integral-skin fine-cell PP foams utilizing this process. However, the presented methodologies are not solely applicable to the PP material grades presented in this thesis or to PP material grades in general. It is envisioned that RRFM will be implemented to process a wide variety of integral-skin polyolefin-based foams.

This thesis also describes the design, analysis, development, build, and optimization of an industrial-grade lab-scale RRFM experimental setup. The developed

methodologies and obtained results are equally applicable to smaller-scale and larger-scale systems.

1.7 Thesis Format and Outline

This thesis comprises 6 distinct chapters.

Chapter 1 provides an introduction to the various topics and entities that govern the addressed engineering problem linked to the rotational foam molding plastics processing technology.

Chapter 2 presents a comprehensive literature review and theoretical background, based on extensive research work, of the methodologies that facilitate understanding a variety of themes applicable to the engineered solutions presented throughout this thesis. Topics covered include a variety of fundamental aspects related to rotational molding, rotational foam molding, extrusion, and relevant materials such as polymers and CBAs.

Chapter 3 discusses the evolution of the proposed engineered solution, namely Rapid Rotational Foam Molding, to its current form. A thorough review of the various remedial technologies developed throughout the design process is presented along with the pertaining physical embodiments that respectively implement these solutions.

Chapter 4 discusses the groundwork performed with respect to developing the feasibility assessment experimental plan of the devised solution using a set of PP-based resins and a CBA as experimental materials.

Chapter 5 carefully analyzes the results generated through the implemented experimental plan, including a variety of comparisons and observations that reveal important information about the entities that govern the devised remedial processing technology.

Chapter 6 concludes the thesis by summarizing the most important findings and presenting a plan for future work.

Chapter 2: Literature Review and Theoretical Background

2.1 Introduction

In this chapter a literature and patent review will be carried out to investigate the different aspects that directly and/or indirectly conditioned the development of the Rapid Rotational Foam Molding technology.

Two unique aspects define the backbone of the material presented in this chapter: (1) the relevant existing processing technologies with their underlying theories; (i.e., a detailed technological overview of conventional rotational molding, rotational foam molding, and melt extrusion) and, (2) the fundamentals associated with the materials and resources used throughout the experimental work pertaining to the thesis; (i.e., polymers, blowing agents, etc.) are also presented.

2.2 Relevant Processing Technologies

2.2.1 Conventional Rotational Molding

2.2.1.1 Introduction

Conventional rotational molding, or rotomolding, evolved to be a plastics fabrication technology that is commonly used to manufacture single-piece, hollow or double-walled, large-sized, complex-shaped, seamless, stress free plastic parts. In its present form, conventional rotational molding of plastics can be described through the four distinct

steps outlined in Figure 2-1. The first step involves charging a hollow mold with plastic powder of size mesh-35 (i.e., particulate size of at most 500 [μm]), which is typically reduced from pellet size. In the second step, the mold is closed and heated at an elevated temperature, usually provided by an oven, for a prescribed period of time. The plastic powder eventually melts and evenly adheres to the internal walls of the mold. The third step entails cooling the mold back to room temperature while rotating it bi-axially. The fourth and last step involves stopping the mold rotations and manually removing the solidified part.

1. Mold Charging with Plastic Powder

2. Mold Heating + Bi-axial Rotation

3. Mold Cooling + Bi-axial Rotation

4. Rotations Seized + Part Removal
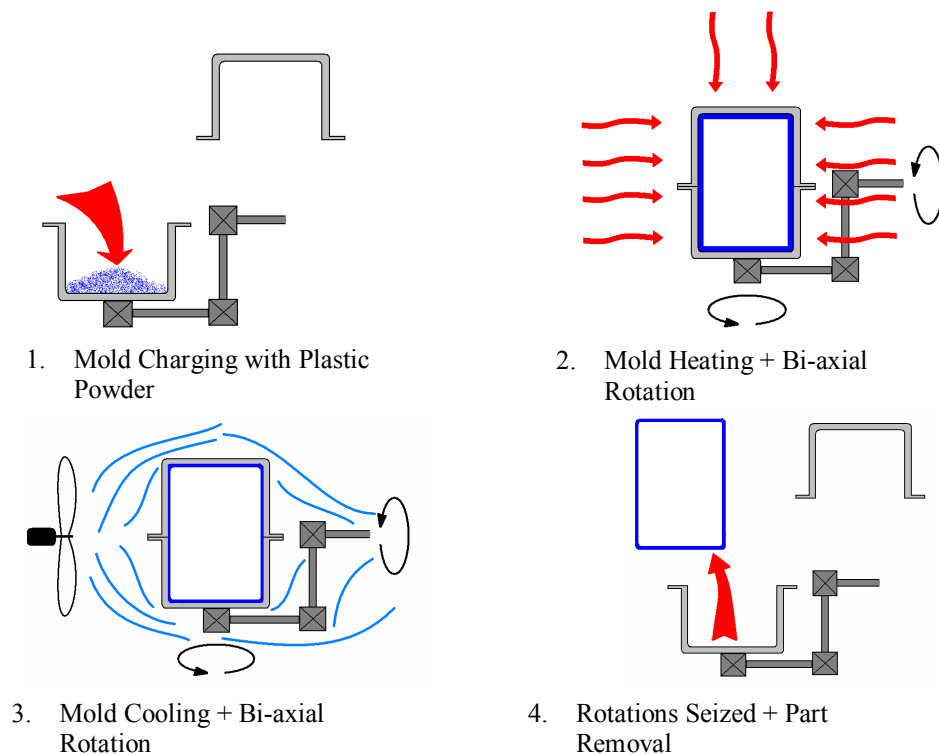
Figure 2-1: Conventional rotational molding processing steps

The first patent describing the fundamentals of rotational molding was filed back in 1855 by an Englishman named R. Peters (British Patent No. 1301) [18,19,23]. In his invention, Peters presented a hollow mold attached to a mechanism, which achieves a rotational motion about two perpendicular axes by utilizing a set of bevel gears. He

recommended molten metals or substances in fluid or semi-fluid state to be used with his invented apparatus. In his patent document, Peters stipulated the bi-axial rotation of the mold containing the substance until even distribution of the substance within the mold is attained; a pipe was used to vent excess gases from the mold core and water cooling was employed.

In 1905, Voelke published a patent (U.S. Patent No. 803,799 [22]) to process paraffin wax in a non-porous mold from a liquid form to a solid form by means of cooling the mold while rotating it about two perpendicular axes [23].

In 1910, Baker and Perks patented (U.S. Patent No. 947,405 [27]) a rotational casting apparatus (a preliminary form of rotational molding) that they used in creating chocolate eggs from ingredients charged to the mold in molten mixtures [27]

Clewell and Fields were the pioneers in processing polymeric materials with rotational molding. In 1941, they patented (U.S. Patent No. 2,265,226 [28]) a preliminary rotational molding procedure that was used to mold vinyl chloride based components. In the mid 1940s and early 1950s, this procedure provided the basis for manufacturing vinyl plastisol moldings [23,28]. During this period, rapid development of rotational molding equipment took place as well.

The development of the polymer polyethylene (PE) by the U.S. Industrial Chemicals Company occurred in 1960. Ever since, due to their enhanced properties and excellent economics, PE rotomolded components have become a main competitor to vinyl plastisols and plastics manufactured using other molding processes [23].

2.2.1.2 Current Status of Rotomolding in North America

Currently, there are approximately 123 North American rotomolders with considerable contribution to the manufacturing of rotomolded articles. The current top five North American companies, ranked based on sales value are: Toter Inc. (Statesville, NC), Step 2 Co. LLC (Streetsboro, OH), Norwesco Inc. (St. Bonifacius, MN), Promens North America (South Bend, IN), and Centro Inc. (North Liberty, IW). The overall combined turnover of these five companies in 2008 was around $550 million [29].

The top five goods categories presently manufactured by North American rotomolders are: agricultural/industrial tanks, recreational/sporting goods, non-tank industrial goods, consumer products, and pallets/skids/packaging components [29].

There are three process-related requirements that govern the resins used in rotomolding: (i) the resin's availability in powder or liquid form, (ii) the resin's thermal stability during processing, and (iii) the good flow properties of the resin [18]. In this context, the top five plastic resins consumed by the North American rotomolders are LLDPE, HDPE, Cross-linked PE, LDPE, and Nylon, these resins comprise over 90% of the materials used in rotomolding today [30]. Other commonly used resins in the North American rotomolding industry include various grades of Polycarbonate (PC), Polypropylene (PP), and Polyvinylchloride (PVC).

2.2.1.3 Rotomolding Equipment

According to related statistics released in the year 2005 [30], there are five principle machine configurations of rotomolding equipment presently used throughout the North American rotomolding industry. Stated in descending order of usage, these are: the carousel independent arm configuration, the carousel fixed turret configuration, the

shuttle configuration, the clamshell configuration, and the rock 'n' roll configuration. All these machine types include the necessary capabilities/equipment to achieve bi-axial rotation, heating, cooling, and servicing procedures. The basic requirements of rotomolding machinery are presented next, followed by an emphasis on the most important rotomolding machinery present in the industry today.

Basic Requirements of Rotomolding Machinery

All rotomolding machines must allow accomplishing four distinct fabrication tasks; these are: (i) heating, (ii) cooling, (iii) servicing, and (iv) bi-axial rotation during the first 2 stages. The requirements that define each task are stated as follows [18,31,32]:

(i) **Heating Stage:** The rotomolding setup has to raise the interior temperature of the mold to the sticking level of the material as soon as possible. The machine has to allow the uniform heating of the mold during the powder sintering stage. It is required that the temperature profiles within the molds be precisely controlled during this segment to prevent the degradation of the processing material.

(ii) **Cooling Stage:** It is essential that the rotomolding system provides the capabilities to evenly cool the mold while rotating to prevent part defects such as warping, porosity, and non-uniform skin thickness. Air cooling and fine mist cooling are common cooling methods used in the industry.

(iii) **Servicing Stage:** The primary goals during this stage are ease of finished part removal and efficiency in supplying molds with raw material.

(iv) **Rotation during Heating and Cooling:** In rotational molding, molds are mounted on an arm assembly to allow their 360° rotation about two

perpendicular axes; a horizontal axis (mold central axis) and a vertical axis. The most commonly implemented respective mold-to-arm rotations ratio is 4:1; this allows achieving satisfactory skin thickness uniformity. Conventional arm designs include straight arms, offset arms, and rock 'n' roll mechanisms. More information is provided in [32].

The Carousel Machine

Generally, carousel machines have four arms arranged at 90° angles apart and are present at heating, cooling, servicing, and auxiliary cooling stations. One or more spindles are connected at one end to a turret or central hub and at the other end to the respective molds at the arms. The arms are motorized and controlled independently of the central hub. The main advantage of this machine is its ability to manufacture a variety of parts, possibly comprised of different materials, in a simultaneous manner, due to four available arms. The main disadvantage of this machine is the fact that all arms are attached to one global frame, which at times results in events when the process is delayed to cope with the processing time and or task of the slowest station [31]. Figure 2-2 depicts a typical carousel configuration.
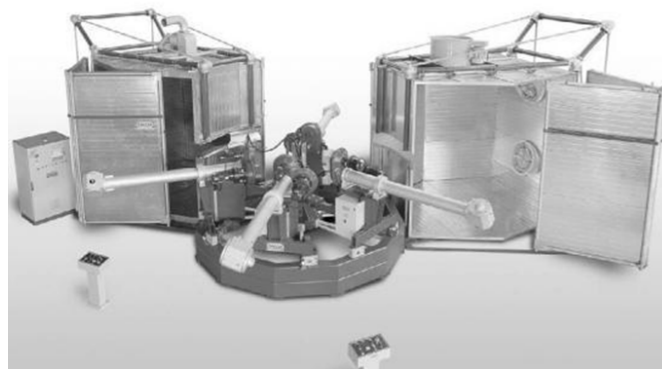
Figure 2-2: Independent arm carousel rotomolding machine [31]

The Shuttle Machine

The shuttle mechanism was created for the purpose of minimizing the space occupied by the rotomolding apparatus. Figure 2-3 depicts a typical shuttle configuration. The setup of this system comprises two bi-axially rotating arms, placed on rails for linear mobility, with an oven in-between them. The mold associated with one arm is allowed into the oven for heating purposes by utilizing the rails, while the other mold is serviced with resin and/or allowed to cool at the same instant. This setup is considered one of the most efficient rotomolding setups, as utilizing it permits minimal downtime [31].

Figure 2-3: Two-station shuttle machine [31]

The Clamshell Mechanism

The clamshell machine is ideal for smaller shop floors as it occupies minimum space. The oven of this machine encloses the arm-mold assembly as seen in Figure 2-4. The oven closes and opens during respective heating and cooling/servicing cycles in a manner analogous to that of a "book" [31]. More than one arm can be included with this setup, which adds to its complexity, maintainability, and cost.
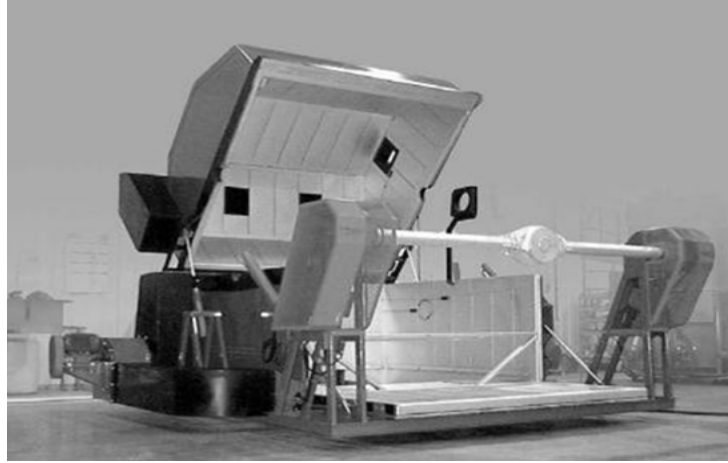
Figure 2-4: Clamshell machine [31]

The Rock 'N' Roll Mechanism

This type of rotational molding machinery is typically used for parts with a large length-to-width ratio that are non-round in nature (Figure 2-5). These unique machines rotate a particular mold 360° in one direction while tipping it at 45° above and below the horizontal contour in another. In terms of economics, rock 'n' roll machines usually cost less than the other types of rotomolding machinery [31].
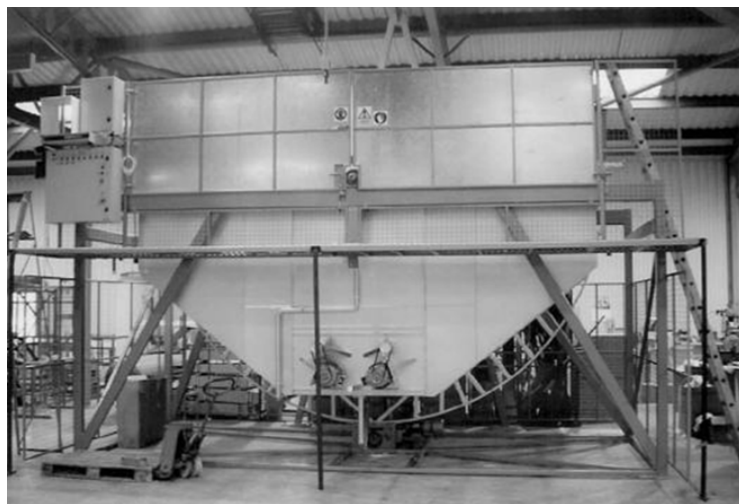
Figure 2-5: Rock 'n' roll rotomolding machine [31]

2.2.2 Rotational Foam Molding

2.2.2.1 Introduction

In many instances, it is highly desirable to introduce a foam layer or core in the interior of hollow rotomolded articles for purposes of enhancing the overall mechanical properties, economics, buoyancy, and insulation capacity.

To obtain a foamed layer/core within the non-foamed polymer skin, the current technique utilizes an extrusion melt compounding procedure to compound a blowing agent with a thermoplastic resin and introducing the resulting foamable blend, after forming it into solid pellets, to the mold, either at the outset of the process with the nonfoamable skin-forming resin (single-shot practice), or at a desired instant, during the course of the same processing cycle, after processing the skin layer (interruptive practice).

Subsequent to the continual heating, by means of prescribed temperature profiles, and the simultaneous rotation of the mold, the foamable resin melts and forms a layer adjacent to that of the skin. Afterwards, the blowing agent decomposes, at a temperature beyond the melting temperature of the resin, to release a gas (usually CO_2 or N_2), which in turn generates voids within the molten polymer matrix, forming the sought foam core/layer [33-35].

2.2.2.2 Foamable Resin Preparation in Rotational Foam Molding

In order to produce articles exhibiting a foam layer or foam core in rotational foam molding, it is necessary to create a suitable foamable resin; this is achieved by mixing a

plastic resin with a CBA and any relevant additives in predetermined quantities that convey a desired VER[1] and CBA decomposition behaviour. In this context, there are two established procedures to prepare foamable resins; these entail a dry blending approach and a melt compounding approach [33-35].

The dry blending mixing approach comprises placing the appropriate amounts of plastic resin (ground from pellets to powder), CBA, and any pertinent additives in a suitable container and then manually or automatically shaking it until the contents are appropriately blended. This practice generates a foamable resin that can be used with any of the prescribed rotational foam molding practices [33-35].

The melt compounding approach involves using an extruder or an extrusion based process to uniformly compound/blend the ingredients of the foamable resin, and then extrude a profile comprising the used polymer blended with non-decomposed CBA particles that are dispersed and evenly distributed through it. The obtained extrudate is then cooled through a cooling bath, pelletized, and sometimes pulverized back to powder form for usage in rotational foam molding. Processing temperatures throughout the extrusion course should be set so as to not permit the premature decomposition of the CBA during blending [33-35].

2.2.2.3 Polymer Foaming Mechanism

Ideally, a desirable polymer foaming process should be comprised of the following steps: (i) the dissolution of the foaming agent, (ii) bubble nucleation, (iii) bubble growth, and (iv) bubble stabilization [36,37]. The details of the mentioned steps are presented herein,

---

[1] The volume expansion ratio (VER) describes the change in volume of a particular polymer or material as it changes form from a solid structure to a foamed structure.

it is worth noting, however, that the discussed sequence is not always simple to accomplish in practice.

(i) Dissolution of foaming agents within polymeric systems occurs either by thermal activation, as is the case when using CBAs and some PBAs, or by state change due to the introduction of volatile liquids released under pressure, as is the case with most PBAs. The dissolution process typically occurs at desired instances when the polymer is in a molten state and has reached a temperature range that preserves desired strength to handle and keep the resulting gases [36-38].

(ii) Bubble nucleation is associated with the birth of very small bubbles (nuclei) in the polymer matrix and can be homogenous; i.e., when the system has no impurities or nucleants and is in a single homogenous phase, or heterogeneous; i.e., in the presence of additives and/or nucleants. The nucleation procedure occurs when excess gas separates in the form of bubbles within the polymer melt upon exceeding the polymer's solubility limit (saturation). The amount of generated bubbles depends on the number of nuclei generated within the system. Visibly, nucleation is distinguished through observing a creaming texture on the polymer mass without significant volume increase [36-38].

(iii) Bubble growth occurs due to the diffusion of excess gas dissolved in the polymer, and is linked with the increase in volume of the polymer mass and its rising action. The growth of the cell depends on the pressure difference between the inside of the cell and the surrounding medium. The extent of the achieved growth depends on the surface tension associated with the polymer, which is indicated by its melt strength and melt elasticity. Larger surface tension promotes less nuclei growth and vice versa. Cell wall rupture upon growth results as a consequence to the low surface tension of a

polymer, either as a property of the polymer, or due to improper processing parameters (foaming temperature, amount of foaming agent, gas concentration, etc.), or as a result of cell wall drainage due to low melt strength of the polymer at elevated temperatures [36-38].

(iv) After cell growth is complete, cell stabilization should take place. During this stage, the gas must not escape the cell so rapidly, causing cell shrinkage. The stabilization of the foam structure relies on the solubility and diffusivity of the gas in the polymer matrix. This can be controlled by elevating the polymer viscosity either by reducing the processing temperature or by increasing the polymer's molecular weight [36-38].

Cell Coalescence and Cell Coarsening

Two undesirable phenomena can take place in a particular foaming process if the proper processing entities are not well defined and/or set; these are, cell coalescence and cell coarsening. Cell coalescence occurs when two or more adjacent cells merge to form one large cell due to the instability of the cell wall separating them. Cell coarsening is the collapse/drainage of a smaller bubble into an adjacent larger bubble resulting in a bubble size that is larger than both; this is due to the gas diffusion from one bubble to another [39]. Low melt strength and poor melt elasticity of the foaming resin and relatively high processing temperatures are common causes of such phenomena.

2.2.2.4 Rotational Foam Molding: Theoretical Background

This section outlines the theoretical background related to the successful manufacture of integral-skin completely foamed core thermoplastic articles utilizing the rotational foam molding method.

Required Amount of Material for Solid Skin

It is essential to first investigate the parameters that would allow achieving a desired rotomolded solid skin with a uniform thickness. A cylindrical mold, as depicted in Figure 2-6, will be used as a reference part to illustrate the approach to calculating skin thickness parameters in rotational molding.
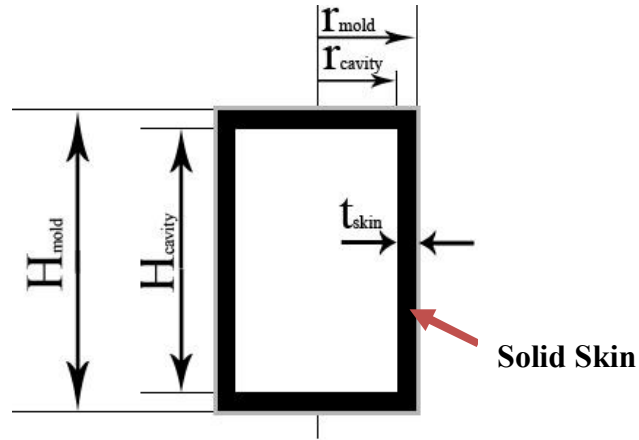
Figure 2-6: Solid skin schematic and parameters for a cylindrical mold

The volumes of the presented cylindrical mold (V_{mold}) and the cavity within the shown skin (V_{cavity}) can be expressed using [40-42]:

$$V_{mold} = \pi(r_{mold})^2 H_{mold} \qquad (2.1)$$

$$V_{cavity} = \pi(r_{cavity})^2 H_{cavity} \qquad (2.2)$$

And,

$$r_{mold} = r_{cavity} + t_{skin} \qquad (2.3)$$

$$V_{skin} = V_{mold} - V_{cavity} \qquad (2.4)$$

Substituting Equation (2.3) into Equation (2.1) and utilizing Equation (2.4), which represents the total volume occupied by the skin material V_{skin}, the mass of the polymer

resin needed to process a skin layer of thickness t_{skin} for the shown molding, $m_{polymer}$, can be calculated using [40-42]:

$$m_{polymer} = \rho_{resin}V_{skin} \tag{2.5}$$

Where ρ_{resin} is the density of the potential skin resin. It is worth noting that the presented approach is applicable to any mold shape upon using the appropriate equations to define the volume of the respective mold and relating such equations with the skin thickness through relevant dimensional parameters.

Formulating the Foam-creating Material

Considering the same cylindrical mold presented in Figure 2-6, it is desired to completely fill its hollow core with foam, in a configuration similar to the one depicted in Figure 2-7.
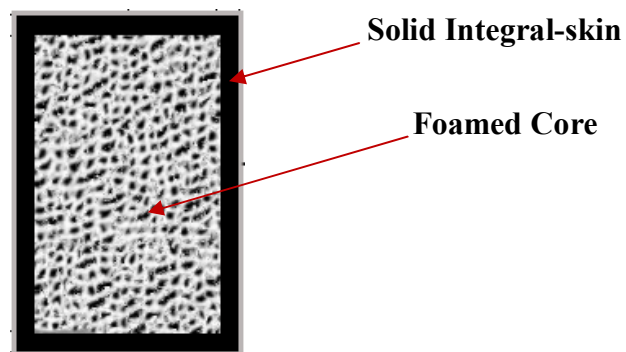
Figure 2-7: Integral-skin foamed core part schematic

As mentioned earlier, a typical foamable formulation includes a plastic resin and a CBA. During processing, the CBA engages in an expansion process, where a gaseous phase is dispersed through the polymer melt. The quantities of the respective formulation constituents that are introduced to the mold depend on the desired volume expansion ratio (VER); that is, the ratio between the final volume occupied by the foam (required to

equal V_{cavity} in the presented case) and the initial volume occupied by the base resin used to create it V_I. VER is defined as [40-42]:

$$VER = \frac{V_{cavity}}{V_{initial}} = \frac{(V_{initial} + V_{gas})}{\frac{m_{polymer}}{\rho_{resin}}} = 1 + \frac{V_{gas}}{\frac{m_{polymer}}{\rho_{resin}}} \tag{2.6}$$

where V_{gas} in represents the gas volume in the created foam.

The amount of CBA, expressed as a weight percentage of the designated foaming resin weight, required to achieve the essential expansion can be determined using [51][43]:

$$\% \, CBA = 100 \cdot \frac{m_{CBA}}{m_{polymer}} \tag{2.7}$$

CBAs typically come in powder form, and are often characterized in terms of their gas generation capacity (ϕ); that is, the volume of gas generated per unit mass of CBA powder used (typical units: [cm^3/g]). This factor can be incorporated into Equation (2.7) by implementing the following equivalent relations [40-42]:

$$V_{gas} = V_{cavity} - V_{intial} = \phi \cdot m_{CBA} \tag{2.8a}$$

$$\therefore m_{CBA} = \frac{V_{cavity} - V_{intial}}{\phi} \tag{2.8}$$

Substituting Equation (2.6) into the expressions obtained in Equation (2.8) and Equation (2.3), after rearranging the following is obtained [40-42]:

$$m_{CBA} = \frac{V_{cavity} - \left(\frac{V_{cavity}}{VER}\right)}{\phi} = \frac{V_{cavity} \cdot \left(1 - \frac{1}{VER}\right)}{\phi} \tag{2.9}$$

$$m_{polymer} = \frac{V_{cavity} \cdot \rho_{resin}}{VER} \tag{2.10}$$

The resulting terms can be substituted into Equation (2.7) to obtain a direct expression that relates the amount of CBA with its gas yield capacity, the desired VER, and the total volume of the cavity to be filled [40-42]:

$$\% \, CBA = \; 100 \cdot \frac{\frac{V_{cavity} \cdot \left(1 - \frac{1}{VER}\right)}{\phi}}{\frac{V_{cavity} \cdot \rho_{resin}}{VER}} = 100 \cdot \frac{VER - 1}{\phi \cdot \rho_{resin}} \tag{2.11}$$

The gas yield factor, ϕ, provided by the CBA manufacturer corresponds to the gas yield at standard (room) temperature and pressure[2], and hence should be given the subscript STP (ϕ_{STP}). In this context, the gas yield has to be corrected with respect to the crystallization temperature of the polymer, as at this temperature, the material freezes and no more volume changes are possible [40-45]. The expression used to correct the gas yield factor with respect to the crystallization temperature of the polymer is:

$$\phi = \phi_{STP} \cdot \frac{V_C}{V_{room}} = \phi_{STP} \cdot \frac{T_C}{T_{room}} \tag{2.12}$$

where V_C, T_C, V_{room} and T_{room} correspond to the gas volume at the crystallization temperature, the absolute crystallization temperature, the gas volume at room temperature, and the actual room temperature, respectively.

Further corrections to the CBA gas yield factor were introduced by Pop-Iliev *et al.* [45]. The presented corrections account for the gas losses experienced during the rotational foam molding cycle due to the nature of the used resins (e.g., PP or PE), the effects of the CBA's decomposition nature and ability to efficiently blow gas through the polymer melt, the effects of polymer viscosity, the effects of the used VER, and finally the effects of the rotational foam molding method used.

2.2.2.5 Evolution of Rotational Foam Molding

The first invention related to a single-cycled multi-charge process that generates integral-skin foam articles dates back to the year 1956 (U.S. Patent No. 2,950,505), when Frank

---

[2] Standard temperature is room temperature, and is expressed in Kelvins to be 293 K. Standard pressure is 1 atm.

Jacob introduced his invention titled *"Method of Molding a Plastic Article having a Cellular Body and Protective Skin"* [46]. The particulars of the invention included a process where a mold is initially filled with a skin-forming thermoplastic powder, then closed and heated until the plastic particulates sinter and form a semi-solid plastic layer adjacent to the mold wall. The mold is then opened and any non-bonded plastic particles are manually removed. Next, the mold is charged with expandable polystyrene (PS) beads (at that time, Dow Chemical Company provided such beads) that comprise the foam core material; the beads are placed adjacent to the non-foamable skin material. The mold is then closed and heated till the skin-forming resin completely sinters and the beads expand and generate the foam layer [46].

The discussed practice, however, was not performed in a rotating mold, and hence was not directly related to rotational foam molding, but was one of the concepts that later led to conceiving the rotational foam molding ideology.

In 1966, Kleine *et al.* published a patent under the title *"Process for Producing Hollow Bodies Reinforced with a Foamed Structure"* (U.S. Patent No. 3,505,137) [47]. The main idea behind this invention included removing a portion of the used mold with a skin section attached to it (while still hot), and then depositing a thermoplastic foamable resin through the resulting mold opening. The mold is sealed and then heated at appropriate temperatures to trigger the foam formation process. The removed skin portion is finally welded to the resulting structure.

In the patent document, the authors also stated that the mold can be rotated for ease of plastic distribution. The disclosed patent provided the ground-work associated with the interruptive rotational foam molding processing technology.

Interruptive (multi-shot) rotational foam molding was developed further by Jerome Lemelson in 1975. In his patent document (U.S. Patent No. 3,875,275) titled *"Method for Molding Composite Bodies"*, Lemelson stated that he was able to create integral-skin foam core structures by means of introducing hollow frames or reinforcing members (Figure 2-8) within a uni-axially rotating mold [48]. Resins combined with compatible blowing agents were allowed into the mold using the frames/members, after creating a non-chilled solid skin layer. Consequently, upon further heating, the blowing agents decompose within such resins causing a completely or partially foamed core contained by the preformed skin.
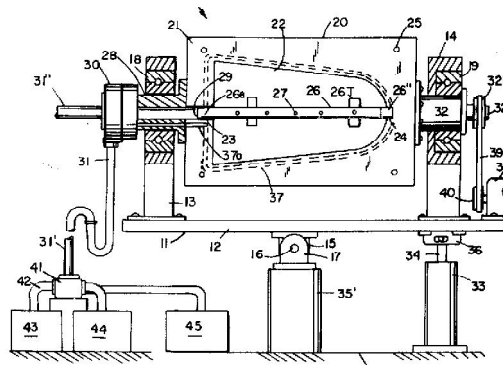
Figure 2-8: Illustration of a hollow frame/member used to introduce foamable resins [48]

The principles of continuous (single-shot) rotational foam molding were first introduced by Mori *et al.* in 1976 (U.S. Patent No. 3,962,390) [49]. This patent presented the technology by which non-foamable and foamable resins are introduced to the mold at the outset of the rotational molding cycle. The foamable resin prescribed in the patent is one that exhibits a higher heat capacity, usually 50% more, than the non-foamable skin forming resin; implying that it takes a longer period of time to melt [49].

Other inventions associated with the advancements achieved with regards to rotational foam molding include but are not limited to: U.S. Patent No. 3,914,361 by N.

Shina and K. Hosoda, International Patent No. W/O 95/19877 by R. Crawford and P. Nugent, International Patent No. W/O 96/15892 by B. Graham, U.S. Patent No. 5,532,282 by D. Needham, U.S. Patent No. 5,830,392 by J. Strebel, and U.S. Patent No. 5,928,584 by C. Lee.

2.2.2.6 Particulars of the Current Practice

<u>Materials Consideration</u>

The rotational foam molding process is very sensitive to materials quality. The characteristics of the materials used for comprising the different layers of an article manufactured using this process vary substantially from one layer to another.

Solid skin layers are usually manufactured using a free flowing plastic powder of mesh-35 size; this allows an even and rapid distribution of the material as the mold rotates during the skin forming processing segment. The melt flow index (MFI) of a material, in [g/10 min], is the quantitative measure, determined using standard procedure ASTM D1238, which provides information on the ability to flow of the material. The higher the melt flow rate value, the easier flowing the material is. For rotomolding of hollow articles with a solid skin, it is desirable to use material grades that have a MFI in the range of 2 to 8 [g/ 10 min] [19,23].

The selection of the resin used in creating the foam layer or core is dependent on the properties and morphological nature of the base polymer used. Generally, it is important to select appropriate resin grades that foam well and allow achieving uniform cell density, large cell population density, and desired average cell size. Important factors that govern the achievement of such attributes entail that the chosen resin should possess adequate melt strength and melt elasticity [19,23].

There are several actions, pursued during the current practice, that facilitate forming compatible skin and foam formulations capable of producing composites of distinct solid skin layers encasing foam structures. The most common procedure involves maintaining a size difference between non-foamable and foamable resins in rotational foam molding such that the non-foamable resin exhibits an overall smaller particle size [49]. During the single shot practice, this allows the sintering of skin-forming resin first, due to its larger contact area with the hot inner mold surface, followed by the processing and formation of a foam layer/core through the larger-sized foamable resins/pellets.

Another technique includes using a non-foamable skin resin of lower melting point than the foamable resin. The processing cycle is then modified to include a secondary higher temperature setting to trigger the sintering and the subsequent decomposition of the CBA embedded into of the pertaining foam-forming resin.

Continuous and Interrupted Rotational Foam Molding Cycles

Currently, rotational foam molding is conducted using a continuous practice or an interrupted practice, the particulars of each are presented herein in the context of processing integral-skin polyolefin foams.

Continuous (Single-Shot) Rotational Foam Molding: A schematic illustrating this procedure is provided in Figure 2-9.

The processing steps start by charging a mold with predetermined amounts of two types of plastic resins at the inception of the rotational molding cycle. The first type is a non-foamable resin, which is used to form the solid non-foamed skin of the end-part. This resin is typically of mesh-35 size (i.e., 0.5 [mm] particulate diameter) and has good flow properties suitable for rotational molding.
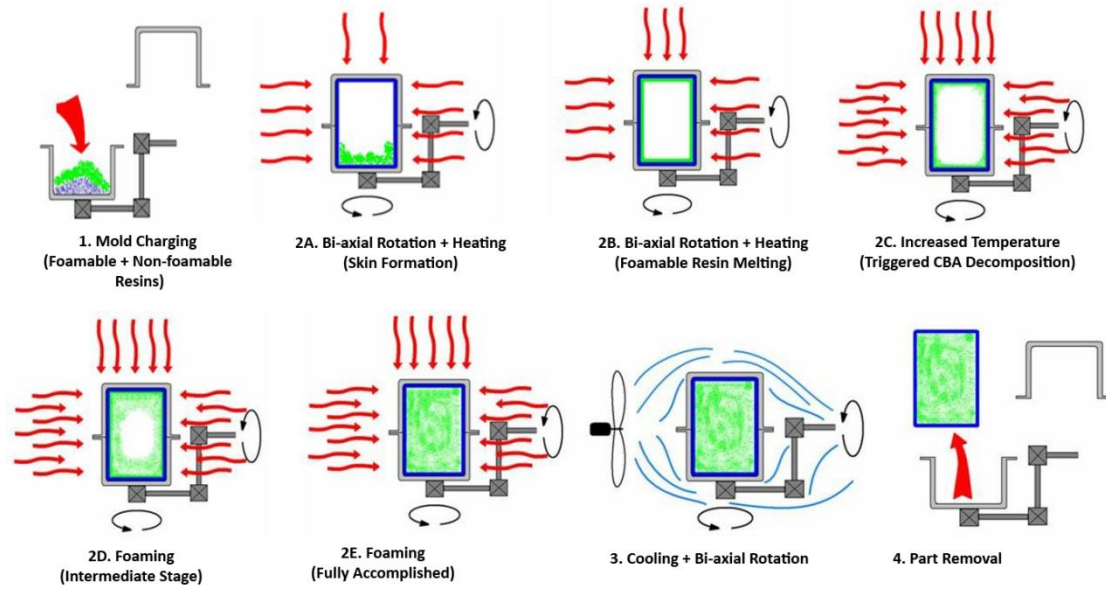
Figure 2-9: Single-charge rotational foam molding processing steps

The second resin is a foamable resin, which is comprised of a plastic resin extrusion melt compounded with a thermally sensitive CBA, in proportions corresponding to the desired plastic volume expansion ratio (VER). The foamable resin is usually coarser in size and/or exhibits a larger heat capacity value than that of the non-foamable resin. The mold is closed and heated in an oven while rotating bi-axially about 2 perpendicular axes. The non-foamable resin melts first and adheres to the inner mold walls due to its smaller size (i.e., more contact with the inner mold walls) and/or less heat capacity value (i.e., less thermal energy is needed to melt it). As the heating process resumes, the foamable resin melts and forms a layer adjacent to that of the molten skin layer. The temperature of the mold is then raised beyond the decomposition temperature of the CBA causing it to decompose and release gas within the molten foamable polymer. Upon the completion of the foaming process, the mold is cooled and then the part is removed.

Interrupted (Multiple-Shot) Rotational Foam Molding: The processing steps used to obtain an integral-skin foamed core rotomolded structure using this method are similar to the ones mentioned above for the single-charge practice, with the exception of the method by which the foamable resin is introduced to the mold during the processing cycle. With this method, a thermally-insulated drop box located either inside or outside the mold is used to deposit the foamable blend at an intermediate stage of the rotational molding cycle, typically after the skin layer is formed, through a pneumatically-actuated gate connected with the mold body. Figure 2-10 illustrates a mold and drop box assembly used in interrupted rotational foam molding [50].
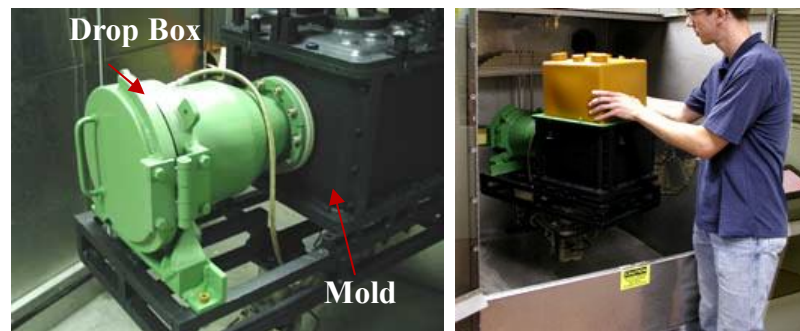
Figure 2-10: Drop box-mold assembly in interrupted rotational foam molding [50]

It can be observed that the design of the illustrated drop box is such that its location is outside the mold; this facilitates the addition of materials and blends comprising more than one layer during the rotational molding processing cycle.

Plastic bags are another commonly used method by which foamable blends are introduced to molds at intermediate stages of the processing cycle. Such bags are placed inside the mold, attached or unattached to a releasing mechanism, and are triggered at an appropriate time during the process to melt and assimilate accordingly, with the structure of the end-part, allowing the formation of the desired foam layer or core.

2.2.3 Polymer Extrusion

<u>Introduction</u>

Polymer extrusion is a polymer processing method, in which a solid thermoplastics material is melted or softened, and then forced through an orifice or die of a desired cross-section and cooled [51,52]. Possible structures created using extrusion include tubes, pipes, sheet, film, wire coatings, and a wide variety of profiles. Extrusion is achieved using extruders, which function as plastic melt pumps. The most common types of continuous extruders include single-screw extruders and intermeshing twin-screw extruders [32,51-53].

The extrusion process is briefly explained using the schematic in Figure 2-11, which presents a detailed section view of a single-screw extruder. The main components of the shown apparatus include a metallic barrel with a screw. The screw is actuated using an electric motor connected to a gear drive. The barrel has a feed throat at one end coupled with a conical hopper, the other end feeds a die exhibiting the desired profile. The described barrel-screw arrangement is at least divided into 3 sections: a feed section, a compression section, and a metering section [52,53].

The plastic resin is fed into the hopper in the form of pellets or powder, which then falls onto the screw by means of gravity at the feed section. The resin is then compressed and melted as it is transported by the screw along the barrel length through the compression section [53].
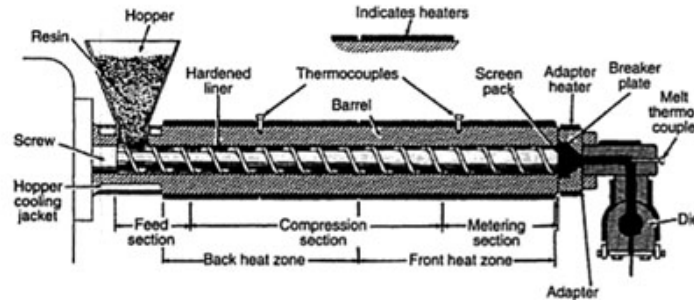
Figure 2-11: Sectioned view of a conventional single-screw extruder [53]

The plastic melting process occurs mostly by utilizing the friction generated between the barrel, plastic, and screw as well as a set of band heaters along the barrel length. The plastic melt is mixed throughout the metering section and then promoted to exit the extruder barrel through the die by means of the pressure generated during processing [53].

It is worth noting that twin-screw extruders function in the same manner as that of single screw extruders; however their design contains two intermeshing screws, that may be co-rotating or counter-rotating, within the barrel instead of one [53].

Historical Background

Extruders were primarily rubber processors until 1935, when Paul Troester developed the first polymer extruder in Germany [54]. The early age rubber extruders were steam heated. In 1935, these extruders acquired electrically heated barrels and added length, which permitted greater melting capabilities. Around 1950, Roberto Colombo explored the apparatus of intermeshing co-rotating twin screw extruders [55] while Carlo Pasquetti developed the concept of intermeshing counter-rotating twin screws extruders [56].

The early research and development work on extrusion was mainly concerned with the conveying of the molten composites in the extrusion process. The first

publication known was an anonymous article often incorrectly accredited to Rowell and Finlayson who wrote an article with the same title and in the same journal six years later. Throughout the 1950s numerous studies on the extrusion process emerged, in 1953 members of the polymer chemicals department of EI Duponts & Co presented the original development in the extrusion theory. However, the entire process of extrusion from the feed hopper to the die was not quantitatively described until 1965 [51-55].

Extrusion: Foam Processing Applications

While the evolution of the extrusion process and theory was mainly concerned with its functional optimization, a few processes were extended from it. One of these extensions dealt with foaming plastics. The extruder possessed the required thermal energy and mechanical power for adequate polymer phase change and the required pumping force for conveying the molten composite; this made the extruder an excellent processing unit for thermoplastics foam processing. Considering the thermoplastics foaming nature and the ability of the extrusion to incorporate different applications, foam extrusion was widely adopted in a variety of manufacturing ventures since the 1970's.

The first foam extrusion based product was Styrofoam, created by Dow in 1941 [57]. At that time, common structures manufactured using Styrofoam included the logs used in keeping anti-submarine nets floating on water bodies during WWII as well as six man life rafts for the coast guards. In the mid 1950's, batch produced PS foam sheets were manufactured for commercial/consumer usage. In 1958, the first commercialized LDPE foam was introduced by Dow [57].

2.3 Relevant Materials

2.3.1 Polymers

Definitions

A polymer is a large molecular chain constructed from many smaller structural units called monomers, covalently bonded together in any conceivable pattern [58]. Monomers possess two or more bonding sites that can connect to another monomer to form a polymer structure. The characterization of polymers occurs through investigating the chemical and physical nature of the monomers. An indication of the size of a polymer chain is given by means of its average molecular weight or its degree of polymerization.

The family of polymers is large, as the polymer structure conforms to a variety of materials either natural or synthetic. Figure 2-12 illustrates the various divisions within the family of polymers, with natural and synthetic polymers as the main comprising groups and elastomers placed in-between, since they can be naturally or artificially obtained.
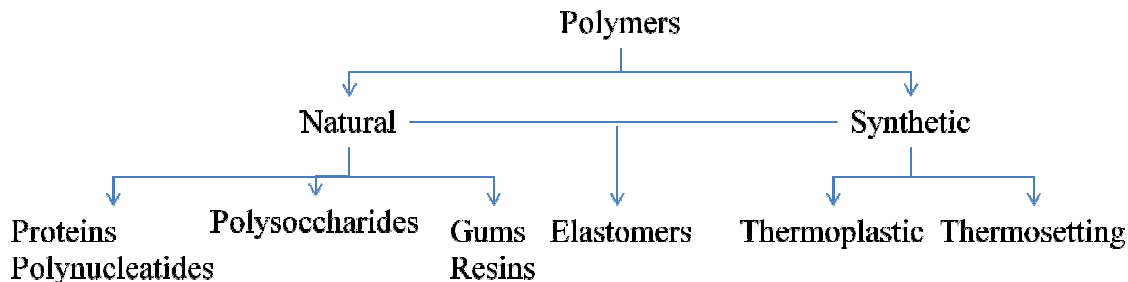
Figure 2-12: General family tree of polymers and polymeric materials [58]

The scope of this thesis is confined to synthetic polymers, which are widely utilized in the plastics industry. Synthetic polymers are divided into thermoplastics and thermosets. Thermoplastics are linear or lightly branched chain polymers that soften and

harden reversibly upon changing temperatures due to the action of the chains sliding past each other. Linear chain polymers have skeletal structures with two ends to them, while branched chain polymers have side chains or branches of significant length as schematically depicted in Figure 2-13.
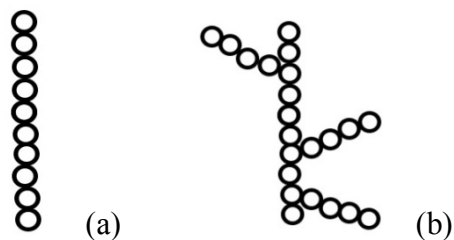
Figure 2-13: (a) linear (straight) polymer chain, (b) branched polymer chain [59]

Thermosets are polymers that can be caused to undergo cross-linking to produce a network polymer; the processing concept of such plastics category is often named curing. The cross-linked configuration is schematically represented in Figure 2-14. Thermosets cannot be softened or reformed again by heat or pressure due to the fixed positions of their comprising chains, they would rather burn [58-61].
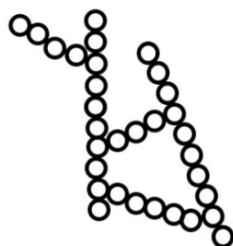
Figure 2-14: Cross-linked polymer configuration [59]

Polymers are prepared by means of a polymerization process; a process of repeating structural monomers or polymers to form long chains. Polymerization can be chemically characterized as either addition (chain growth) polymerization, where

monomers that contain double bonds are added sequentially to the growing end of a chain, or condensation (step growth) polymerization, where monomer, oligomer, and polymer chains combine by the elimination of small molecules from longer chains. Addition polymerization is divided further, depending on the type of chain growth mechanism implemented, to free radical polymerization, anionic polymerization, cationic polymerization, or coordination polymerization. The fundamental differences between both polymerization mechanisms are shown in Table 2-1 [58-61].

Among synthetic polymers, homopolymers are polymers whose structure can be represented by multiple repetition of a single type of repeating unit, which may contain one or more species of a monomer unit, while copolymers are polymers that contain more than one type of repeating unit [60].

Table 2-1: Chain growth and step growth polymerization mechanisms [61]

	Chain Growth Polymers	Step Growth Polymers
Molecular weight during polymerization	Average molecular weight changes very little once polymerization has begun as long as polymer chains form early in the process	Average molecular weight increases with reaction time
Species present during polymerization	Monomer, polymer and propagating chains (at very low concentration)	Monomer, dimer, trimer, oligomer, polymer
Rate of monomer utilization	Constant consumption of monomer during polymerization process	Monomer consumed early in the reaction
Effect of long reaction times	High conversion of monomer to polymer	High molecular weight species

Major Relevant Plastic Grades

High Density Polyethylene (HDPE): This PE grade possesses linear chains due to the polymerization process. Linear chains are easy to compact together, and hence provide ease of processing. HDPE's density ranges between 950 and 970 [kg/m^3] and its melting temperature is around 135 [^{o}C]. Applications of HDPE include containers, bottles, wire insulation, and household appliances [58-61].

Low Density Polyethylene (LDPE): This PE grade entails long and short branches, which prevents the chains from being closely packed. LDPE is soft and flexible, its density ranges between 910 and 920 [kg/m^3] and its melting temperature is about 110 [^{o}C]. Applications of LDPE include bottles, film, garment bags, and toys [58-61].

Linear Low Density Polyethylene (LLDPE): This PE grade is branched and formed of ethylene with addition of small amounts of butene or octene-1. LLDPE's density ranges within 910 and 920 [kg/m^3] and its melting temperature is around 125 [^{o}C]. It is usually used for thin high strength film used in packaging [58-61].

Polyvinyl Chloride (PVC): Possesses linear chains due to the polymerization process. Rigid PVC has a density around 1400 [kg/m^3] and is used for construction and piping applications, while Plasticized PVC has a density around 1300 [kg/m^3] and is used for flexible film sheet and upholstery. The melting temperature of PVC is around 360 [^{o}C] [58-61].

Polypropylene (PP): Can either be linear or branched. PP has a density of about 905 [kg/m^3] and a melting temperature around 165 [^{o}C]. Possesses outstanding

mechanical properties and chemical resistance, and is used for automotive parts, packaging, fibers, luggage, etc. [58-61].

Other major commercial plastics include polystyrene (PS) (density ≈1050 [kg/m^3], melting temperature ≈240 [^{o}C]), polyamides (Nylon 6, Nylon 66, etc.) (density ≈1140 [kg/m^3], melting temperature ≈215-265 [^{o}C]), polyethylene terephthalate (PET) (density ≈1360 [kg/m^3], melting temperature ≈260 [^{o}C]) and polycarbonate (PC) (density ≈1150 [kg/m^3], melting temperature ≈240 [^{o}C]) [58-61].

2.3.2 Materials Characterization

The following sections discuss the fundamentals of the analytical methods used to study the morphological and thermal characteristics of polymer grades and CBAs. Differential Scanning Calorimetry (DSC) and Thermogravimetric Analysis (TGA) methods were used to characterize polymers and blowing agents for experimental work.

Differential Scanning Calorimetry (DSC)

DSC is used to determine the temperature and heat flow associated with material transitions as a function of time and temperature. It also provides quantitative and qualitative data on endothermic (heat absorption) and exothermic (heat evolution) processes of materials during physical transitions that are caused by phase changes, melting, oxidation, and other heat-related changes [62-64].

Typically, a DSC experiment involves the heating and/or cooling of a sample pan using a specified heating and/or cooling rate, relative to a reference (empty) pan in a non-reactive environment enforced by a purge gas (such as nitrogen). Figure 2-15 provides a schematic outlining the DSC methodology. Each pan is placed on a heater; both heaters

are required to heat the pans at identical rates. The heater under the sample has to supply more energy and provide more heat than the one under the empty reference pan. The difference in heat generated between the two heaters, which is termed heat flow, is then plotted verses temperature/time [62-64].
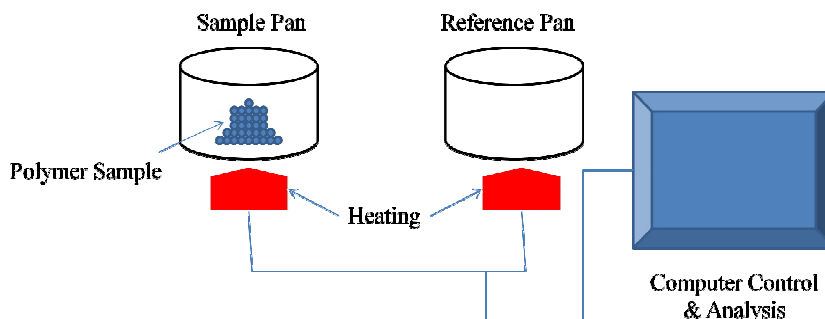
Figure 2-15: Schematic outlining the DSC procedure

DSC can be used to find the heat capacity of a certain material or substance, this is the amount of heat required to raise the temperature of the investigated material by 1 degree. Heat capacity is mathematically defined as follows [62-64]:

First, the value of heat flow is represented by:

$$\frac{heat}{time} = \frac{q}{t} \qquad \left[\frac{Joules}{Second}\right] \qquad (2.13)$$

However, the heating rate is given by:

$$\frac{Temp.Increase}{time} = \frac{\Delta T}{t} \qquad \left[\frac{^{\circ}C}{s}\right] \qquad (2.14)$$

Finally, heat capacity is described as:

$$C_P = \frac{heat\ flow}{heating\ rate} = \frac{q}{\Delta T} \qquad \left[\frac{J}{^{\circ}C}\right] \qquad (2.15)$$

This is essentially the amount of heat (e.g., [J]) per unit temperature (e.g., [°C]).

Several material properties could be found by observing a DSC curve. The first parameter is the glass transition temperature T_g of a substance. Below this temperature, the polymer is hard and brittle, while above it, the polymer becomes soft and flexible. Some polymers are used below T_g like polystyrene ($T_g \approx 100$ [ºC]), which is used in applications like computer casings and model vehicles. T_g is indicated on a DSC curve by a step (observe Figure 2-16), which includes an increase in heat flow and heat capacity of a material [62-64].
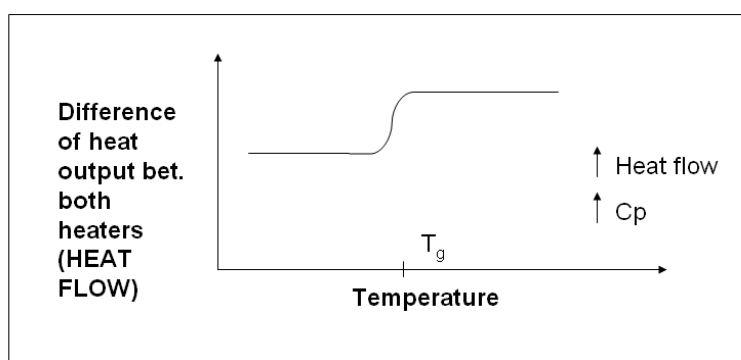
Figure 2-16: Glass Transition Illustration

Glass transition occurs in amorphous or partially amorphous polymers; that is materials with chains that are not ordered into crystals.

As a polymer is heated further in the DSC, a large dip in the curve is observed. This phenomenon denotes the polymer's melting phase. The temperature at which this change in the curve starts is called the onset melting temperature, while the peak of the dip is conventionally known as the polymer's melting temperature T_m. Melting occurs in crystalline or semicrystalline materials and is explained by the falling of the polymer atoms from their order and the collapsing of the crystalline structure. Melting is an endothermic phenomena as it absorbs heat from the environment. Hence, during melting, the heater under the sample will be required to provide even more heat to keep the

desired rate. The area under the melting curve is called the latent energy of melting, which is the energy that is absorbed when the substance undergoes a physical phase change without change in temperature. Figure 2-17 illustrates the melting phenomena emphasized with using a DSC-generated curve [62-64].
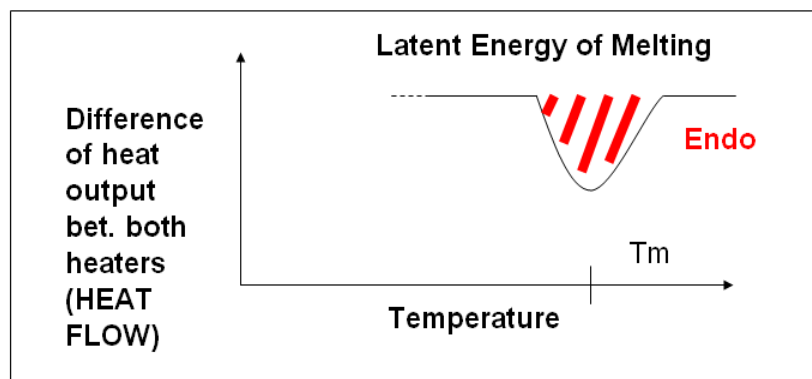
Figure 2-17: Melting phenomena represented by a DSC curve

After the material is heated beyond its melting temperature and held isothermal for a period of time to ensure that any previous thermal history is completely erased, the sample is then cooled at a specified rate. During cooling, a peak is observed. This peak corresponds to the crystallization phase of the investigated material. Before this phase, polymer atoms move around frequently, in an attempt to be arranged in an ordered setup, until the crystallization temperature is reached. At this temperature, enough energy has been gained by the polymer for the atoms to be arranged in crystals. Crystallization is an exothermic process, and the area under the crystallization curve represents the latent heat of crystallization. This is the energy released when the material undergoes a phase change. Figure 2-18 demonstrates the DSC view of the crystallization phenomena [62-64].
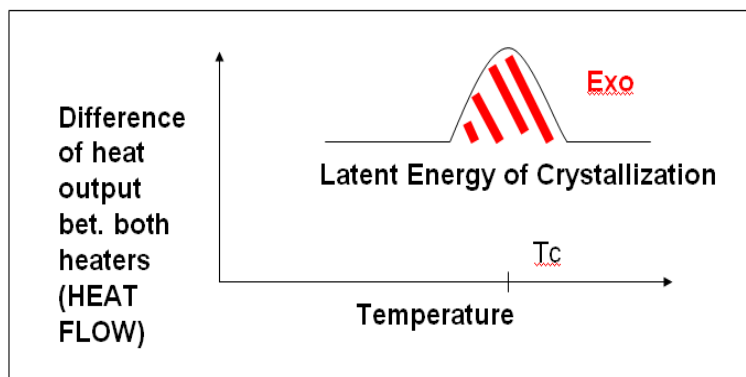
Figure 2-18: Crystallization Phenomena

One of the important factors that could be determined using DSC is the degree of crystallinity of a polymer. This is analytically determined by first determining the latent heat of melting $\Delta H_{melting}$ and the latent heat of crystallization $\Delta H_{crystallization}$ using the area under the melting and crystallization curves, respectively [62-64]:

$$\Delta H_{melting} = \frac{heat\,flow\_melting}{mass\,of\,material} \cdot temperature \qquad \left[\frac{J^o C}{g.s}\right]$$

$$\Delta H_{crystallization} = \frac{heat\,flow\_crystallization}{mass\,of\,material} \cdot temperature \qquad \left[\frac{J^o C}{g.s}\right] \tag{2.16}$$

Hence, the percentage of crystallinity is given by:

$$\%crystallinity = \frac{\dfrac{\Delta H_{melting} - \Delta H_{crystallization}}{H_{melting}^*}}{total\,sample\,mass} \bullet 100 \tag{2.17}$$

Where: $H_{melting}^*$ is the amount of heat absorbed by one gram of material during melting.

Thermogravimetric Analysis (TGA)

TGA measures weight changes in a material as a function of temperature (or time) under a controlled atmosphere [65-67]. TGA utilizes heat to measure the occurrence of reactions and physical changes in materials. This allows the measurement of the mass

change associated with transition and thermal degradation. TGA is also capable of recording change in mass resulting from dehydration, decomposition, and oxidation of a sample with time and/or temperature. Typical applications are those that require the measurement of the thermal stability and composition of a material [65-67].

The conventional TGA apparatus is mainly formed of a sensitive balance, a furnace, a sample handler, a thermocouple, and an inert purge gas. The system is controlled through a software program that accepts input from the user and regulates the experimental process accordingly. Figure 2-19 shows a schematic outlining the main components of a TGA [65-67].
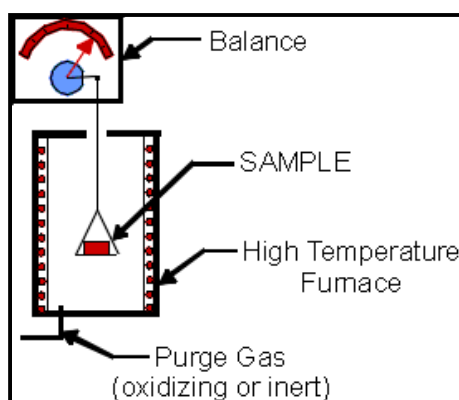
Figure 2-19: Main components of a Thermogravimetric Analyzer

A TGA experiment starts by weighing the evaluated sample, inputting the weight into the software, and then placing it in a sample pan. The sample pan is made from an inert material, for example platinum, which promotes a nonreactive environment. The sample pan is then placed in its location on the apparatus and the experimental procedure is setup using the controlling software. Upon starting the experiment, the balance monitors the weight of the sample, which is recorded at time intervals using the aid of the software.

Figure 2-20 illustrates a sample plot generated using the TGA Q50.
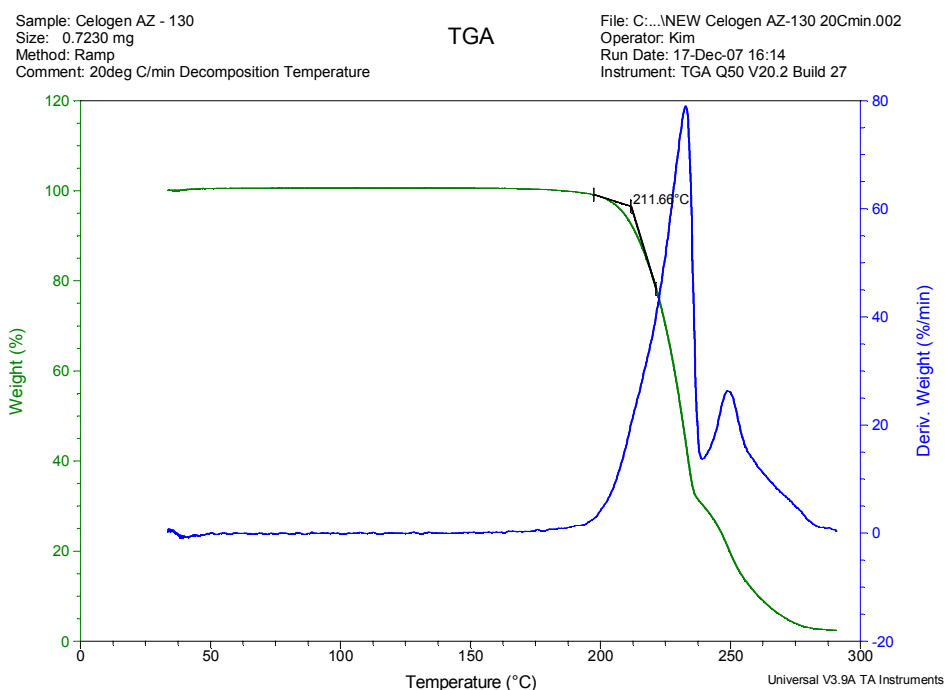
Figure 2-20: TGA sample plot

The material evaluated is a chemical blowing agent (CBA) of type Celogen AZ. It can be observed that the weight percent is plotted against the temperature change. The decomposition temperature of the CBA as shown on the plot is about 212 [°C] and the weight of the sample approaches zero as the decomposition process is fully completed; measurements obtained from the plot are performed using the peak integration tool in the TA Thermal Advantage Software. The results shown are typical of the CBA, as it decomposes to release gas within this temperature limit. The blue curve shown on the plot represents the change in weight percent over time, which has a peak with the onset temperature of 212 [°C].

2.3.3 Polypropylene: Structure and Properties

Generally, polymerizing propylene, a gaseous byproduct that results from refining petroleum, yields polypropylene (PP) [68,69]. The polymerization procedure occurs in appropriate reactors under precise temperature and pressure profiles. Catalysts are used to provide a site for the reaction to occur; the general form of the polymerization process is illustrated in Figure 2-21.
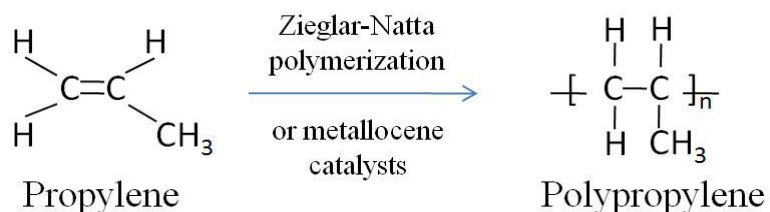
Figure 2-21: Polymerizing of propylene [68,69]

The definition and form of the polymer PP were susceptible to radical developments after 1950, with the Ziegler-Natta discovery of catalysts capable of synthesizing stereoregular PP, that is PP molecules that have definite three-dimensional patterns [68-71]. In principle, the discovered catalyst system regulates the way by which a monomer and a growing chain approach each other during the polymerization process [69]. Furthermore, the chemical nature of the catalyst governs the specific orientation by which the propylene monomer adds to the polymer chain (stereospecifity) [68,69]. Prior to this discovery, the preliminary form of polymerized propylene was comprised of a branched low molecular weight oil of little applicability.

PP Tacticity

PP tacticity is an indicator of the arrangement and orientation of methyl groups attached to alternate carbon atoms within a respective chain; such characteristic is significant as it provides information about the physical properties of a particular PP material [60,61,68,69].

Isotactic PP (i-PP) is the most common commercial form of PP, where pendant methyl groups are all in the same configuration and side of the polymer chain. Figure 2-22 illustrates a portion of a PP chain exhibiting such attributes. Isotactic PP is a semicrystalline solid, it exhibits the highest crystallinity among other PP configurations; this imposes good physical, mechanical, and thermal properties [60,61,68,69].
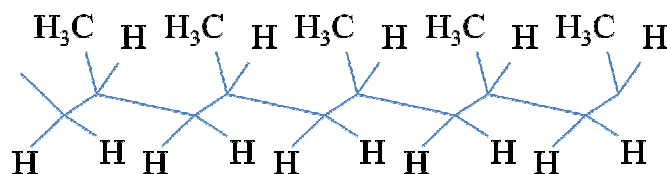
Figure 2-22: Isotactic PP (i-PP) structure and arrangement [68]

Syndiotactic PP (s-PP) this type of PP structure is produced commercially using metallocene catalysts, which are coordination compounds consisting of transition metal ions such as Zr or Ti with one or two cyclopentadienyl ligands. Syndiotactic PP it has alternate pendant methyl groups on opposite sides of the polymer backbone, with opposite configurations. Figure 2-23 illustrates a portion of a PP chain exhibiting such attributes. This arrangement dictates less stiffness than an i-PP but better impact and clarity properties [60,61,68,69].
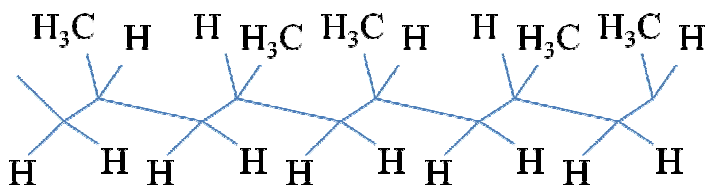
Figure 2-23: Syndiotactic PP (s-PP) structure and arrangement [68]

Atactic PP (a-PP) in this type of PP, the pendant methyl groups are randomly arranged about the polymer backbone. Figure 2-24 illustrates a portion of a PP chain exhibiting such attributes. This arrangement dictates the least crystallinity among all PP arrangements, resulting in is an amorphous and sticky form of PP used in applications like adhesives and roofing tars [60,61,68,69].
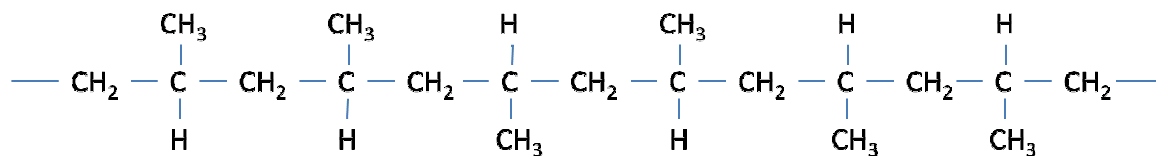
Figure 2-24: Atactic PP (a-PP) structure and arrangement [68]

Polymerization Catalysts

Catalysts are substances, typically comprising organometallic transition metal complexes, which increase the rate of the reaction while enduring no change in their chemical state. There are two commonly used catalysts developed for PP polymerization; Ziegler-Natta catalysts (multi-sited catalysts), and metallocene catalysts (single-sited catalysts) [60,61,68,69].

In their preliminary form (1950s), Ziegler-Natta catalysts were comprised of transition metal halides (e.g., $TiCl_3$) mixed with an organometallic compound (e.g., triethylaluminum). Such catalyst composition initially yielded PP grades that are only 30-

40% isotactic. Further development raised the isotacticity to 80% (1960s), along with a need to perform a secondary processing operation to remove catalyst residues. Typical isotacticity magnitudes achieved nowadays can reach about 95%, improvements included enhancing the reactivity of the used transition metal halides to increase the active sites present during polymerization as well as the introduction of supporting heterogeneous catalysts (e.g., $MgCl_2$) and Lewis base constituents (e.g., the benzoic acid ester), which aid in achieving higher stereospecificity and terminate the need to remove catalytic residues [60,61,68,69].

Metallocene catalysts are organometallic compounds (e.g. Fe, Ti, Zr), with a sandwich like spatial arrangement and identical active sites, placed between two cyclic organic compounds. The present constituents of metallocene catalysts comprise $ZrCl_2$ as the transition metal with cyclopendadiene and an aluminoxane; such catalysts are commonly used to generate the commercial form of s-PP [60,61,68,69].

Molecular Weight Distribution and Melt Flow Rate

Polypropylene has an average molecular weight (M_w) between 220,000 and 700,000 [g/mol]. Generally, longer PP chains have higher molecular weight and lower melt flow index (MFI) values; PP MFIs range between 0.3 and 1000 [g/10 min]. Higher molecular weight implies increased toughness and melt strength, which results in better impact resistance, elongation, and reduced moduli, strength, haze, and crystallization temperature [60,61,68,69].

In terms of applications, PP grades with MFIs less than 2 [g/10 min] are used for extrusion related and foaming purposes (foaming, blown film, etc.), where high melt

strength is required, while PP grades with higher MFIs are used in coating, injection molding, and fiber spinning applications.

The molecular weight distribution (MWD) is the ratio between M_w, the average molecular weight, which represents the weight of a polymeric chain at a given molecular weight, and M_n, the number average molecular weight, which represents the number of polymer chain molecules at a given molecular weight. The MWD range for PP is between 2 and 11. PP can either have a narrow MWD, with molecular chains exhibiting the same length, or a broad MWD, when such chains greatly vary in length. Shear sensitivity of molten PP is highly affected by the nature of the MWD; Figure 2-25 illustrates a plot entailing the viscosity of PP as a function of the applied shear rate.

A. Broad Molecular Weight Distribution
B. Narrow Molecular Weight Distribution
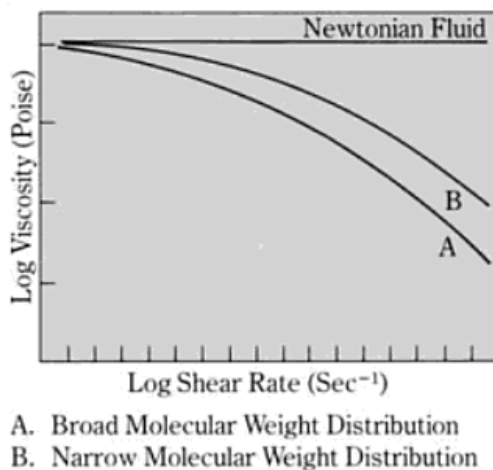
Figure 2-25: Shear sensitivity of molten PP [68]

When analyzing the figure, it is evident that PP grades with broad MWDs are more sensitive to shearing than these exhibiting narrow MWDs, which makes them suitable for usage with processing technologies that require extensive and complex shaping operations such as injection and blow molding. On the contrary, narrow MWD PP grades are more suitable for extrusion and fiber spinning applications [69].

Morphology vs Characteristics

The morphology of respective PP structures highly affects their pertinent characteristics. Parameters like the melting and glass transition points, mechanical properties, and haze and sterilization levels can be investigated with respect to morphological qualities by using thermal analysis methods and other techniques. A major morphological attribute that directly influences the mentioned parameters is the degree of crystallinity. An increased crystallinity level in materials corresponds to higher strength, chemical resistance, melting point, and opaqueness. In principle, this is due to the increased order imposed on the arrangement of the crystals. Amorphous materials, on the contrary, are formed of crystalline regions surrounded by disordered, spaghetti like, amorphous structures with entangled polymer chains; these are characterized as tougher, more ductile, and transparent materials [60,61].

As thermoplastic polymers with crystalline content melt, the arranged crystal structure deteriorates, and then starts reforming again at a point during the cooling process when the onset recrystallization temperature is reached. Melting temperatures tend to be higher with increased polymer crystallinity; this is due to the larger number of crystals destabilized in order to achieve melting. Quantitatively stating, perfectly i-PP sustains a melting temperature of 171 [^{o}C], while the commercial form of i-PP has a melting temperature that merely ranges between 160-166 [^{o}C], such notable reduction pertains to the presence of an amorphous (atactic) phase along with the crystalline phase that signifies i-PP. Moreover, when the amorphous phase is dominant, as in the case of s-PP grades (only 30% crystalline), the melt temperature can reach as low as 130 [^{o}C].

The glass transition temperature is the temperature at which an amorphous material content becomes brittle on cooling or soft on heating. PP grades experience glass transition at a temperature range between -35 and -26 [^{o}C], attributing to the amorphous constituency. Theoretically, above glass transition temperatures, polymer chains are permitted to vibrate within the free volume resulting from the non-orderly nature of amorphous regions, and as glass transition temperatures are reached, such action is confined or restricted, causing material brittleness and demoted impact resistance properties [68,69].

The mechanical properties of PP are radically influenced by the magnitude of crystallinity. Increased crystallinity is associated with increased stiffness, yield stress, and flexural modulus, in addition to reduced toughness and impact endurance. For instance, the assessment of the flexural modulus of highly crystalline PP yielded values up to 2500 [MPa], while for low crystallinity PP, analogous values reached a maximum of only 1600 [MPa] [68,69].

Oxidation, Degradation, and Chemical Resistance

Non-stabilized PP resin is highly susceptible to oxidation/degradation at typical processing temperatures, this has been ascribed to the reactive nature of the tertiary hydrogen on the carbon atom bonded to the pendent methyl group within PP's chemical structure. The oxidation process is commonly referred to as "chain scission", this is due to the incurred reduction in molecular weight resulting from splitting the respective PP chains to shorter ones [72,73]. Oxidation/degradation demotes PP's mechanical properties and substantially increases its deformation under loading. Main factors that

cause degradation include exposure to extreme mechanical stress, elevated heat, or possibly polymerization deficiencies [72,73].

The constituents of PP are only nonpolar atoms, i.e., carbon and hydrogen. In terms of chemical resistance, this allows it to resist chemical attacks imposed by polar chemicals like soaps, oils, or alcohols. Yet swelling, degradation, and softening of PP can be caused by means of nonpolar chemicals such as hydrocarbons or chlorinated solvents [68,69].

PP Commercial Forms

There are three main commercial forms of PP; homopolymer PP, random copolymer PP, and block copolymer PP [60,61,68,69].

Homopolymer PP is the most widely used PP material; it is made from a single monomeric precursor and has a semi-crystalline structure that results from the stereospecific linking of propylene monomers. The semi-crystalline nature of homopolymer PP dictates the presence of two phases within its structure; an amorphous phase and a crystalline phase. The amorphous phase is formed of an i-PP and an a-PP, with the i-PP crystallizing during processing. Primary applications of homopolymer PP grades include extruding it to form fibers and filaments for upholstery, carpet, etc., thermoforming it into packaging containers and structures, and injection molding it to form appliances, hardware, furniture, toys, etc. [68,69].

Random copolymer PP is formed by polymerizing propylene and a low percentage of ethylene, 1-butene, or 1-hexene (7% or lower) as co-monomers in the same reactor. This conjunction results in improved impact properties of random copolymer PP over homopolymer PP. Random copolymer PP is similar in structure to i-PP, however,

the comonomer units disrupt the stereoregular arrangement of propylene molecules and cause an affect similar to increasing atacticity; that is, an apparent decrease in crystallinity and increase in polymer chain mobility. Random copolymer PP grades have a reduced melting temperature and specific gravity; typical grades are used in applications pertaining to films, blow molding (e.g., bottles), and injection molding (e.g., food containers) that require high clarity and low impact strength.

Impact copolymer PP grades are physical mixtures of homopolymer PP and random copolymer PP formed in a cascading manner within the reactors by means of metallocene catalysts. Ethylene content in the overall mixture is usually between 6-15 [wt%], however it forms 40-65 [wt%] of the random copolymer content. Increased ethylene enhances the impact properties at the expense of stiffness. Impact copolymer PP grades are mainly used in the injection molding of parts associated with appliances, automobiles, packaging, furniture, etc. [68,69].

2.3.4 PP foams: Related Studies

This section summarizes the devised methodologies and previous studies performed to achieve PP foams throughout the available plastics processing technologies. Although a variety of publications investigate the respective matter, the findings still remain relatively limited, with respect to other polymers like PE and PS, this is typically due to the melt rheology drawbacks, with respect to foaming, associated with PP.

In 1972, Parrish disclosed a process by which low density closed-cell PP foam sheet (cell diameter: at least 500 [μm]) was prepared by flash extrusion with reduced bubble nuclei formation [74]. In his experiments, Parrish mixed an i-PP grade, namely PF 6623, with foaming agents like florotrichloromethane and dichlorotetrafluoromethane in

appropriate quantities. Two extruders were used for preparation purposes, one for melting PP and the other for mixing it with the foaming agent along with cooling the achieved blend. The resultant blend was foamed and pumped at respective designated foaming temperature and pressure values (typically 140 [^{o}C] and 600 [PSI]), through a third extrusion based operation, into a die that formed continuous extruded PP foam sheets [74].

In 1973, Harada *et al.* developed a more efficient method to extrude foamed PP sheets made from a composition comprising crystalline and non-crystalline PP, PE, and a CBA. The constituents, less the CBA, were compounded in an extruder and then formed into pellets. The pellets in turn were mixed with the CBA in a second extruder at designated temperatures to form a foam sheet with high impact resistance and good texture [75].

In 1981, Ueno *et al.* prepared an enhanced PP formulation for foaming purposes from constituents comprising highly crystalline PP resin kneaded with 1,2 polybutadiene resin (1,2 PB), mixed with hot xylene, and a blowing agent [76]. The presence of 1,2 PB allows PP to be extrudable over a wider range of foam processing temperatures, and diminishes the irregularities in foam by enhancing the strength of the PP melt.

Fukushima *et al.* published a patent in 1985 [77]. The invention introduced a method to extrude highly expanded PP foams with improved melt strength and free from unevenness in surface by using a PP resin having a specified melt tension. In this "material-enhancement" based invention, the particulars of the blend used are such that it comprises a PP resin with a melt tension value of 3 [g] or more at 190 [^{o}C] and a maximum/minimum melt ratio of 2.5 or less fed into an extruder after mixing with a

volatile foaming agent and two or more of high and low density PEs, PB-1, ethylene vinyl acetate copolymer, styrene-butadiene rubber, ethylene-ethyl acrylate, and others. The resulting PP blend exhibits minute variance in viscosity, which gives an extruded product having melt strength suitable for foaming, such that cells can be uniformly formed without breakage at high expansion ratios [77].

Recent developments in PP resins capable of achieving desired foaming were commenced by resin manufacturers such as Montel (PP grade Higran, U.S. Patent No. 7,049,524) and Borealis (PP grade Dapoly HMS) [6]. Increasing the melt strength of the polymer is now typically attained by introducing long chain branching into the normally linear chain structure. This results in resins exhibiting high melt strength and strain hardening, which allows the cell walls to stabilize without rupture upon achieving expansion [6].

Prior efforts to devise processing tactics that achieve different polymeric foams utilizing rotational molding have been discussed earlier in this chapter. Nevertheless, processing PP foams in rotational molding was not explicitly disclosed until the year 2000, when the first patent entailing a rotational molding processing methodology to achieve PP foams was introduced by Park *et al.* [78]. The proposed process entailed first melt compounding a suitable CBA with a PP resin of selected rheological properties in an extrusion based operation and then introducing the resulting blend in pellet form to a mold, attached to a rotational molding setup, and then instigating the rotational molding cycle. This is achieved by the selection of a CBA and a promoter to release foaming gas into the PP resin at a temperature which is high enough to eliminate undesirable effects of

poor sintering, but low enough to avoid foaming the resin when its melt strength is too weak to support proper cell formation [78].

PP Foams: Conclusions

The literature examined in view of processing PP foams provided an outline of the main difficulties binding the process as well as a variety of methods, to consider these difficulties, via process or material based strategies. It was concluded that the principle challenge in processing PP foams lies in the intricacy of controlling and retaining the desired cell size due to the weak material melt strength and the low solubility of gases in PP. The processing of quality integral-skin PP foams in rotational molding is particularly involved, which often creates undesirable outcomes such as a premature decomposition of blowing agents, which can demote the skin uniformity by foam invasion into the skin, which in turn deteriorates the skin-foam interface.

2.3.5 Blowing Agents

In the realm of foam applications, a blowing agent (also referred to as foaming agent) is an additive material, which brings about a reduction in polymer density by the introduction of gas cells [73]. There are two groups of blowing agents; physical blowing agents (PBAs) and chemical blowing agents (CBAs) [6,52,68,73].

PBAs are compressed gases or volatile liquids introduced to the polymer at selected instances of the foaming process. Compressed gasses are injected into the polymer melt under high pressure, and as the pressure is relieved, the gas becomes soluble in the polymer and forms bubbles. N_2, air, and CO_2 are typically used. Volatile liquids on the other hand are promoted to change state –from liquid to gas- when heated

at the selected processing temperatures. Volatile blowing agents are organic chemicals in nature; examples include hydrocarbons (HC), chlorofluorocarbons (CFC), hydrochlorofluorocarbons (HCFC), and hydrofluorocarbons (HFC). Recently, the usage of such liquids has been confined to limited applications due to the adverse effects that they impose on the environment, in other applications they have been replaced by more ecologically friendly aliphatic hydrocarbons like pentane, butane, and propane [5,6,52].

The selection of PBAs in foaming applications is reliant on several factors. These include: the PBAs environmental acceptability; its toxicity, flammability, and compatibility with the used plastic; its boiling point, solubility properties, molecular weight, and vapor pressure in the used temperature range [5,6,52].

CBAs are solid compounds, organic or inorganic, mostly provided in powder form, which decompose at processing temperatures to liberate gas that forms cellular structures [32]. CBAs can be classified into two main categories; endothermic CBAs, which require energy during decomposition and typically release CO_2 along with minor portions of other gases, and exothermic CBAs, which release energy during decomposition and typically release N_2 and with minor portions of other gases upon decomposition. The most popular CBAs for plastics usage include: ABFA, azidocarbonamide (AZ), or 1,1-azobisformamide (exothermic, typical decomposition range: 204-213° C); OBSH, p-p'-oxybis, or benzenesulfonyl hydrazide (exothermic, 157-160 [$^{\circ}$C]); TSSC or p-toluene sulfonyl semicarbozide (exothermic, 228-236 [$^{\circ}$C]); 5-PT or 5-phenyltetrazole (endothermic, 238-249 [$^{\circ}$C]) [6,32,52,68].

Selecting CBAs for a particular polymer foaming process is based on several factors related mainly to the used polymer and process. The most important factor is the

compatibility of the decomposition temperature range of the CBA with that of the polymer processing. Other factors include the gas liberation; that is the volume of gas generated per unit mass of CBA used, the rate of gas release, the particle size of the CBA, and the shape and form of the end-use product [6,32,52,68].

2.4 Concluding Remarks

This chapter provided a thorough discussion, based on a conducted literature review, of the pertinent background and theory involved in devising the solutions to the engineering problems treated by the performed research and experimental work. Topics covered included a variety of fundamental aspects related to rotational molding, rotational foam molding, extrusion, and relevant materials such as polymers and CBAs.

Next, Chapter 3 discusses the particulars binding the evolution of the proposed solution that was generated based on a careful consideration of the investigated theoretical and methodical aspects.

Chapter 3: Design and Development of a Novel Technology and its Respective Experimental Setup

3.1 Problem Statement

The manufacture of rotational moldings with a distinct non-foamed outer skin that encapsulates entirely a foamed core or layer requires both non-foamable and foamable plastic resins to be charged into the mold within the same rotational molding cycle. As discussed in Section 2.2.2.6, this could be achieved in the conventional practice either by interrupting the molding process, or continuously, in a single-shot fashion by charging the mold with predetermined quantities of both non-foamable and foamable resins simultaneously at the outset of the cycle, so that the use of drop boxes or plastic bags becomes unnecessary [1,5,11,17-19, 24-26].

In comparison with plastics processing technologies such as blow molding and thermoforming, which are used to manufacture comparable end-products, the greatest disadvantage of the rotational molding process is its lengthy cycle time. The cycle time is long due to the inherent nature of the process, which requires the temperature of the rotated mold to be elevated from room temperature to beyond the melting temperature of the enclosed plastic, for shaping to take place, and then cool it back to room temperature [1,5,11,17-19, 24-26]. The cycle duration is prolonged further as rotational molding is used to process articles with an integral-skin foam core/layer; this is due to the insulative effects of the foam, which hinder the real-time control of the processing entities.

In addition to the lengthy cycle times, integral-skin foam moldings achieved using the conventional practice often incur events when the decomposition of the CBA occurs prematurely; compromising the skin thickness uniformity and at times causing the invasion of the foam structure into the skin layer, weakening the skin-foam interface. These undesirable incidents demote the overall quality of the generated moldings, deteriorating their mechanical properties, buoyancy, and aesthetics.

3.2 Extrusion-Assisted Rotational Foam Molding (EARFM)

The research related to developing the EARFM process was primarily motivated by the important need for overcoming the fundamental disadvantage of rotational foam molding process; its length cycle times. This is in order to improve the quality of the manufactured moldings and increase the efficiency of the process. Thus, the fundamental rationale of EARFM relies on the fact that it would be definitely desirable to decouple the heating segment of the process by introducing a much more efficient plastic fabrication method, such as extrusion.

Conversely, unlike the prior practice, which requires the foamable resin to be produced in a remote extrusion-based melt compounding operation involving a carrier resin and a CBA to produce decomposition-free foamable solidified pellets, in this extrusion-assisted processing concept, non-chilled foamable extrudate is directly introduced into a uni-axially rotating hot mold via a specially designed "injection" port, subsequent to which it is further heated to trigger the decomposition of the CBA for foaming, and then externally cooled to solidify the product and prepare it for removal.

Figure 3-1 depicts the EARFM processing concept in the form of a flow chart. The operating principle of the EARFM technology can be described as follows: first, a

non-foamable resin is inserted into the mold. The mold is then closed, rotated bi-axially, and heated in an oven at a desired temperature for a period of time to accomplish the formation of the solid skin.
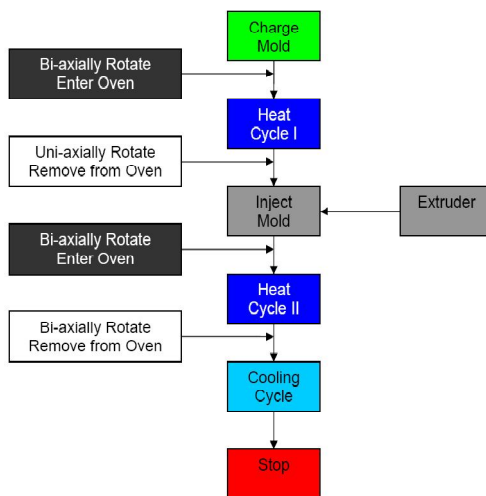
Figure 3-1: EARFM processing flow chart
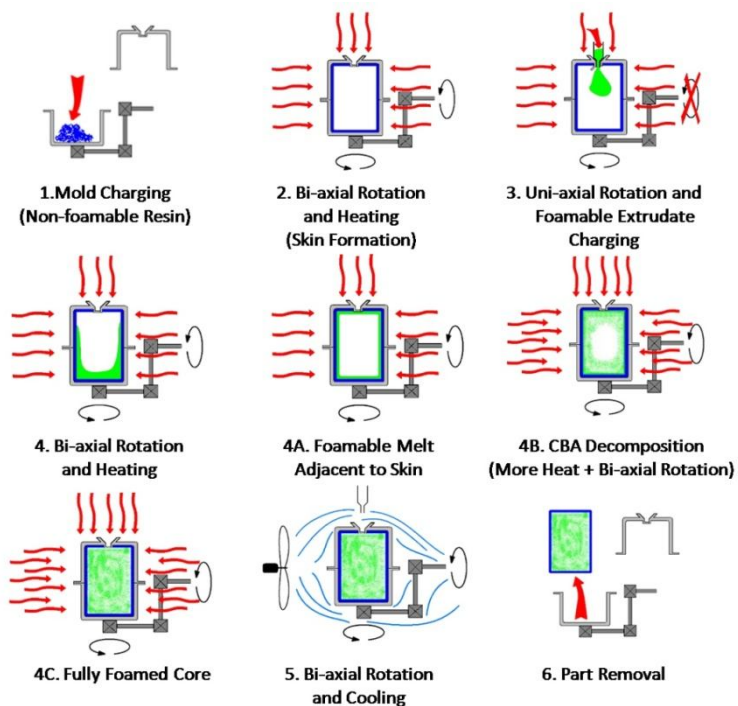
Figure 3-2: Operating principle of EARFM

The mold is removed from the oven, kept hot, and its rotation is switched to a uni-axial mode in order to allow its coupling with an extruder, this is to enable the direct injection of an appropriate amount of foamable extrudate within the preformed non-chilled skin boundaries. Afterwards, the mold rotation is switched to a bi-axial mode and the mold is inserted back into the oven at a desired temperature for an appropriate time period to trigger the decomposition of the CBA. Upon the completion of forming a foam core within the solid integral-skin, cooling takes place, and the obtained solidified integral-skin cellular part is removed from the mold. The described operating principle is schematically represented throughout Figure 3-2, with respect to producing a skin-surrounded foamed article.

The EARFM process was a preliminary remedial solution that was developed with a sole purpose to treat the lengthy cycle times associated with the conventional rotational foam molding process. The next section provides an overview of the design and engineering methodologies used to achieve the experimental setup that closely mimics the EARFM processing technology.

3.3 Design of the Experimental Setup

3.3.1 Overview

In order to assess and experimentally verify the advantages of EARFM versus the conventional rotational foam molding technique, it was essential to design and develop a fully-functional prototype apparatus that efficiently combines extrusion with rotational molding to serve as an experimental setup. In this context, an industrial-grade, custom-made, heavy-duty, lab-scale, semi-automatic, experimental setup dedicated for EARFM

has been successfully designed, developed and built. Altogether, the experimental setup combines five main components: an extruder, a bi-axially rotating mechanism, a mold, an oven, and a system that allows the integration of these components to perform the process.

The design, construction, experimental, and developmental work of the experimental setup was completed, collaboratively, by an engineering team. A chart presenting the hierarchical division of the project tasks among the project team members, as well as the identity/designation of each of the members at the time of accomplishing the respective tasks is presented in Figure 3-3.
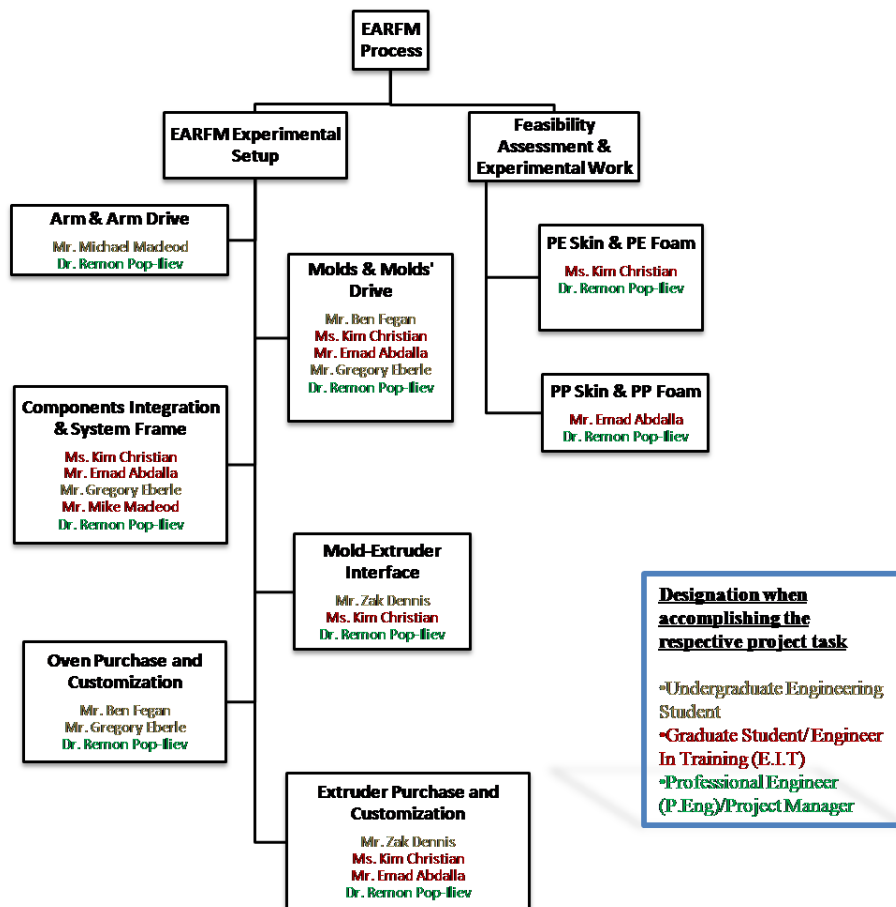
Figure 3-3: Project hierarchical division & engineering team identity

The complete design study in view of achieving an optimized system and component configuration is now presented.

3.3.2 Principal Functional Requirements and Design Parameters

A global set of functional requirements (FRs) and the corresponding design parameters (DPs) pertaining to each component in view of accomplishing the EARFM experimental setup are presented in this section.

FR #1: A plastics processing apparatus that is capable of continuously melt compounding CBAs with thermoplastic resins. This apparatus must have a heated nozzle that allows sealing its tip upon an input signal from the user; this is to prevent the leakage or waste of the compounded melt at stages of the process when not in use. The apparatus must also have a control system with adjustable processing parameters

DP #1: The extruder is the most suitable device to achieve the required functions. Thus an extruder is to be selected based on further decomposition of functional entities.

FR #2: A mechanical device that is able to rotate the used mold both uni-axially and bi-axially in a manner such that one rotation is about the central axis of the mold and the other rotation is about an axis perpendicular to it. Furthermore, such rotations must be independent of each other and separately controllable; this is to provide adjustability when running experimental trials. The device components must withstand high temperatures due to heating and must also fit within the boundaries of the heating apparatus (the oven) during the mold heating process. The device should operate safely within the workspace in order to preserve the wellbeing of the users.

DP #2: A bi-axially rotating arm comprised of a shaft concentric with another shaft, with two distinct drive systems, is capable of achieving the indicated functional requirements.

FR #3: A plastic shaping tool that capable of withstanding high processing temperatures and is easily permanently attachable to the rotational drive system on one end and temporarily attachable to the extruder output nozzle at the other end while rotating uni-axially is to be designed. The tool must include an interfacing mechanism that will allow injecting the foamable extrudate within the boundaries of the already formed non-chilled solid skin without damaging it. A venting system must be provided to avoid pressure buildup in the mold due to processing. The tool must be designed for ease of part removal once the processing sequence is completed. The material comprising the tool should be chosen so as to maximize heat transfer and minimize corrosion with the intention that the integrity of the surface finish of the molded part remains over extended period of use.

DP #3: The discussed functional requirements were translated to a design parameter that consists of a mold with a specially designed sealing valve, which allows the interfacing process to smoothly take place.

FR #4: A heating apparatus that exhibits proportional-integral-derivative feedback control (PID) with a simple user interface to program the desired temperature profiles must be selected and retrofitted to cope with the mold heating requirements. The apparatus must allow the entrance and exit of the rotating arm with the mold in a semi or fully-automated manner.

DP #4: A forced convection oven is to be selected, purchased, and retrofitted to accommodate the indicated functional requirements.

FR #5: A system that combines all the aforementioned design parameters must be devised, such that the adequate functionality of the experimental setup with respect to the EARFM process is accomplished in the most efficient manner.

DP#5: A global frame embracing the stationary and moving components is to be designed to attain an optimal implementation of the EAFRFM processing concept.

3.3.3 Engineering Target Specifications

Quality Function Deployment (QFD) techniques were used to translate the developed design parameters and functional requirements into an engineering specification that will in turn be used to design, dimension and shape the physical embodiments of the design parameters that will govern the engineered system. A House of Quality (HofQ) matrix was developed to correlate each subsystem under one set of requirements (Figure 3-4), whereas a separate HofQ was derived for each subsystem during the detailed design process. The use of this engineering tool aids in determining the targeted technical specifications, while comparing them to the functional ("customer") requirements and the current state of the art in this respect.
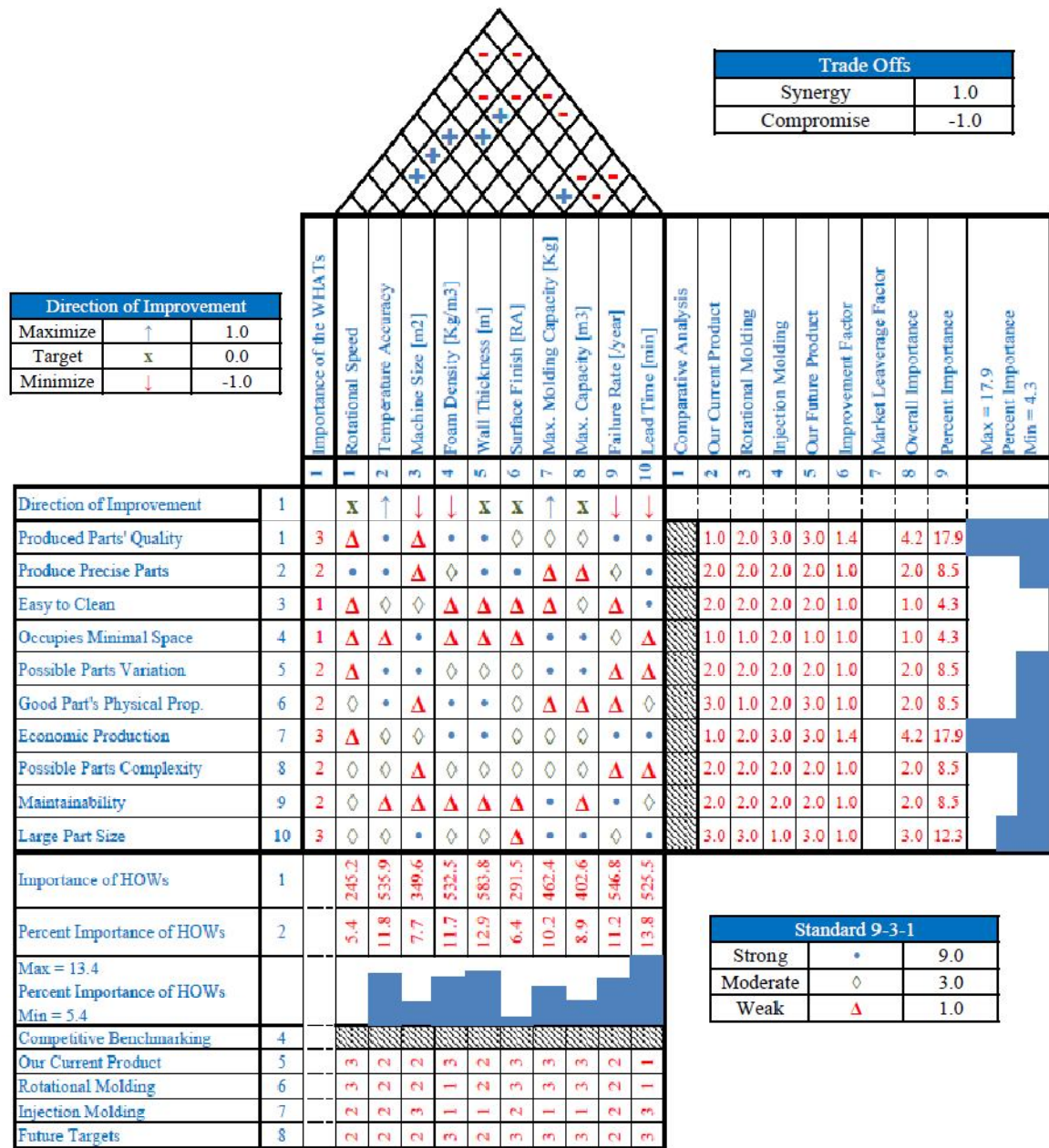
Figure 3-4: Global HofQ matrix

3.3.4 Concept Generation

Operator safety and device reliability, ease of function, fabrication, assembly and maintenance were the most important criteria considered for determining the favorable global processing layout concept that combines the physical equipment needed to

accomplish EARFM. Such layout will aid in interpreting the optimal sequence of processing steps, the configuration of the different components that comprise the designed system, and the custom embodiments that are required to allow safe and reliable equipment interactions.

Different processing layout concepts were generated, developed, and then evaluated. The achievement of this task at the outset of the design process allows defining the detailed objectives that govern the design or the selection of the system components. The final generated layout concepts are presented as follows:

Concept 1

Figure 3-5 depicts schematically a layout concept that has the oven in a fixed position while the arm-mold assembly and the extruder are free to translate linearly. Implementing the EARFM processing technology using this layout concept, the arm-mold assembly is first repositioned inside the oven for skin formation then translated out of the oven and coupled with the extruder by means of moving the extruder towards the arm-mold assembly for foamable extrudate introduction into the mold. Afterwards, the arm-mold assembly and the extruder are disengaged, and the arm-mold assembly is inserted back in the oven for further heating and consequently foam formation action. Mold cooling is subsequently employed and the part is removed from the mold.

Concept 2

Figure 3-6 depicts schematically a layout concept that comprises a stationary rotator, a translating oven, and a translating extruder. Implementing the EARFM processing technology using this layout concept entails repositioning the oven at the inception of the process to service the arm-mold assembly by heating the mold during bi-

axial rotation and forming the desired skin. The oven is then retracted and the extruder is translated towards the arm-mold assembly and promoted to fill the mold with the foamable extrudate. Once this step is accomplished, the oven is translated to enclose the mold for further heating in order to decompose the CBA and form the desired foam core within the preformed skin. Mold cooling is subsequently employed and the part is removed from the mold.

Concept 3

Figure 3-7 depicts schematically the third processing configuration concept that was considered. This concept relies on the translation of the arm-mold assembly to interact accordingly with the oven and the extruder, which are held stationary in place. Implementing the EARFM processing technology using this layout concept entails repositioning the arm-mold assembly towards the oven, after charging the mold with the nonfoamable skin resin, at the inception of the process to form the desired skin. The mentioned assembly is then translated from the oven towards the fixed extruder in order to acquire the foamable extrudate. Upon accomplishing this step, the arm-mold assembly is translated back into the oven for further heating to trigger and complete the foam expansion process. The mold is subsequently cooled and the part is removed.
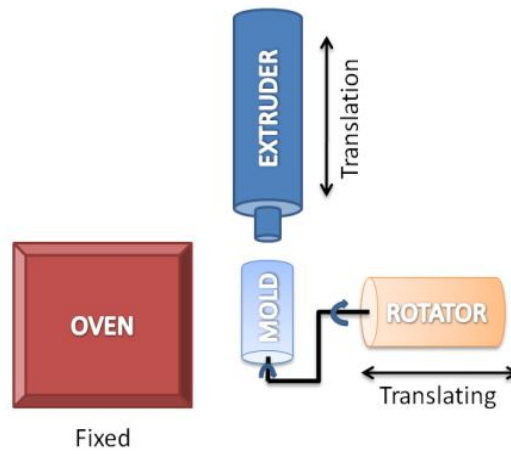
Figure 3-5: Processing Concept 1 – translating extruder and arm-mold assembly, fixed oven
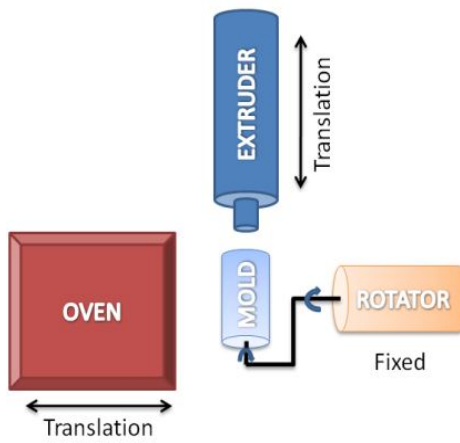
Figure 3-6: Processing Concept 2 – translating extruder and oven, fixed arm-mold assembly
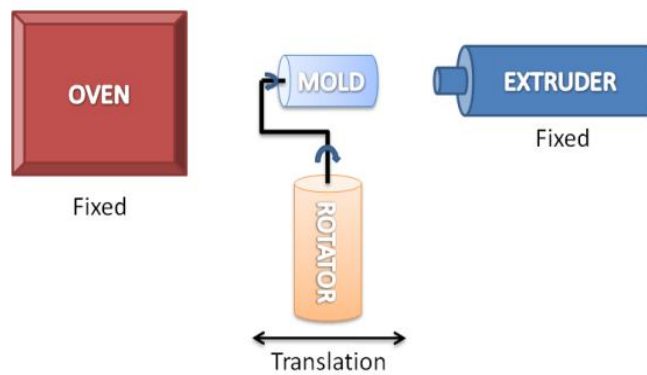
Figure 3-7: Processing Concept 3 – translating arm-mold assembly, fixed extruder and oven

3.3.5 Concept Evaluation

An advanced decision matrix (also known as belief decision matrix) approach was used to evaluate the generated layout concepts. This method relies mainly on calculating belief values, using assigned knowledge and confidence probabilities, that each concept will succeed in satisfying the established design criteria and others. The design criteria are stated next. The concept evaluation approach is thoroughly defined in [79]:

__Design Criterion 1__

The level of complexity associated with the concept. This includes the number of parts involved and the confidence and knowledge possessed by the designers with respect to the ability of each physical embodiment to repeatedly accomplish the desired function.

__Design Criterion 2__

The level of complexity of the functions achieved by physical embodiments associated with each concept. This includes the motion achieved by each components as well as the reliable functionality of the interacting components during the processing course.

__Design Criterion 3__

The access available to each of the processing equipment and components during the processing cycle and at assembly and maintenance procedures.

__Design Criterion 4__

Readiness of the concept for manufacturing, assembly, and maintenance

The resulting decision matrix is shown in Table 3-1. It indicates that Concepts 1, 2, and 3 had total satisfaction values of 66.79%, 70.14%, and 75.82%, correspondingly.

Table 3-1: Advanced decision matrix used to aid concept selection

| Criteria | Component | Importance (Sum = 100) | Belief Value - Concepts | | | Belief = p(k) x p(c) + (1-p(k)) x (1-p(c)) / p(k) - Probability based on knowledge / p(c) - Probability based on confidence |
			1	2	3	
Design Complexity (number of parts)	Oven	4	0.82	0.50	0.82	
	Extruder	4	0.52	0.52	0.82	
	Rotator Arm	6	0.50	0.82	0.58	
	Mold	6	0.50	0.82	0.58	
Function Complexity (motion/interaction/ process control)	Oven	6	0.91	0.50	0.91	
	Extruder	7	0.50	0.50	0.91	
	Rotator Arm	5	0.68	0.91	0.68	
	Mold	6	0.50	0.75	0.50	
Accessibility to System Components	Oven	6	0.50	0.82	0.68	
	Extruder	8	0.68	0.68	0.75	
	Rotator Arm	8	0.82	0.68	0.82	
	Mold	8	0.82	0.68	0.82	
Readiness for Manufacturing, Assembly, Maintenance	Oven	4	0.91	0.50	0.91	
	Extruder	6	0.50	0.50	0.91	
	Rotator Arm	8	0.75	0.91	0.75	
	Mold	8	0.75	0.91	0.75	
Total Satisfaction = Σ (Importance • Belief)			66.79	70.14	75.82	

Based on the presented results, Concept 3 was selected for the final layout design of the EARFM experimental setup. This choice was based on several reasons. First, the arm is the easiest component to move due to its relatively low weight and simpler electrical and material delivery connections. In addition, this layout provides the best access to all components; this is an important factor since this system is intended for research use, which requires continuous adjustments of operational parameters as well as the integration of new components as required. The chosen layout also requires the lowest motion accuracy, since it is only necessary to translate the arm and control its position while keeping all other subsystems fixed. Moreover, the incorporation of cooling equipment with the chosen setup is simple compared to other concepts.

3.3.6 Experimental Setup Final Design

This section focuses on the design parameters and details devised for each of the components comprising the experimental setup used to implement the EARFM processing technology. A CAD representation of the experimental setup assembly is displayed in Figure 3-8 below. The comprising components include an arm and mold assembly, a carriage attached to a translational mechanism, an extruder, and an oven.
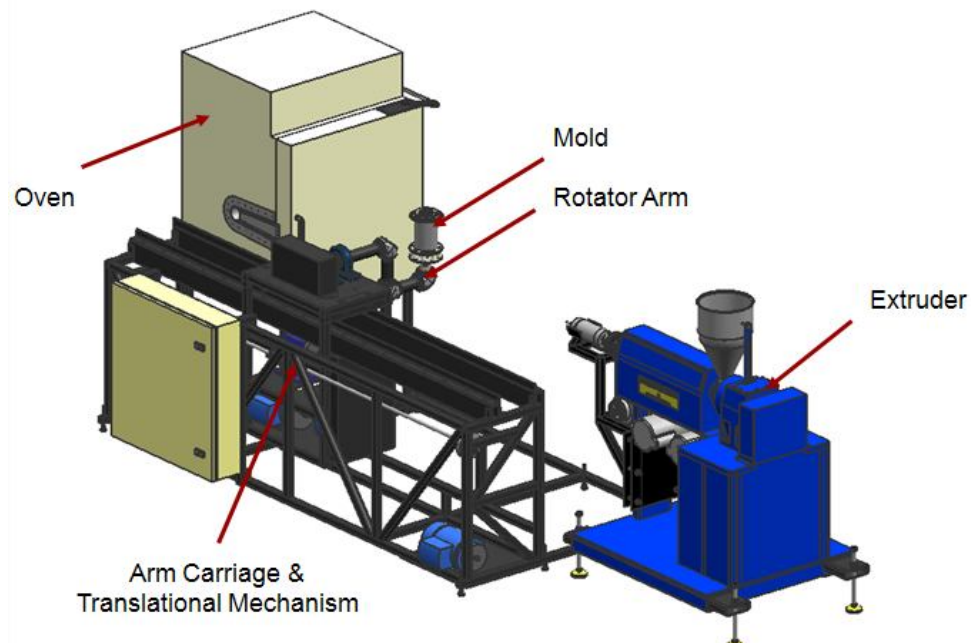
Figure 3-8: EARFM experimental setup - CAD representation

Rotator Arm: The final design of the rotator arm is depicted in Figure 3-9. The main design factors considered were the mechanical and thermal load tolerance, and the functionality in terms of accomplishing the required arm and mold RPM. Additionally, the design of the arm was constrained by the technical specifications of the extruder and oven that were purchased. The arm rotates the mold in 2 perpendicular axes; these are labeled in the figure as the x-axis and the y-axis. Rotation about the x-axis is achieved by

connecting the external arm shaft at its base to the drive system using a chain and sprocket setup. Rotation about the y-axis is achieved by transmitting power to the mold mount, using a different drive system, by means of 3 pairs of miter bevel gears situated at the corners of an internal shaft assembly that is concentric with the external arm body.
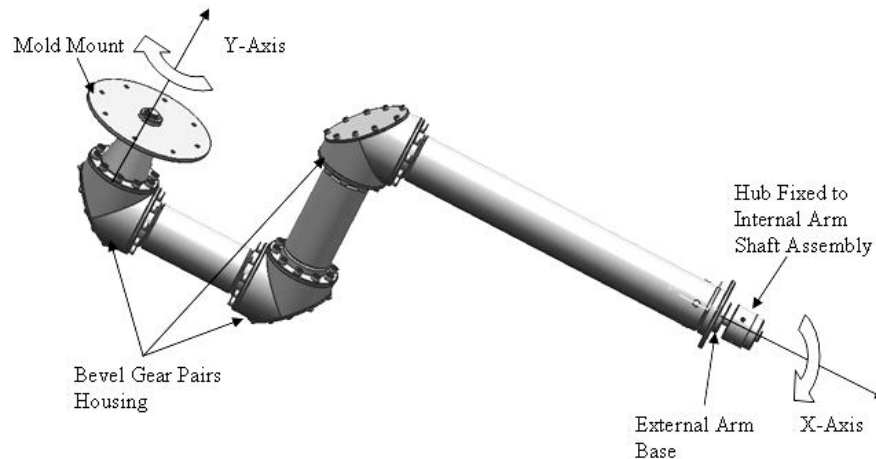
Figure 3-9: Final design of the rotator arm

*Finite Element Analysis***:** Structural and thermal analyses were performed on selected components throughout the design process. As an example, finite element analysis methods were used to reach the optimal dimensions of the rotator arm and determine its mechanical performance under thermal loading. The different loads imposed on the arm were manipulated using a CAD package. The 3D model of the arm was meshed, and then the material AISI Steel 1018 was applied to the resulting model. A 40 [N] force due to the weight of the mold was applied to the arm at a location corresponding to the centre of gravity of the mold; this force was imposed in a dynamic cyclic manner for a period of 1000000 [cycles]. Another 100 [N] force representing the weight of the offset arm portion was applied to the arm base. A centrifugal force due to the maximum angular

velocity of 20 [RPM] was also applied in the axis of arm rotation. Finally, a thermal load of 300 [ºC] was applied to the section of the arm exposed to heating in the oven.

In summary, under these conditions, the simulation was rendered and the results (shown in Figure 3-10) showed that a maximum displacement and stress of magnitude 0.9054 [mm] and 1740 [MPa] were present respectively. Such results were important in determining the fatigue resistance and thermal expansion of the structure, which guided the selection of the different arm components such as the various bearings and fasteners.
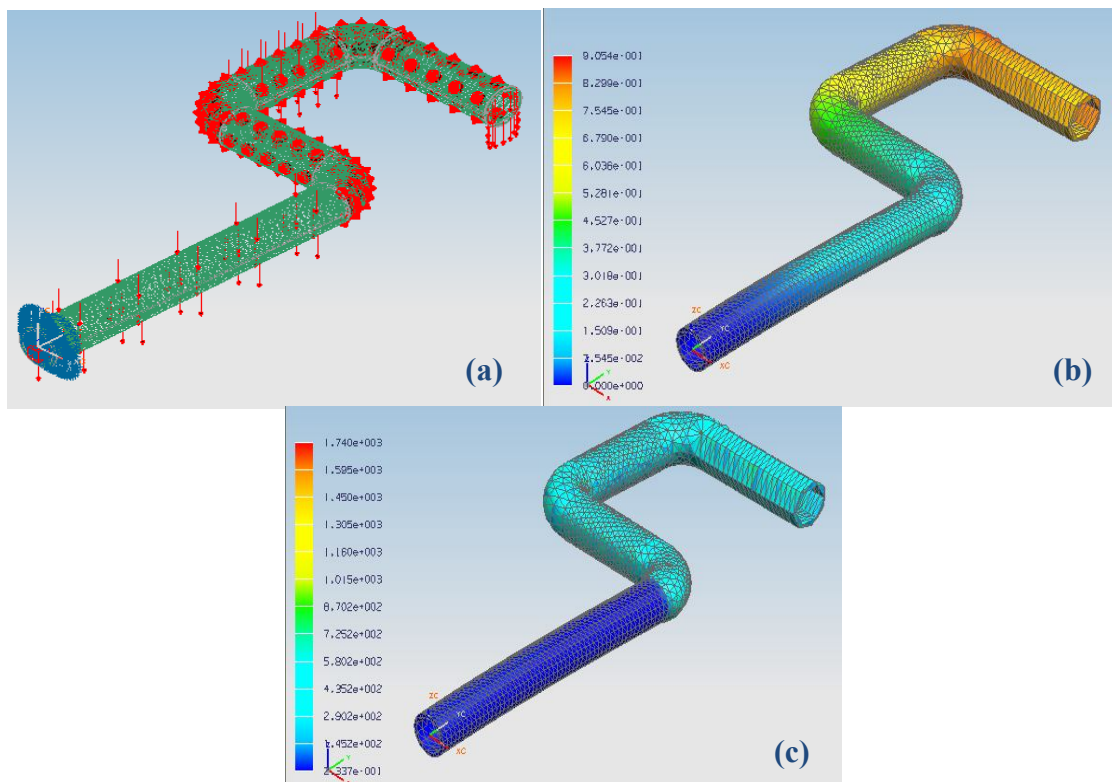
Figure 3-10: (a) FEA: loads application (b) FEA - displacement results (c) FEA - stress results

Arm-mold Translational Mechanism: The arm is required to translate back and forth at different times during the processing cycle between the extruder and the oven while preserving the prescribed mold rotation regime. A linear translation mechanism was designed for this purpose and its assembly with the rotator arm and mold is depicted in

Figure 3-11(a) and Figure 3-11(b). The translational mechanism operates like a cart fixed on a track. The cart is represented by a frame embracing the arm-mold assembly and the respective drive system, which contains two motors, two speed reduction boxes, and eight sprockets with chain connections for power transmission. The translational mechanism is actuated by means of a lead screw connected to a ball-nut that is permanently fixed to the carriage; the lead screw is driven by a motor through a chain connection. The fixed link between the carriage and the ball-nut allows the carriage assembly with its comprising embodiments to translate when the lead screw is driven by the motor mounted to the main experimental setup embracing frame.
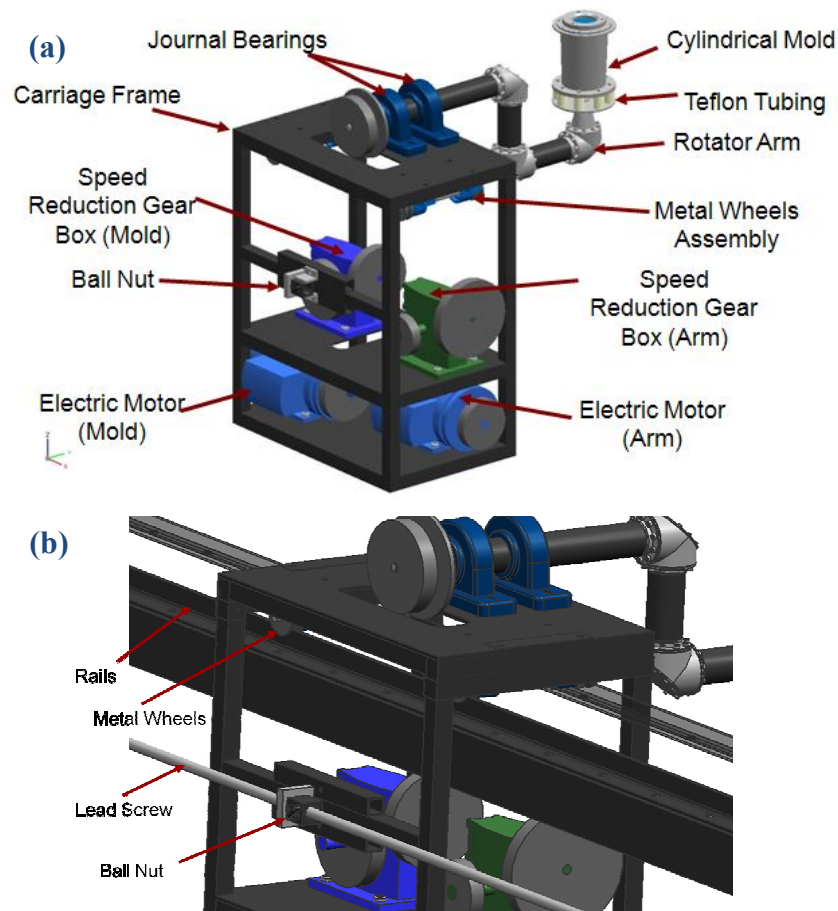
Figure 3-11: Arm-mold assembly attached to carriage and translational mechanism

Mold: A cylindrical mold was designed for the preliminary experimental trials. The mold included a 2º draft angle for easy part removal. Also, in order to assemble the mold to the rotator arm and aid its interface with the extruder, two flanges with bolt holes were welded to the ends of the tapered cylinder. One end of the mold contains a venting tube to avoid pressure buildup during the process. The selected material for the mold was Aluminum 2014. This aluminum alloy has a thermal conductivity value of 192 [W/m-K], which will maximize the heat transfer into and out of the mold.

Mold and Extruder Interface: During the foamable extrudate injection phase, the extruder nozzle enters the mold, pierces the existing skin, and injects the extrudate. To facilitate this interconnection and to keep the extrudate in a molten state, a single cavity pneumatic valve gate hot runner was purchased from Husky [80] and assembled at the output port of the extruder. For purposes of sealing the mold immediately after the foamable extrudate injection, a valve that became commonly known as the "pizza" valve was designed and manufactured (Figure 3-12).
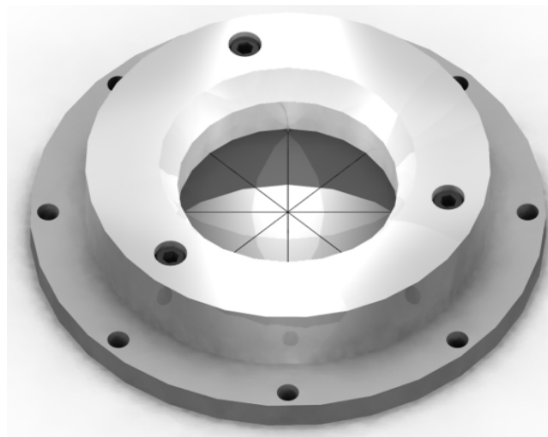
Figure 3-12: "Pizza" Valve CAD Assembly

The material selected for the pizza valve was stainless steel shim of 2 [mm] thickness formed to its final shape using high precision laser cutting. This choice was made due to the enhanced ductility of the material, and thermal and corrosion resistance. Due to the pizza like cut, the mold will be completely sealed when processing the skin, however, during the foamable extrudate induction, the physical pressure applied by the extruder nozzle to the outer surface of the pizza valve will simply allow the nozzle to protrude through slits of the valve, followed by protruding the non-chilled skin, into the core of the mold and deposit the extrudate. Upon achieving the desired filling level and disengaging the mold-extruder interface, the pizza valve will spring back into place; self-healing any generated voids by means of the yet molten plastic. Figure 3-13 presents a pictorial of the pizza valve and nozzle interaction during the typical filling stage
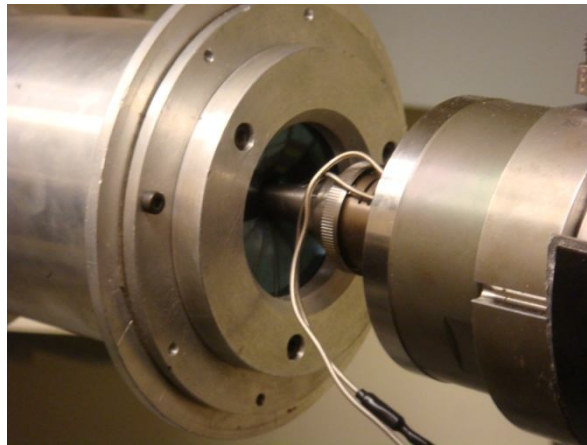
Figure 3-13: Pizza valve and hot runner interaction during filling – EARFM technology

Oven Selection and Customization: An industrial-grade forced convection oven was selected to serve the purpose of the designed experimental setup; this is to provide temperature stability at the processing environment. The internal dimensions of the oven are: $635 \times 635 \times 635$ [mm^3]. Its maximum operating temperature and heating rate are

300 [ºC] and 15 [ºC/min], respectively, with a temperature control resolution of ± 0.5 [ºC].

The purchased oven was retrofitted to accommodate the bi-axially rotating arm during the mold heating phase with minimal heat loss. This was achieved by employing two measures. First, a slot was created on one side of the oven to allow the smooth translation of the arm into and out of the oven. The slot was designed with tight tolerance in order to minimize the heat escape that can result when the oven-arm interaction takes place. The second measure involved automating the opening and closing of the oven door using a pneumatic actuator attached to one side of the door. The oven was placed on a frame with an adjustable height; this frame provides flexibility when aligning the mold, extruder, and oven on the same operating axis. A pictorial view of the customized oven is shown in Figure 3-14.

Side View   Isometric View
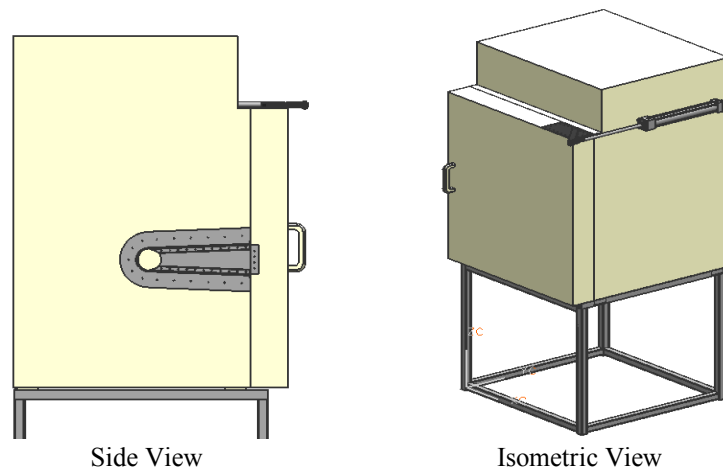
Figure 3-14: Oven CAD representation

Extruder Selection and Customization: A custom built, refurbished heavy-duty single screw extruder by Wayne Machine and Die Co. was purchased for the purpose of this project (Figure 3-15). The extruder has a 32 [mm] screw diameter with a

compression ratio of 24:1. The extruder's drive system is equipped with a 7.5 [hp] motor with a torque delivery accuracy of ±1% and a maximum screw [RPM] value of 100 [81]. As an additional feature, a melt blending system was purchased with the selected extruder. This system is solely present to aid in the dispersion the CBA particles within the foamable resin. The bi-metallic lined barrel of the extruder contains seven temperature control zones. Three zones are in the barrel, one is in the melt blending system, one is in the adaptor, and two are in the die zones.

Figure 3-15: Extruder - Wayne Machine and Die Co.

3.3.7 Safety Features

Operator safety was considered throughout the design, construction, and operation phases of the experimental setup. Accordingly, a variety of safety features and policies were implemented. In terms of physical measures, all motors, gear boxes, chain-sprocket setups, and moving components were carefully housed by means of sheet metal covers that were designed and assembled by Mr. Gregory Eberle. Furthermore, two emergency

stop buttons, incorporated with the extruder design, and another one with the arm-mold-carriage assembly were placed in an operator accessible location within the experimental setup.

In terms of regulatory measures, a variety of warning signs were placed at locations were the equipment operators could be susceptible to injuries or burns due to interacting with the equipment of the experimental setup. Safety gear, including safety eyewear, footwear, gas masks, and thermally insulating gloves were required to be worn at all times by the operators.

3.3.8 Preliminary Experiments Utilizing EARFM

A preliminary set of experiments was performed using PE as the constituting material for processing the skin and foam layers of the integral skin foamed core cylindrical shaped test articles. The choice of PE as a pilot testing material was based on its excellent processing properties and wide processing window, which allows it to simultaneously attain a suitable level of performance in rotational molding and foaming applications. Upon proving the feasibility of EARFM using PE skin/PE foam, the usage of PP skin/PP foam was to follow. The obtained results concerning the PE rotomolded composites processed using EARFM were thoroughly discussed in [82] and [kims thesis].

The EARFM processing technology proved to considerably reduce the excessive time consumed by the heating segment of the conventional processing cycle employed to achieve integral-skin rotomolded foams. In principle, decoupling the heating segment associated with melting the foamable pellets in the conventional practice and achieving it through promptly injecting a foamable blend, that is melt-compounded in an extruder, into a uni-axially rotating hot mold, considerably reduced the overall processing time,

increased the quality of the achieved parts, and eliminated the need to generate foamable pellets and then use them it in a time and energy intensive heating procedure to achieve the required processing task.

3.4 Extrusion-Assisted Direct-Foaming Rotational Molding (EADFRM)

3.4.1 Introduction

Despite the achieved savings and the overall improvements attained in the quality of the moldings exploited by EARFM, further attempts were made to reduce the heating time and energy consumed by the devised processing methodology. Such attempts targeted the elimination of the second heating segment that is imposed to trigger the foaming process.

The research and experimentation efforts spent in the context of the mentioned objective resulted in a principally modified processing technology that relied on completely decoupling the foaming segment, rather than just decoupling the heating segment in EARFM, and achieving it by means of the extruder. The redesigned process became known as Extrusion-Assisted Direct-Foaming Rotational Molding (EADFRM), where a desired foamable blend, consisting of a pre-proportioned quantity of plastic resin mixed with CBA, is compounded within the extruder and promptly pumped, as a foaming melt, within the pre-processed non-chilled skin boundaries contained by the uni-axially rotating hot mold.

The introduced fundamental alterations not only abolished the need to utilize a second heating step, but also provided additional opportunities to completely eliminate

adverse phenomena like skin degradation due to overheating and the premature decomposition of the CBA prior to the designated instant within the process.

3.4.2 EADFRM - Experimental Setup Modifications

Several modifications were successively applied to the experimental setup so as to proficiently implement the developed EADFRM technology.

The first change entailed replacing the hot runner by a thermally controlled conical nozzle of a larger diameter to preserve the rapidity and structure by which the foaming polymer is extruded into the mold (Figure 3-16(a)).

Subsequently, the pizza valve slits were altered from a straight cut (center to circumference) to a spiral cut (Figure 3-16(b)) such modifications were executed with the intention to permit its smooth operation when in contact with the redesigned nozzle during filling and to prohibit equipment damage due to the involved physical/mechanical interaction.
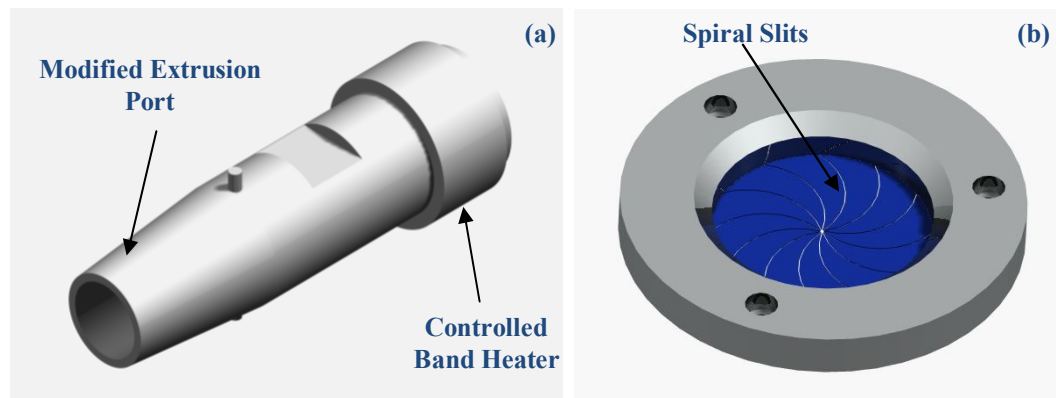
Figure 3-16: Modified nozzle and pizza valve for EADFRM

3.4.3 Extrusion-Assisted Direct-Foaming Operating Principle

The processing concept to achieve an integral-skin foamed core article using EADFRM can be summarized in 4 unique steps, these are presented as follows:

Step 1: At the beginning of the process, the mold is manually charged with a predetermined amount of non-foamable plastic resin in powder form, which will be used to create the solid skin of the part.

Step 2: The arm and mold assembly are inserted into the oven by means of the carriage and translational mechanism. The mold rotates in a biaxial manner within the oven, utilizing the arm. This stage is accomplished at a material-dependent elevated temperature for an accordingly set period of time to create the skin. Simultaneously, the extruder is charged with predetermined amounts of dry blended polymer resin with CBA, suitable for achieving polymeric foam that exhibits a desired volume expansion ratio (*VER*) at a set melt temperature.

Step 3: The arm and mold assembly are then translated towards the extruder, with the arm rotation switched to a uni-axial mode and the mold aligned with the extrusion port; the extrusion port penetrates the mold up to a designated extent. The extruder is subsequently promoted to fill the hot mold with extrudate comprised of the desired foam for a period of time dependent on the melt flow rate and screw [RPM]. The filling process occurs at the mold end through the modified pizza valve, which was designed to seal the mold during the conventional rotational molding cycle, facilitate the introduction of foam to it during the foam filling stage, and allow the skin to self-heal after the filling process is accomplished; this occurs due to its enhanced spring back ability, which allows the skin to settle back at its original location, undamaged.

Step 4: The arm is then bi-axially rotated and the mold is cooled, allowing the appropriate distribution and further expansion of the foam to completely fill the cavity, and the formation of a suitable interface relating the skin and foam layers of the part. The cooled part is accordingly removed from the mold after a set cooling period.

The EADFRM operating principle is illustrated by the series of schematics in Figure 3-17:
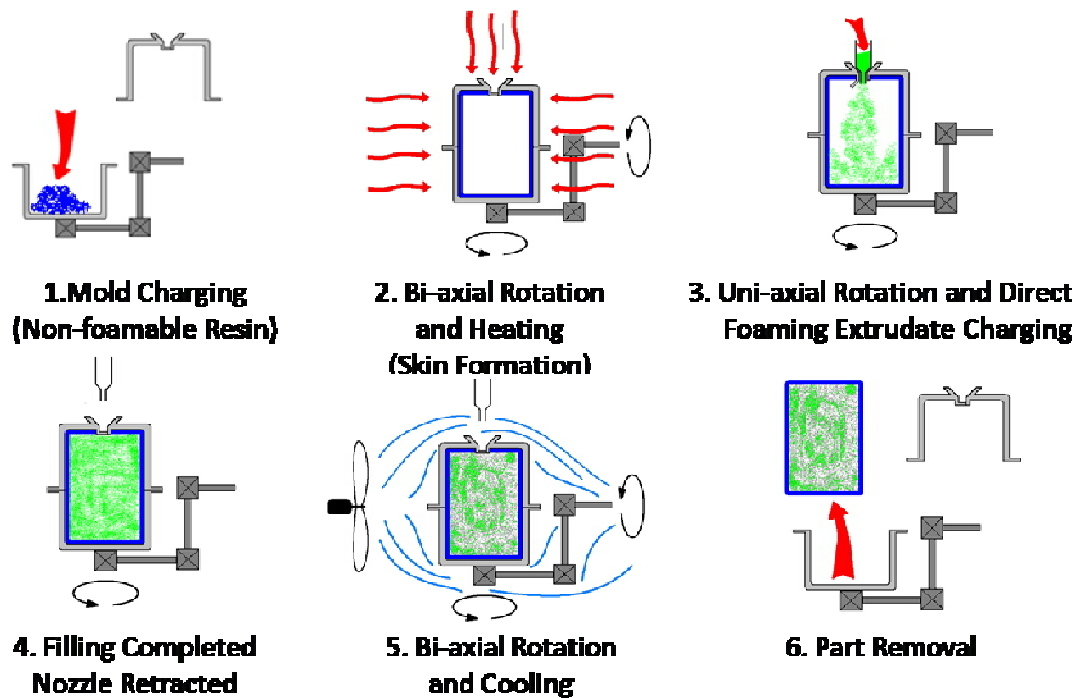
Figure 3-17: Operating principle of EADFRM

3.4.4 Preliminary Experimental Trials Utilizing EADFRM

Three unique batteries of experiments were executed to assess the performance of EADFRM with respect to the manufacture of articles comprising an integral PP skin surrounding a PP foam core, these comprise: (1) the processing of solid-skin hollow rotomolded PP articles, (2) the processing of skinless fully foamed inner core rotomolded PP articles, and (3) the processing of integral skin foamed core PP-constituted structures.

A complete set of entities pertaining to the material formulations and obtained morphologies was published in Ref. # [25] and [83]. A sample experimental log magnifying the parameters implemented to achieve integral skin foam core rotomolded articles using EADFRM along with the status and condition of the obtained moldings is presented in Table 3-2.

Table 3-2: Experimental log associated with the preliminary experimental trails of EADFRM

exp #	Oven time min	Melt T °C	Z1 Temp °C	Z2 Temp °C	Z3 Temp °C	DZ1 Temp °C	DZ2 Temp °C	DZ3 Temp °C	Melt Pres PSI	RPM	Fill Time (min)	Cool Time (min)	Status	Notes
1	17.5	193	190	200	215	215	215	230	550	95	3:30	45	better, almost completely full, some foam escape from pizza valve	Profax 6523 Homopolymer VER 3 750g & 9.5 g CBA
2	15	198	190	200	215	215	215	230	550	95	3:00	45	Large Gap in the middle again, Venting problem, some foam escape	Profax 6523 Homopolymer VER 3 750g & 10.5 g CBA
3	15	203	190	200	215	215	215	230	470	95	3:00	45	Large Gap in the middle again, Venting problem, some foam escape	Profax 6523 Homopolymer VER 3 750g & 12 g CBA
4	15	199	190	200	215	215	215	230	500	95	3:00	45	Half Full, half the problem solved some foam escape from pizza valve	Profax 6523 VER 3 700g & 12.5 g CBA, NEW Venting
5	15	199	190	200	215	215	215	230	500	95	3:00	45	Half Full, half the problem solved, some foam escape from pizza valve	Profax 6523 VER 3 700g & 9.5 g CBA, NEW Venting
6	20	199	190	200	215	215	215	230	400	95	3:30	45	Large Gap in the middle again, Venting problem, some foam escape from pizza valve	Profax 6523 VER 3 750g & 9.5 g CBA, SNAKE Venting
7	20	199	190	200	215	215	215	230	400	95	3:30	45	Large Gap in the middle again, Venting problem	Profax 6523 VER 3 700 & 14 g CBA, regular vent with slits, mesh and wool
8	20	199	190	200	215	215	215	230	400	95	3:30	45	Large Gap in the middle, some foam escape from pizza valve	Profax 6523 VER 3 750 & 14 g CBA, regular vent with slits, steel wool, AZ-130
9	30	203	195	210	225	225	225	225	300	95	3:30	45	Gap smaller, good skin-foam interface, some foam escape from pizza valve	Profax 6523 VER 3 600 & 15 g CBA, concentric vents with slits, steel wool, AZ-120, 3mm skin
10	30	210	200	215	230	230	230	230	350	95	3:30	45	Good filling, missing extra ventillation	Profax 6523 VER 3 600 & 18 g CBA, concentric vents with slits, steel wool, AZ-120, 3mm skin, 3 vents
12	30	207	195	205	225	225	225	230	450	95	3:30	45	Gap in the middle	Profax 6523 VER 3 600 & 20 g CBA, concentric vents with slits, steel wool, AZ-120, 3mm skin, 3 vents

3.4.5 EADFRM – Processing Concerns

In spite of the proven applicability of EADFRM as a remedial engineered solution treating the processing drawbacks of conventional rotational foam molding and the initially developed EARFM technology, several processing concerns became apparent during the preliminary experimental trials. As implied by the remarks noted in Table 3-2, the attained moldings often entailed unpredictable quality and morphology at the

interface location pertaining to the inconsistency of the pizza valve in achieving its designated task; that is, to completely seal the mold and act as a one way gate during foam filling. Additionally, a variety of venting challenges were faced due to the inadequate venting procedure initially used.

Figure 3-18(a) shows an exemplary integral-skin foam core cylindrical shaped molding of insufficient interface quality at the filling location. It can be readily deduced that an incident of foam invasion into the adjacent skin layer is present, it is also emphasized that a portion of the pizza valve cracked due to friction with the extruder nozzle and became incorporated with the molding at the interface location. Figure 3-18(b) shows a different molding of which the pizza valve has failed to seal the mold due to the intense foam expansion, causing the foam to escape the mold body and the failure of the respective experiment.
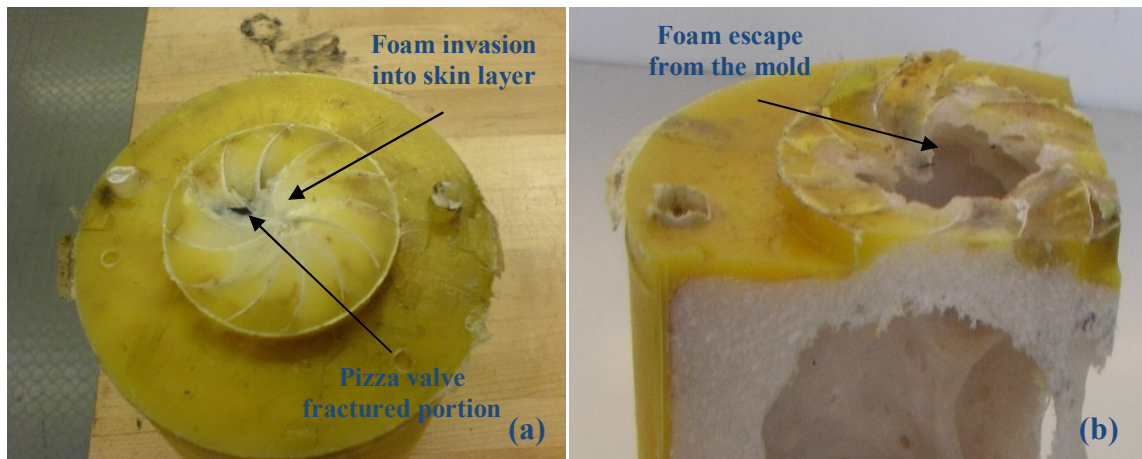
Figure 3-18: Processing concerns pertaining to the pizza valve design

The variable performance of the pizza valve generated an additional processing related challenge, specifically, the difficulty in removing the cooled part from the mold. This is due to solidified skin/foam portions trapped within the slits of the valve, which

often created a labor intensive demolding practice as well as the need to replace the damaged pizza valve repeatedly.

3.5 Rapid Rotational Foam Molding (RRFM)

In response to the processing issues encountered with EADFRM and EARFM, a further improved remedial processing technology was developed under the name of Rapid Rotational Foam Molding (RRFM).

3.5.1 RRFM Processing Fundamentals

In principle, the RRFM and the EADFRM technologies operate in a similar manner, with the sole purpose of attaining high quality integral-skin foam core rotomolded articles. The fundamental difference between both technologies lies in the procedure by which the extruder-mold marrying is accomplished during the foam filling step. In RRFM, instead of the pizza valve concept, a newly designed interface with insulated boundaries was incorporated as an interchangeable constituent of each of the designed molds. During the skin processing step, the interface seals the mold, allowing it to fully enclose the skin. Following this step, and as the non-chilled mold is prompted to approach the extruder, the interface is physically disengage by the operator from the mold body along with a molten portion of the skin adhering to its surface. Such behaviour is aided by retarding the heat transfer at the interface's boundaries via incorporating thermally insulating material in its design, which facilitates the parting of the skin portion linked to it from the overall skin structure when in molten state. Once the interface is removed, the extruder is simply advanced to deposit the foaming polymer within the non-chilled skin through the resulting mold opening. The parted skin portion, yet kept in molten state, is placed back

via the interface to its location in the mold so as to seal the opening after foam filling is accomplished. The forces applied by the foam layer on the outer skin layer during the course of foam stabilization and cooling allows the skin to heal and act as one structure that completely and homogeneously encapsulates the foam core. The processing principle employed to achieve an integral-skin foamed core article using RRFM can be illustrated using the schematics presented in Figure 3-19. A detailed flow chart of the process is presented in Figure 3-20.
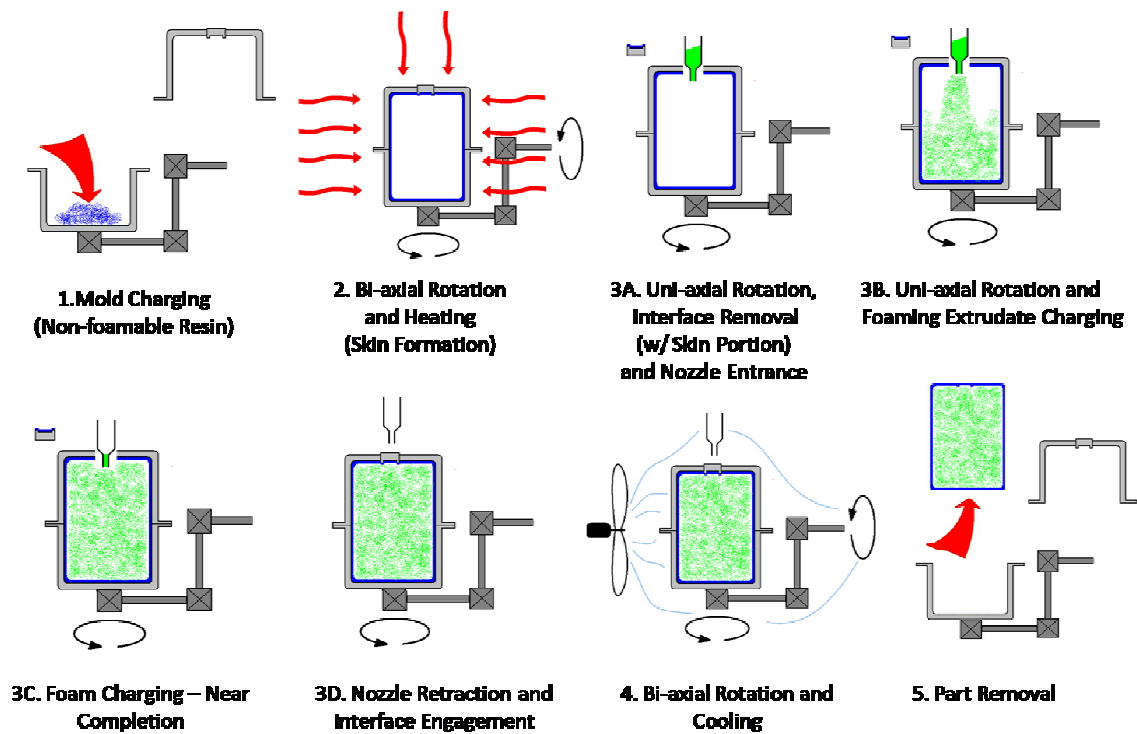
Figure 3-19: Operating principle of RRFM
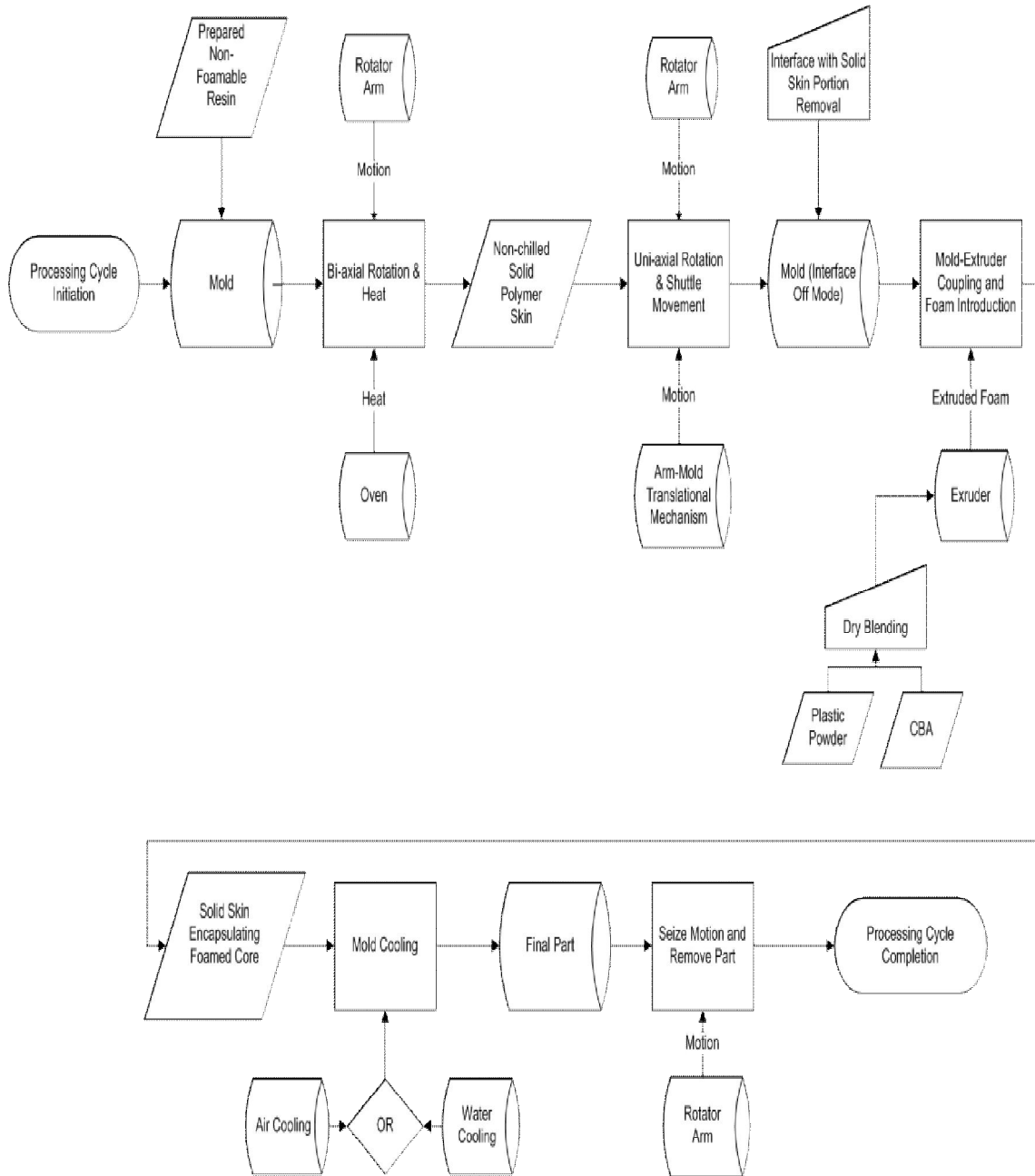
Figure 3-20: RRFM processing flow chart

3.5.2 RRFM - Experimental Setup Modifications

The modifications employed to alter the existing experimental setup in order to cope with the RRFM process were mainly associated with the mold interface assembly that replaced the aforementioned pizza valve concept. The designed mold interface assembly is shown in Figure 3-21; it consists of three main components: the insulation cap, the mold interface and the mold connection adaptor. The mold connection adaptor is mounted onto the mold by means of bolts. During skin processing and after achieving the foam filling segment, the mold interface is locked onto the mold adaptor via a set of incorporated metal extrusions that secure the interface, upon rotating it, within corresponding guides precisely machined into the mold connection adaptor. The mold interface includes a channel that is filled with high temperature ceramic fiber insulation, which in turn facilitates the parting of the skin portion under the mold interface from the overall skin structure. The insulation cap holds the ceramic fiber securely within this channel during processing.
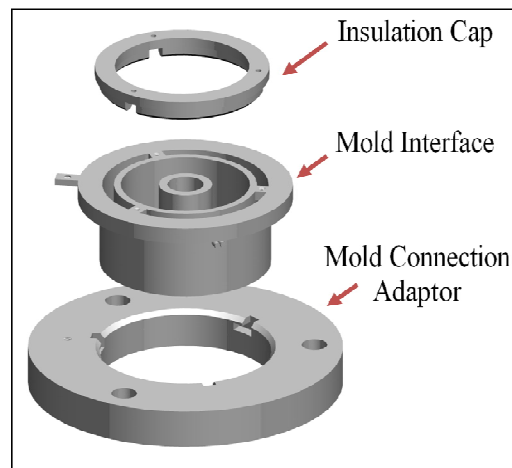
Figure 3-21: RRFM mold interface assembly

The mold interface and insulation cap assembly are completely detachable from the mold body during filling by means of a "quick release" T-shaped handle that locks into a designated compartment within the mold interface. After injection is complete, the interface can be reattached to the mold to allow the created foam to expand and adhere to the semi-molten polymer attached to the interface, ultimately producing a better quality mold interface section of the final molding. Figure 3-22 shows the redesigned mold interface assembly with respect to the cylindrical mold.
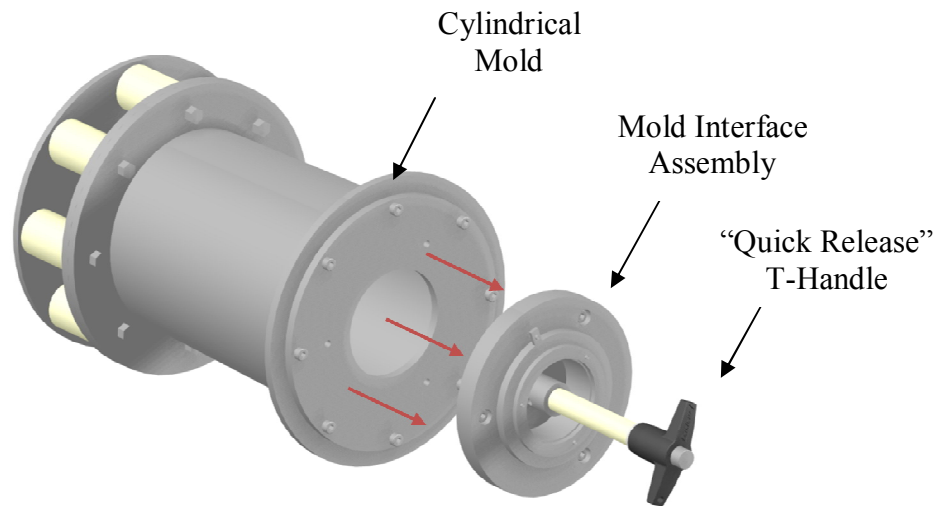
Figure 3-22: The insulated mold interface assembly relative to the cylindrical mold

The predicated interface behavior was also validated through the preliminary experimental trials. Figure 3-23 shows a series of "snapshots" photographed at different instances of the RRFM process to present the method of operation of the interface assembly. Figure 3-23(a) shows the cylindrical mold approaching the extruder nozzle while rotating uni-axially about its central axis; the quick release T-shaped handle is shown engaged with the interface assembly to instigate its removal process. Figure 3-23(b) illustrates the removal of the mold interface with the skin portion adhering to its

lower surface at an instant prior to foam filling. Figure 3-23(c) demonstrates the tactic used to preserve the molten state of the skin portion attached to interface while foam filling is in process; that is, the interface assembly is exposed to the elevated temperature of the oven. Finally, Figure 3-23(d) shows a cut-out from a sample part showing the achieved high quality morphology at the skin-foam interface due to the engineered interface design.
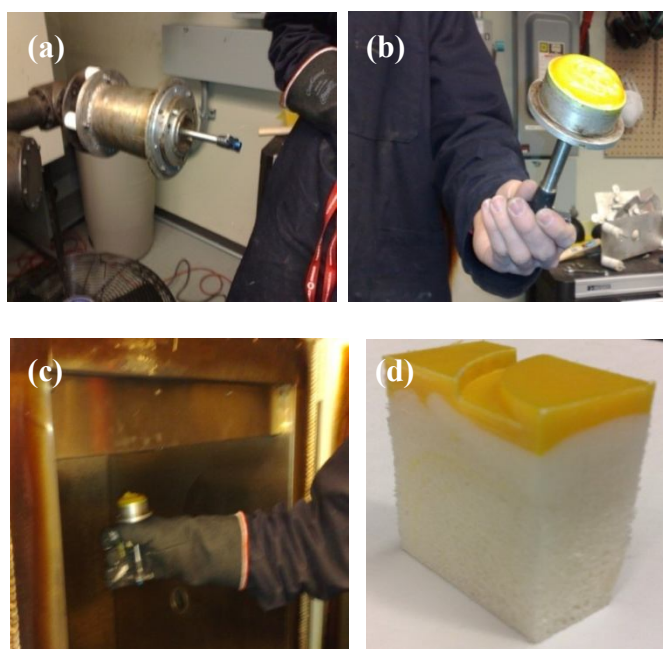
Figure 3-23: (a) Interface locked onto the mold, (b) Interface removal with skin portion, (c) Preserving the interface temperature, (d) Final morphology about the interface area

3.6 Summary

In principle, the evolution of RRFM as an efficient processing technology for the manufacture of integral-skin polyolefin foams was discussed in detail throughout the sections of this chapter, along with the design, development, and build of the experimental setup that implements this novel processing concept. A variety of

experimental trials were initially conducted to prove the feasibility of RRFM as a method to process integral-skin PP/PP foams. Additionally, the mentioned experimental batteries investigated the processing parameters that allow achieving satisfactory cylindrical and flat shaped moldings pertaining to the discussed processing concept.

3.7 Achieved Time and Energy Savings

The potential cycle time savings associated with the RRFM process compared to the previously discussed remedial processes and to conventional rotational foam molding proves to reach up to 35%.
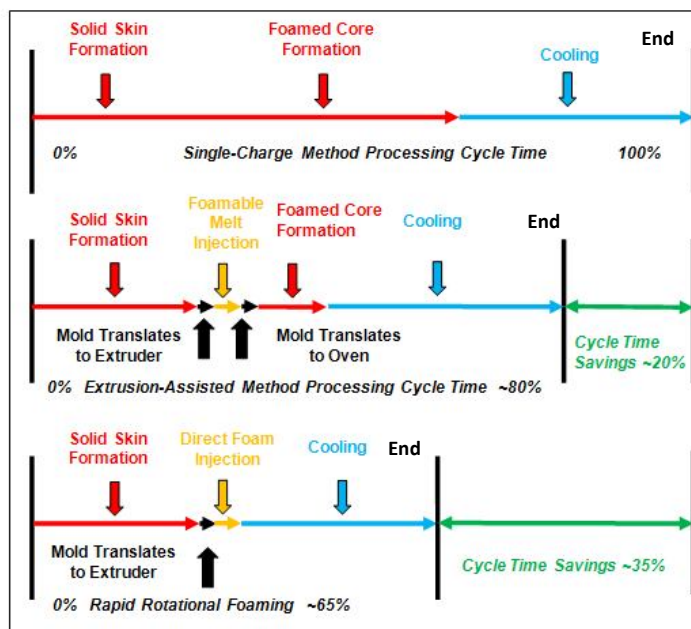
Figure 3-24: Processing cycle time reductions achieved through RRFM

As illustrated in Figure 3-24, approximately 20% of the incurred savings, when compared to the total processing cycle time of conventional rotational molding, resulted from the reduction of the overall heating cycle time of the foam core production. A further 15% savings in cycle time of this newly modified RRFM process can be contributed to the

reduction in travel time of the mold in addition to a reduction in heating cycle time due eliminating the use of the oven to trigger foam formation.

The next chapter discusses the experimental plan that was devised to prove the feasibility of processing three different skin-foam material blends using RRFM. The successful accomplishment of such a venture authenticates the wider materials/ processing window generated by the novelty demonstrated in RRFM, especially after identifying the difficulty in accomplishing similar PP-based manufacturing endeavors using the conventional practice.

Chapter 4: RRFM – Processing Experimental Plan

4.1 Introduction

Throughout this chapter, the devised applied processing proposal and the involved experimental plan used in assessing the performance of RRFM with respect to processing integral-skin PP cellular composites will be emphasized. The groundwork pertaining to the performed experiments is presented first, followed by the devised experimental plan and the presentation of the rationale governing its particulars.

4.2 Materials and Resources Used in Experimentation

4.2.1 PP Grades

Four different PP resin grades were obtained from Lyondell Basell prior to the preliminary experimental trials; the respective resin codes along with their basic commercial properties are listed in Table 4-1

Table 4-1: PP resins obtained for experimentation purposes

	PP Resin	PFHL451H	PFSR257M	PF6523	PFSB786
Properties	MFI [g/10min]	2.0	2.0	4.0	8.0
	Density [g/cm^3]	0.902	0.902	0.900	0.902
	Homopolymer (H) or Copolymer (C)	H	Random C	H	Impact C
	Tacticity	i-PP	i-PP	i-PP	i-PP

The obtained PP grades were carefully selected to reflect a wide variety of characteristics; from systematic differences in MFIs to a selected variation in material nature from PP homopolymers to PP copolymers. The resins, received in pellet form, were initially pulverized at Ingenia Polymers to mesh 35 powders; this is to test their processability as solid skin constituents in RRFM, and when used for foaming purposes, to enhance and facilitate their dispersion and distribution characteristics with the CBA.

4.2.2 CBA

The CBA used to formulate the foamable resin was of type Celogen AZ-120 (exothermic CBA) and was obtained from Chrompton Chemicals. The molecular constituents of this thermally activated CBA are azodicarbonamide with amorphous silica. Celogen AZ-120 was selected after comparing its performance and base properties with Celogen OT and Celogen AZ-130; this is due to the compatibility of its pertaining decomposition temperature range with the obtained PP grades as well as its small particle size, which assists the dispersion and distribution properties during the implemented dry blending procedure. Table 4-2 highlights the most important characteristics of Celogen AZ-120.

Table 4-2: Properties of Celogen AZ-120

CBA: Celogen AZ -120 (exothermic)	
Chemical Composition	Azidocarbonamide, Silica
Bulk Density [kg/m^3]	7961 – 9755
Gas Yield φ [cm^3/g]	210 – 220
Decomposition range [^oC]	205 – 213
Gas Composition	N_2, CO_2, CO, NH_3
Particle size [μm]	2.0 – 2.4

4.2.3 Molds and Venting

Two different shaped molds, fabricated using Aluminum 2014, were used throughout the final set of conducted feasibility assessment experiments; a cylindrical shaped mold and a flat plate shaped mold (Figure 4-1).
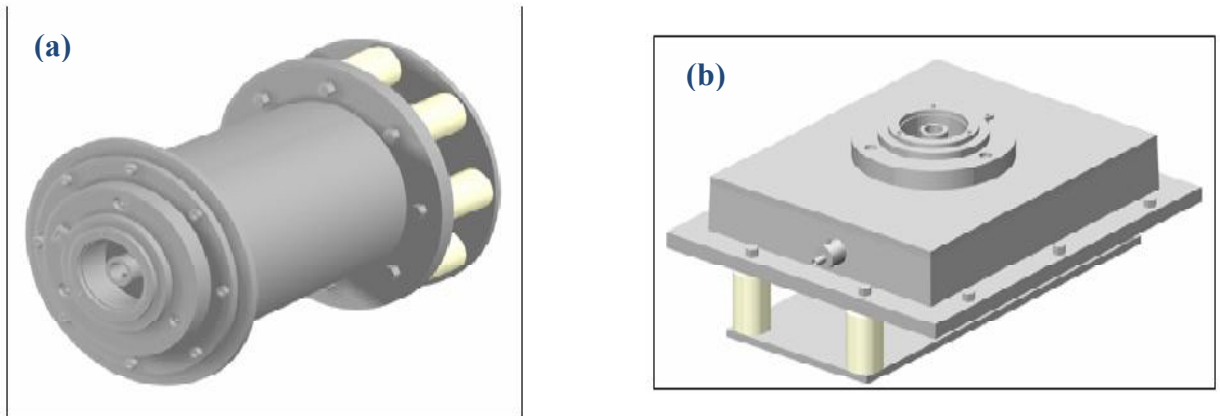
Figure 4-1: (a) Cylindrical mold (b) Flat plate mold

<u>Cylindrical Mold</u>

The cylindrical mold has a base radius of 11 [cm] and a total height of 17 [cm] which sets its total volume to be ~1400 [cm^3]. A 2° draft angle was incorporated in the mold design to facilitate part removal. The mold was offset from the rotating flange of the arm by means of 8 identical Teflon® tubes; the presence of such tubes aids in aligning the center of the mold with the arm's center of rotation and acts as an insulating means to prevent unwanted heat exchange effects that can arise from the direct arm-mold contact.

As for the venting design, three vents were integrated at different locations within the cylindrical mold structure; one vent, ~4 [cm] long, was placed at the center of the mold's base and the other two vents, ~6 [cm] in length, were placed through two holes drilled within the mold interface adaptor at a distance of ~4 [cm] radially away from its

center. The venting tubes are cut from Teflon® stock and exhibit an inner diameter of 0.3175 [cm] and an outer diameter of 0.635 [cm]. Teflon® was used due to its low coefficient of friction, which facilitates vent removal, as well as its excellent thermal properties. It is worth noting that the venting tubes were partially closed with steel wool prior to the skin processing segment, and then unclogged during the foam filling and successive cooling segments to evacuate the accumulated processing gasses.

Flat Mold

The flat plate mold has dimensions of 23 x 18 x 3.5 [cm] (length x width x depth) respectively, which sets its total volume to be ~1450 [cm³]. This mold also included a 2° draft angle to facilitate part removal. The mold was offset from the arm's rotating flange by means of 4 identical Teflon® tubes that serve insulation and positioning purposes. Six vents were used to evacuate processing gasses generated within the mold during the processing cycle. Two vents, ~3 [cm] long, were located at the center of each of the mold's far vertices, whereas the four other vents, ~2 [cm] in length each, were located at every bottom corner of the mold. Once more, all six vents were partially closed with steel wool during skin processing and then uncluttered during the remaining steps of the process.

4.2.4 Thermal Analysis Characterization

DSC Experimental Procedure and Results

The DSC apparatus used to investigate the thermal transitions of the obtained resins was the DSC Q20 of TA Instruments. The apparatus was initially cleaned and then calibrated by running a high purity material (e.g., indium, zinc, etc.) through its melting point using

a preset software-aided temperature profile and procedure. The purpose of the calibration procedure is to establish a quantitatively defined relationship between a value of a quantity indicated by the DSC and the true value of the highly pure material; this will allow maximising the accuracy of the generated analysis results.

Upon completing the calibration procedure, the investigated resins, received from Lyondell Basell in the form of pellets that weighed at least 30 [mg] each, endured a reduction in size so as to be compatible with the pan-lid assembly and the specific purpose of investigating the melting and crystallization behaviors through the DSC experiments. A lab knife and tweezers were used to achieve this task (Figure 4-2 (a)).

The cut material was then weighed and enclosed in an aluminum pan and lid setup using a sample press. The sample pan closure was done in an inverted lid manner (Figure 4-2 (b)); this method prevents damaging the sample housing when sealing it with the press, considering the relatively large and uneven sample geometry.
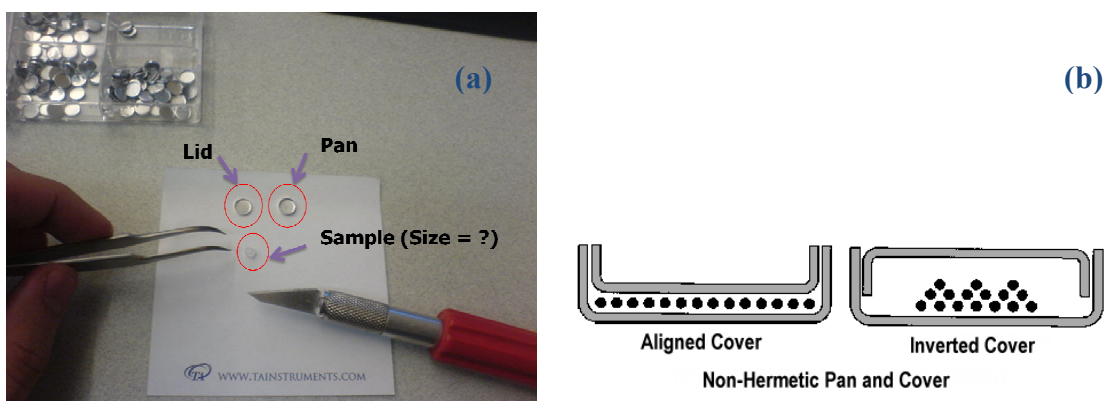
Figure 4-2: (a) Sample preparation setup (b) Lid closure configuration

An identical DSC profile was employed to the four PP grades used; that is, a heating rate of 20 [ºC/min] up to a temperature of 230 [ºC], followed by an isothermal hold at 230 [ºC] for 30 [min], and then a successive cooling rate of 2.5 [ºC/min] down to

room temperature (25 [ºC]). The employed experimental profile complies with the relevant capabilities of the used DSC apparatus, which are presented in Table 4-3 [62].

Table 4-3: Relevant specifications of the used DSC Q20 apparatus [62]

Specification	Numerical Value
Temperature Range	Ambient to 725 [ºC]
Temperature Accuracy	± 0.1 [ºC]
Temperature Precision	± 0.05 [ºC]
Sensitivity	1.0 [µW]

The resulting DSC curves were analyzed to obtain the melting phase onset, the melting phase peak (T_m), the crystallization phase onset, the crystallization phase peak (T_c), and the percent crystallinity of the respective resins. The corresponding DSC curves associated with as-received PP grades PFHL451H, PFSR257M, PF6523, and PFSB786 are shown in Figure 4-3(a) to Figure 4-3(d), respectively.
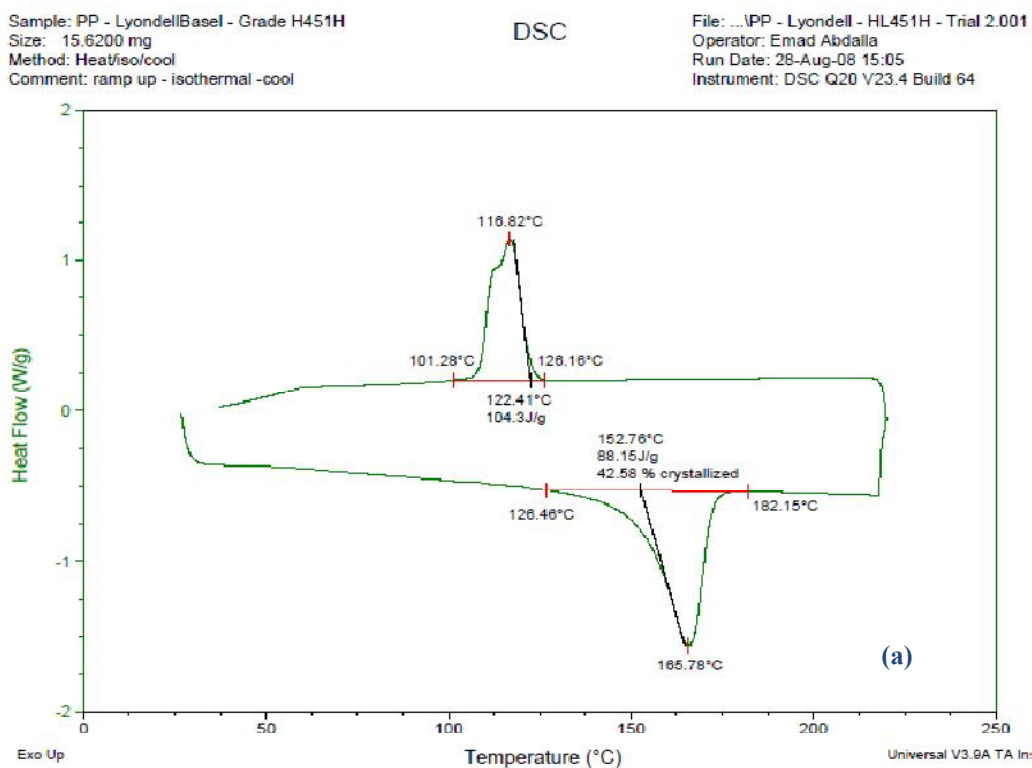
Sample: PP PFSR257M
Size: 17.4700 mg
Method: ramp up/iso/ramp down
Comment: ramp up/iso/ramp down

DSC

File: C:...\DSC Experiments\PP PFSR257Mf.001
Operator: Emad Abdalla
Run Date: 30-Apr-09 14:12
Instrument: DSC Q20 V23.4 Build 64

123.99°C

92.03°C   138.24°C

127.47°C
83.75J/g

130.56°C
67.96J/g
32.83 % crystallized

111.58°C   172.01°C

149.41°C

(b)

Heat Flow (W/g)

Temperature (°C)

Exo Up   Universal V3.9A TA Instrume
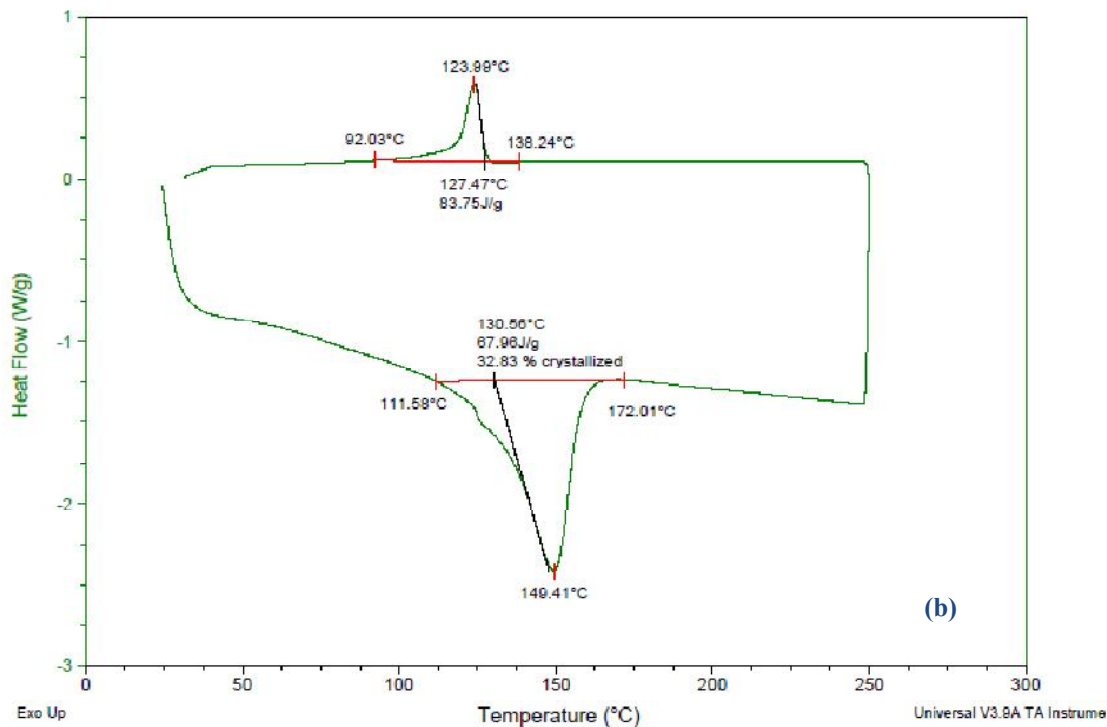
Sample: PP - LyondellBasel - Grade 6523
Size: 19.1400 mg
Method: Heat/iso/cool
Comment: ramp up - isothermal -cool

DSC

File: C:...\PP - Lyondell - 6523 - Trial 2.001
Operator: Emad Abdalla
Run Date: 29-Aug-08 12:19
Instrument: DSC Q20 V23.4 Build 64

112.30°C

90.32°C   123.79°C

115.54°C
108.6J/g

153.91°C
89.75J/g
43.36 % crystallized

132.38°C   180.07°C

166.38°C

(c)

Heat Flow (W/g)

Temperature (°C)

Exo Up   Universal V3.9A TA In
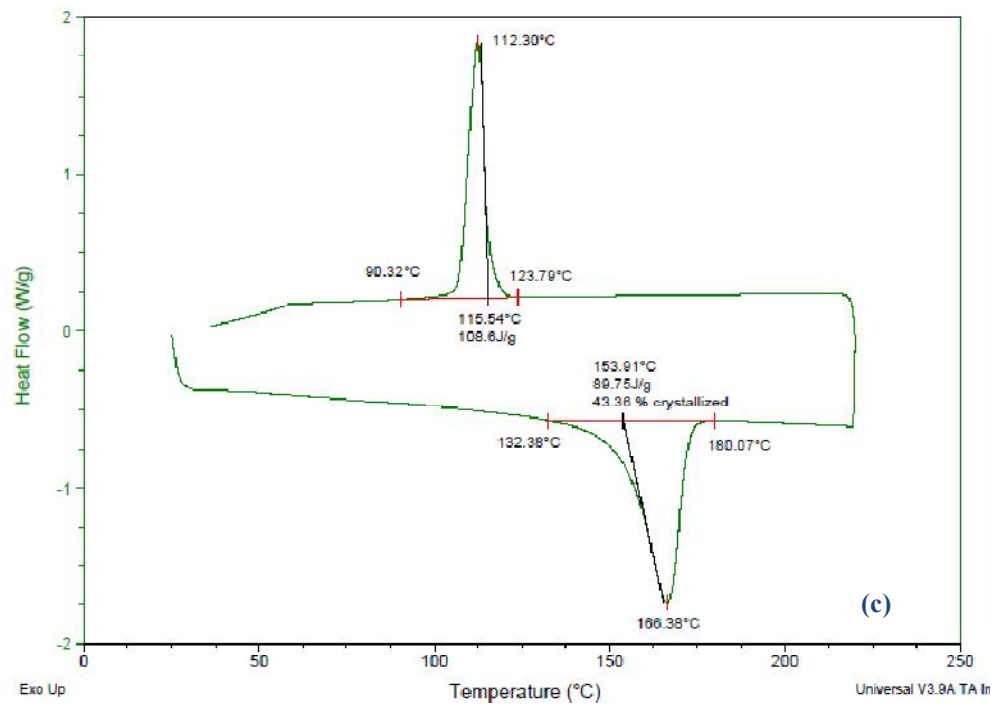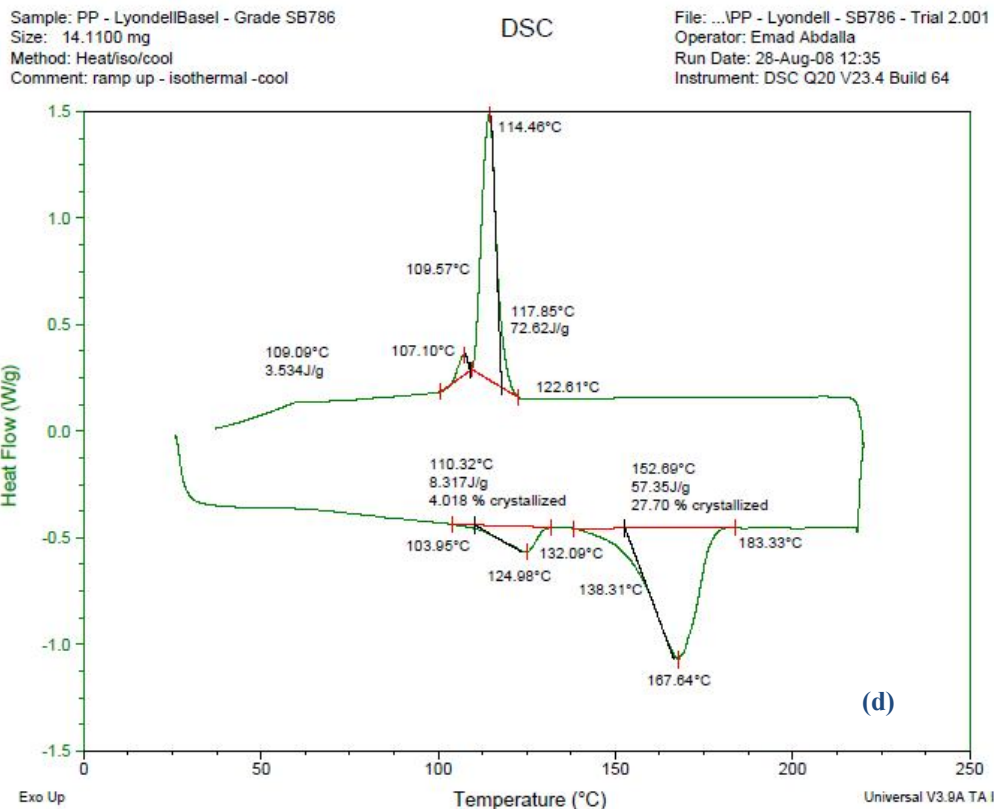
Figure 4-3: Curves generated using DSC for the used experimental materials

The parameters obtained through analyzing all four DSC curves are tabulated in Table 4-4.

Table 4-4: Parameters obtained through the analysis of the DSC output curves

PP Grades	T_m Onset [°C]	T_m Peak [°C]	T_c Onset [°C]	T_c Peak [°C]	% Crystallinity
PFHL451H	126.46	165.78	126.16	116.85	42.59
PFSR257M	111.58	149.41	138.24	123.99	32.83
PF6523	132.38	166.38	123.79	112.30	43.46
PFSB786	103.95/138.31	124.98/167.64	122.61/109.57	114.46/107.10	4/27.7

It is worth noting that the analytical approach of obtaining the percent crystallinity of a particular polymeric substance was discussed in Section 2.3.2 of this thesis. However, the TA Instruments Analysis software can be set to generate the value

associated with this parameter upon inputting the polymer enthalpy (standard heat) in [J/g] into the software interface and integrating the area under the melting peak. The enthalpy value for PP was found from the table of standard enthalpies to be 207 [J/g].

The respective results displayed in the table prove to abide by the researched theories related to PP crystallinity presented in Chapter 2. That is, it is concluded from the analyzed DSC results that the PP grades exhibiting a higher percent crystallinity have higher melting temperatures and more delayed crystallization behaviors. The consideration of the characterized parameters is essential to setting the appropriate experimental entities associated with the RRFM process. For instance, the foaming parameters of the extruder for PP grade PFSR257M will be significantly different than the ones utilized for the other foaming grades, since if set at a similar temperature to the other grades, the deterioration of its melt strength will take place, causing an undesirable end-use foam structure. The crystallization temperature values pertaining to the PP grades used for foaming in this thesis are particularly important in determining the corresponding corrected CBA gas yield parameters for each resin as per the method discussed in Section 2.2.2.4. Table 4-5 displays the calculated corrected gas yield factor with respect to each of the foaming resins.

Table 4-5: Corrected gas yield value for the resins used in foaming

	PFHL451H	PFSR257M	PF6523
Corrected Gas Yield Factor [cm³/g]	274.7265101	279.7580537	271.5201342

TGA Results

A plot emphasizing the weight vs temperature behaviour of Celogen AZ-120 is obtained using TGA model Q50 (Figure 4-4).
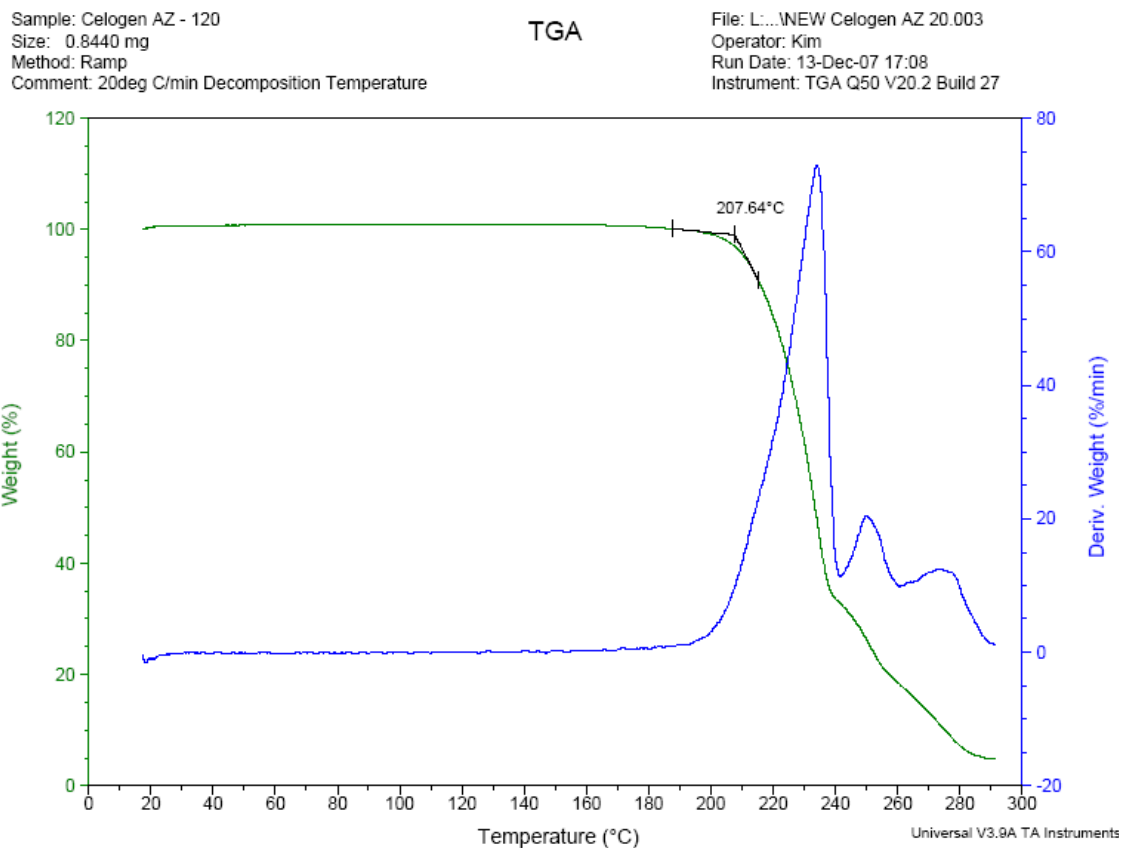
Figure 4-4: TGA performed on Celogen AZ–120

Using the TGA plot analysis tools, the onset decomposition temperature of the CBA appears to occur at 207 [^{o}C]. The complete decomposition of Celogen AZ-120 is achieved at a temperature of ~220 [^{o}C], where the weight of the sample rapidly approaches zero. The stated results comply with the obtained manufacturer's properties of the CBA.

4.3 RRFM Processing Considerations

4.3.1 Integral-skin

A desired skin in rotational molding is one that demonstrates uniform thickness, is bubble free, and has no signs of degradation.

A variety of parameters govern the achievement of a desired skin in rotational molding; these include: the mold and arm RPMs and the ratio between them during processing, the mold heating time and temperature, the successive cooling time and method, the constituting resin, and the respective resin amount used to fill the mold at the outset of the process.

In addition to the abovementioned parameters, it was revealed during the initial set of experimental trials that the processing concept of RRFM imposes supplementary factors that highly influence the integrity of the resulting skin. These include, the RPM of the mold during the foam filling segment, the respective filling time, and the time consumed by the translational mechanism to convey the mold up to the extruder nozzle. Other parameters that are worth considering, but were found to be of less effect on the resulting skin integrity, include the angle of the mold with the normal during filling and the volumetric flow rate of the foaming polymer as it enters the mold.

To investigate the effects of the discussed RRFM-specific skin processing factors, throughout the closing set of experiments, conventional rotational molding skin processing parameters were held fixed at values that previously proved to generate fine skin quality. That is, the skin processing time, the skin thickness, the mold and arm RPM and the ratio between them during skin processing, and the material constituting the skin will all be held fixed at the selected skin processing parameters stated in Table 4-6,

whereas the effects of varying the RPM of the mold during the foam filling segment, the respective filling time, and the time consumed by the translational mechanism to convey the mold up to the extruder nozzle will be studied in contrast with the integrity of the achieved moldings.

Table 4-6: Selected skin processing parameters

Skin Processing Parameter	Selected Value
Skin PP Grade (MFI [g/10 min])	PFSB786 (8)
Skin Thickness [mm]	5.5
Mold Rotations [RPM]	12
Arm Rotations [RPM]	3
Mold [RPM] : Arm [RPM]	4:1
Oven Temperature [^{o}C]	300
Oven Time [min]	27

Experimental groundwork in regards to processing solid skin in RRFM involves calculating the material amount pertaining to the desired 5.5 [mm] skin thickness based on the polymer density and mold volume, and then weighing the corresponding amount of plastic powder to generate the necessary formulation.

The skin-forming powder is then dry blended with ~2 [g] of yellow pigment (grade: PV Fast Yellow H2R – Clariant) in a mixing bag; this is to create a distinction between the skin and foam layers, as the foam layer is kept un-dyed for analysis purposes. The blend then introduced to the mold (cylindrical or flat) after spraying the mold with a mold release agent and the mold is closed accordingly.

4.3.2 Foamed Core

The desired foaming methodology in RRFM is one that generates foam capable of completely filling the hollow core within the preformed skin, has a near uniform cell density, and possesses adequate average cell size and cell density which comply with the predicted outcome of the pre-blended CBA-resin formulation.

Processing desired quality PP foams in RRFM is reliant on a range of factors. The first and foremost factor is the qualitative and quantitative composition of the resin-CBA formulation used to generate the foaming polymer via the extruder; that is, the respective amounts of blended PP-resin and CBA, the rheological and dimensional nature of the resin, and the characteristics of the CBA are particularly important to the quality of the foam achieved.

Moreover, the processing conditions employed by the extruder to generate the foam are an equally imperative factor in processing high quality foams. For the particularly used experimental setup, the operated extruder has three adjustable temperature zones within the barrel and one at the die; the adequate setting of each of these temperatures along with the selection of a congruent screw RPM contribute directly to the quality of the foams processed.

Lastly, the cooling method and duration in addition to ample mold venting, occupy a similarly important role in processing desired quality foams. Table 4-7 summarizes the controllable parameters concerning the foam processing segment of the RRFM technology and the respective terminology used for each parameter throughout the remaining portion of this thesis.

Table 4-7: Parameters governing the foam processing segment

Foaming Parameters Category	Parameters	Symbolic Representation
Formulation-Related	PP Resin Grade	N/A
	PP Resin Particle Size	N/A
	PP Resin Amount	$m_{polymer}$
	CBA Grade	N/A
	CBA %	%CBA
	CBA Particle Size	N/A
Processing-Related	Barrel Zone 1 Temperature	T_{BZ1}
	Barrel Zone 2 Temperature	T_{BZ2}
	Barrel Zone 3 Temperature	T_{BZ3}
	Extruder Die Temperature	T_{DZ}
	Extruder RPM	$RPM_{extruder}$
Other	Cooling Method	N/A
	Cooling Time	$T_{cooling}$
	Venting Method	N/A

Experimental groundwork performed to facilitate achieving a favored foam core includes establishing the resin-CBA amounts that conform to the desired VER (based on the concept discussed in section 2.2.2.4), while including an additional amount for expected losses within the extruder barrel and nozzle. Sifting the CBA to break up any clustered particulates is also necessary to avoid any undesired end-effects. The resin-CBA formulation is then dry-blended in an adequate mixing container for a sufficient period of time to achieve an evenly mixed blend.

The extruder is initially purged to flush-out any previous processing residues and the selected processing parameters are set by means of the extruder control panel. Subsequently, the blended formulation is manually fed into the extruder hopper and the foaming process is initiated as the screw RPM is increased.

4.4 Experimental Plan

A variety of strategies were employed to generate a comprehensive experimental study that proves the feasibility of processing integral-skin PP foams in RRFM; these are presented throughout the following sections.

4.4.1 RRFM - Feasibility through Materials Variation

The first experimental task involved verifying the ability of RRFM to generate foams based on PP-grades of different nature, displaying a calculated and expected VER, and are encapsulated by a solid skin. Furthermore, establishing the compatibility of such foams with the stipulated PP skin-processing grade (PFSB786) and parameters was another subtask to be achieved.

For this reason, three foam core comprising material grades (stated in section 4.2.1) were devised for testing; two PP homopolymers with different MFIs and one PP copolymer. A VER of 4, along with the corrected CBA gas yield values, were used to develop the respective foamable formulations. Details regarding the qualitative and quantitative aspects of these formulations will be presented in section 4.4.6)

4.4.2 RRFM – Process Repeatability

The second experimental task involved testing the repeatability of RRFM. This duty was set to be accomplished once finding a range of processing parameters and entities capable of generating at least three consecutive successful samples using a specific formulation. The definition of successful samples in this context is confined to samples that exhibit a solid non-degraded skin encapsulating a completely foamed core with no significant gaps resulting due to inadequate foam filling.

4.4.3 RRFM - Processing Parameters Variation

Subsequent to achieving successful experimental parameters ranges for each of the used formulations, a parametric variation was implemented to examine the affects of employing the parameters related to the median and two extremes of such ranges on the morphology of the obtained articles. The most important parameters varied in this experimental series included the extruder barrel temperatures at different zones (to vary the melt temperature of the polymer within the extruder), the extruder RPM, and the mold RPM during filling.

4.4.4 RRFM - VER Variation

The manufacture of integral-skin PP foams that attain an intentional variation in foam density was then assessed by processing cylindrical articles that exhibit a 6-VER completely foamed-core surrounded by a PP solid skin of 5.5 [mm] wall thickness. The processing parameters implemented to achieve this task were the ones that proved to exhibit a superlative performance throughout the testing series discussed in the former subsection.

4.4.5 RRFM - Mold Shape Variation

The capacity of RRFM to manufacture integral-skin foam core articles of different shapes and forms was then investigated by implementing the same experimental practice, using a similar adequate set of binding parameters, on the flat shaped mold, and then analyzing the resulting morphologies in order to explore the feasibility of the process in this respect.

4.4.6 Final Experimental Plan

Utilizing the materials characterization results discussed earlier in this chapter as well as the conclusions derived from the preliminary experimental trials, the particulars of the experimental plan that satisfies the feasibility analyses criteria presented in sections 4.4.1 to 4.4.5 were carefully developed. The corresponding plan is thoroughly documented in Table 4-8.

A hierarchical coding scheme was implemented to provide a distinct identification method for each of the conducted experiments and resulting moldings. Alphabetically, the foam-comprising PP resins were classified into the letter "A" for PFHL451H, the letter "B" for PF6523, and the letter "C" for PFSR257M. Numerically, for the experimental series of materials A and B, experiments #1 to #3 involved the process repeatability investigation; that is, conducting three identical processing cycles to investigate the likelihood of achieving a successful molding throughout all three runs.

Experiments #3 to #5 were conducted with the ultimate goal of investigating the effects of varying significant processing parameters such as the extruder barrel and die zones temperatures, screw RPM, and mold RPM during the foam filling segment, on the moldings' morphological characteristics. Experiments #6 and #7 were carried out to obtain cylindrical moldings exhibiting a PP solid-skin surrounding a VER=6 based foam core. Experiments #8 and #9 were conducted to investigate the opportunity of achieving flat plate shaped solid-integral-skin moldings exhibiting 6-fold and 4-fold expanded foam cores, respectively.

Table 4-8: Experimental plan to investigate the feasibility of processing integral-skin PP composites in RRFM (Materials A and B)

	Code	Foam Material	VER	$m_{polymer}$ (g)	%CBA	T_{BZ1} [^{0}C]	T_{BZ2} [^{0}C]	T_{BZ3} [^{0}C]	T_{DZ} [^{0}C]	$RPM_{extruder}$	RPM_{mold}	$T_{cooling}$ [min]
Cylindrical Mold	A1	Resin A PFHL451H	4	380	1.14	170	180	195	180	85	16	45
	A2		4	380	1.14	170	180	195	180	85	16	45
	A3		4	380	1.14	170	180	195	180	85	16	45
	A4		4	380	1.14	175	185	200	180	70	8	45
	A5		4	380	1.14	165	175	190	180	100	12	45
	A6		6	265	1.89	170	180	195	180	85	16	45
	A7		6	265	1.89	175	185	200	180	85	16	45
	B1	Resin B PF6523	4	385	1.16	155	170	185	170	85	16	45
	B2		4	385	1.16	155	170	185	170	85	16	45
	B3		4	385	1.16	155	170	185	170	85	16	45
	B4		4	385	1.16	165	180	195	170	85	16	45
	B5		4	385	1.16	160	175	190	170	85	16	45
	B6		6	300	1.92	160	175	190	170	85	16	45
	B7		6	250	1.92	155	170	185	170	85	16	45
Flat Mold	A8	PFHL451H	6	250	1.89	175	185	200	180	85	16	45
	A9		4	350	1.14	175	185	200	180	85	16	45
	B8	PF6523	6	250	1.92	175	185	200	180	85	16	45
	B9		4	350	1.16	175	185	200	180	85	16	45

A different experimental approach was followed throughout the experiments conducted using material C. The reason behind such change was the compatibility issues faced when using this PP grade with Celogen AZ-120 during the preliminary experimental trials. The large difference between the melt temperature of PFSB257M (Tm ≈150 [^{o}C]) and the decomposition range of Celogen AZ-120 (≈203 [^{o}C] – 213 [^{o}C]) causes the plastic resin to exhibit an exceedingly weak melt strength when processed at temperatures high enough for the decomposition of the CBA. Conversely, if the rein-CBA blend is processed in the extruder with the intention of foaming at the regular resin processing temperatures (≈150 [^{o}C]), the CBA does not completely decompose, hence demoting the desired expansion attitude. Figure 4-5 (a) illustrates a cylindrical molding sample cut-out where an event entailing the first discussed case took place, whereas Figure 4-5 (b) illustrates another event magnifying the second mentioned case.
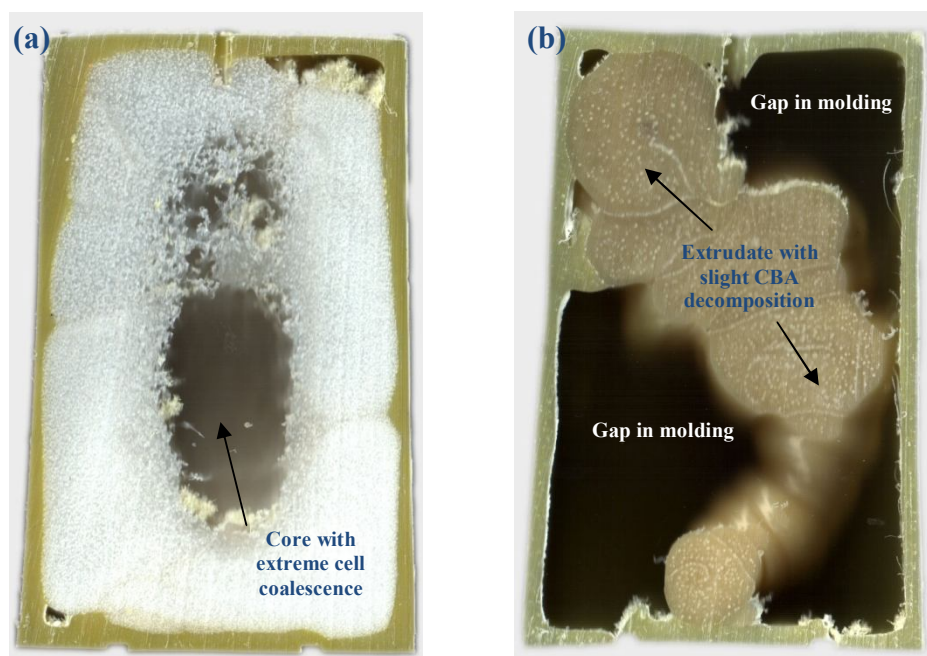
Figure 4-5: PFSR257M foam core - (a) High foam processing temperature causing weak melt strength (b) Low foam processing temperature - non-decomposed CBA

Conclusively, the devised experimental work pertaining to resin C was solely focused on developing a strategy that just simply proves that processing integral-skin foamed core cylindrical and flat shaped articles exhibiting a foam core based on the PP copolymer PFSR257M is achievable. Based on this rationale, the experimental plan entailing the final seven experimental scenarios related to this resin is presented in Table 4-9.

Table 4-9: Experimental plan to investigate PFSR257M as a foam core comprising material

Cylindrical Mold Experiments											
Code	Foam Material	VER	$m_{polymer}$ [g]	%CBA	T_{BZ1} [°C]	T_{BZ2} [°C]	T_{BZ3} [°C]	T_{DZ} [°C]	$RPM_{extruder}$	RPM_{mold}	$T_{cooling}$ [min]
C11	Resin C PF SR257M	4	380	1.14	160	175	190	170	60	16	45
C22		4	380	1.14	150	160	180	170	85	16	45
C33		4	380	3.5 (OT)	135	150	165	165	95	16	45
C44		4	380	1.14	155	160	170	160	95	16	45
C55		4	380	1.14	145	155	160	150	100	16	45
C66		4	380	1.14	145	155	160	150	100	16	45
Flat Mold Experiment											
C77	PF SR257M	4	350	1.14	150	160	170	160	100	16	45

As observed in the Table 4-9, a variety of methods were employed to investigate the processing of PFSR257M as a foam-core comprising material at a VER value of 4. The first experiment, C11, investigated foaming at a temperature that would facilitate the decomposition of Celogen AZ-120 with little extruder screw action. Then, experiment C22 involved a systematic reduction in the extruder barrel temperatures alongside an increase in the screw RPM. Experiment C33 involved further reduction in the barrel temperatures, an increase in the screw RPM, and the usage Celogen OT ($T_{decomposition}$ ≈159 [°C]) as the foaming agent.

Experiment C44 entailed using Celogen AZ-120 as the blowing agent, while setting the barrel zones temperatures closer to each other and increasing the screw RPM. Experiment C55 involved reducing the barrel temperatures further and reducing the increments by which they increase from one barrel zone to another, while increasing the screw RPM to promote the CBA decomposition. Afterwards, experiment C66 comprised a replication of experiment C55 so as to ensure that the achieved parameters are functional.

Finally, experiment C77 involved achieving an integral-skin foam core flat shaped part by adapting the most successful formulation produced through experiments C11-C66.

4.5 Summary

In summary, a comprehensive experimental plan was systematically devised to consider the diverse aspects that govern the RRFM process and prove its feasibility as a reliable and efficient technology in the realm of manufacturing integral skin PP foams. The particulars of the plan were based on a variety of scientific materials characterization techniques in addition to a preliminary set of exploratory experiments that magnified a range of processing aspects simultaneously pertaining to the used materials formulations and the novel RRFM technology.

Next, Chapter 5 presents and evaluates the various results obtained throughout conducting the designed experimental plan.

Chapter 5: Experimental Results and Discussion

5.1 Introduction

The experimental plan devised in Chapter 4 was carefully implemented using the custom-built industrial-grade lab-scale experimental setup specifically constructed and developed to successfully execute the RRFM process.

All through this chapter, the various results linked to the executed experimental runs will be presented and analyzed in detail. The overall skin and foam morphologies were inspected through a set of micrographs obtained by means of scanning electron microscopy (SEM). Solid integral-skin portions were characterized in terms of skin thickness uniformity, surface roughness, and overall skin quality. Foam structures were analyzed based on the achieved average foam density, cell population, and average cell size.

The obtained samples were examined for the quality of the interface binding the adjacent skin-foam layers. The consistent functionality of the insulated interface concept was evaluated throughout the different skin-foam blends.

5.2 Post-Experimental: Specimen Handling

The different moldings generated according to the employed experimental plan were first weighed in order to verify the compliance of the created specific material formulations with the experimentally achieved VER. The samples, cylindrical or flat-plate shaped,

were then cut using a uni-directional revolving powered band saw (Figure 5-1); this is to minimize the effects of the shearing action resulting from the cutting method on the attained cross-sections.

Figure 5-1: Sample cutting procedure

Cylindrical shaped samples were cut open through their absolute center, whereas flat shaped samples were cut once through their absolute center and once near each of the two opposite ends present at the longest dimension of the molding; this choice in cutting locations aids in magnifying processing specifics such as the degree of foam filling, the success of the venting procedure, the skin-foam interface, and the extent of variation in foam density. Furthermore, it facilitates in obtaining additional sample masses to be used particularly for SEM and foam density analysis.

The pieced samples were then scanned using a flat-bed scanner and the resulting images were imported into Adobe Photoshop CS ©. Utilizing the capabilities of the software package, a magnetic lasso tool was used to precisely trace the boundary separating the skin and foam layers. Afterwards, a 30% transparent black-colored mask was applied onto the foam layer of each molding in order to emphasize the overall

morphology; since the "naturally" white foam color interferes with the background of this document.

5.3 Experimental Results

5.3.1 Experimental Series A

The first experimental series involved processing articles exhibiting a PFSB786 solid integral skin ($\approx$5.5 [mm] thickness) binding a PFHL451H completely foamed core. The implemented experimental procedure within this category generated an entirely successful set of moldings; Figure 5-2 depicts a 3-dimensional photographic representation of a typical molding achieved using the employed materials formulations and parameters within this series.

Figure 5-2: Typical cylindrical molding generated throughout experimental Series A

5.3.1.1 Recorded Experimental Values

A variety of entities were documented along the course of the conducted experiments; these include: the processing melt temperatures, the melt pressures, and the final weight of the generated samples. Table 5-1 presents the respective log associated with each of the conducted processing runs according to experimental Series A.

Table 5-1: Measured parameters throughout the experimental Series A

Experiment Code	Constituents	Processing T_{melt} [^{o}C]	Processing Melt Pressure [PSI]	Skin Weight [g]	Overall Part Weight [g]
A1	Skin: PFSB786 (MFI 8 g/10 min) / Foam: PFHL451H (MFI 2 g/10 min)	171 - 183	195 - 0	280	615
A2		170 - 183	200 - 0	280	618
A3		172 - 181	200 - 0	280	613
A4		178 - 185	180 - 0	280	618
A5		171 - 176	225 - 0	280	620
A6		175 - 181	200 - 0	280	460
A7		181 - 187	150 - 0	280	483
A8		176 - 182	150 - 0	280	481
A9		172 - 183	170 - 0	280	533

The melt temperature value is recorded and displayed on the respective extruder control panel by means of a thermocouple that is placed in a designated location that allows it to be in direct contact with the extruder barrel contents. The processing melt temperature range shown in the table entails the resulting range of observed temperatures spanning the time period starting at the introduction of the foamable formulation to the hopper of the extruder and ending at the completion of the foam filling segment. The magnitude of the melt temperature is set by a combination of user entered values related to the barrel zones' temperatures and the screw [RPM], and usually starts at a lower value and then increases during extrudate pumping due to the thermal and frictional factors imposed by the foaming action.

The magnitude of the melt pressure within the barrel is directly influenced by the melt temperature, the desired degree of foaming, and the characteristics of the used material formulation. It can be readily observed from the tabulated values that the melt pressure decreases with increasing melt temperature and decreasing degree of expansion.

5.3.1.2 Validation through Repeatability

Three consecutive successful moldings were achieved as a result of conducting processing scenarios A1, A2, and A3; these are depicted in Figure 5-3. The slight visual variation displayed between the first 2 moldings (A1 and A2) and the third molding (A3), which favors A3, is justified by the particularly improved venting methodology as well as the reduction of the yellow pigment used to comprise the skin. Such practice was employed henceforth due to the resulting improved overall molding aesthetics.
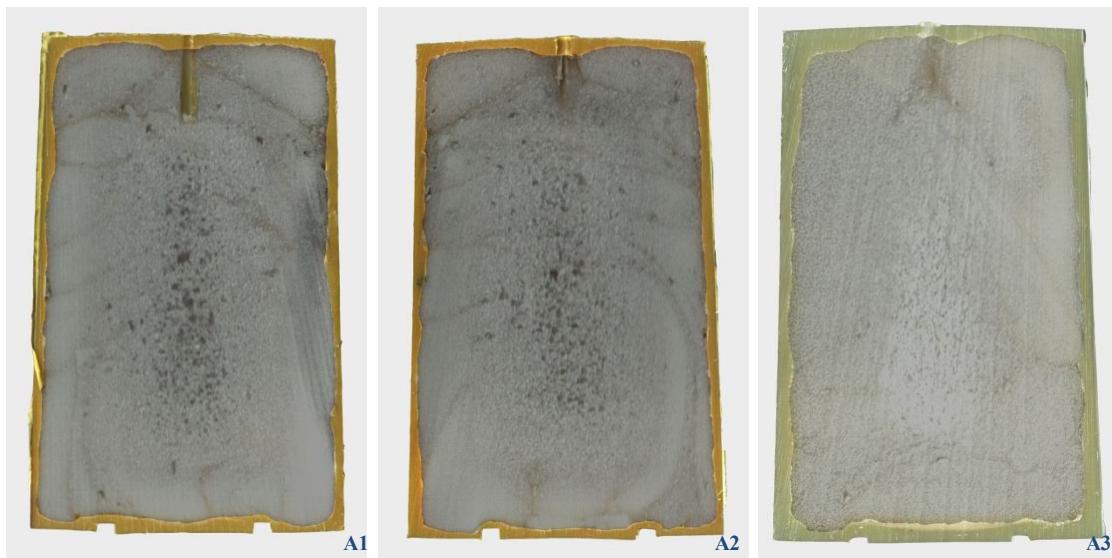
Figure 5-3: Scanned cylindrical moldings associated with experimental scenarios A1-A3

The achievement of three consecutive successful moldings confirmed several facts. First, it was established that a high degree of control over the fundamental

processing environment and critical parameters binding RRFM is comprehendible and has been accomplished. Moreover, no significant filling gaps or perforations at any location throughout the skin-foam boundary or within the distinct skin and foam layers were observed throughout moldings A1-A3. Thus, the success of PFHL451H as a foam-core comprising PP grade in RRFM, which is compatible with skin material PFSB786, was validated.

Additionally, a practical demonstration of the insulating interface's functionality and consistency was established for the presented formulations and is displayed on the resulting moldings.

5.3.1.3 Processing Parameters Variation

<u>Visual Analysis</u>

Figure 5-4 depicts the cylindrical moldings associated with experimental scenarios A3-A5, where a variation in processing parameters was executed.

A3	A4	A5
Intermediate T_{melt} and RPM_{screw}, and Highest RPM_{mold}	Highest T_{melt}, Lowest RPM_{screw}, and lowest RPM_{mold}	Lowest T_{melt}, Highest RPM_{screw}, and Intermediate RPM_{mold}
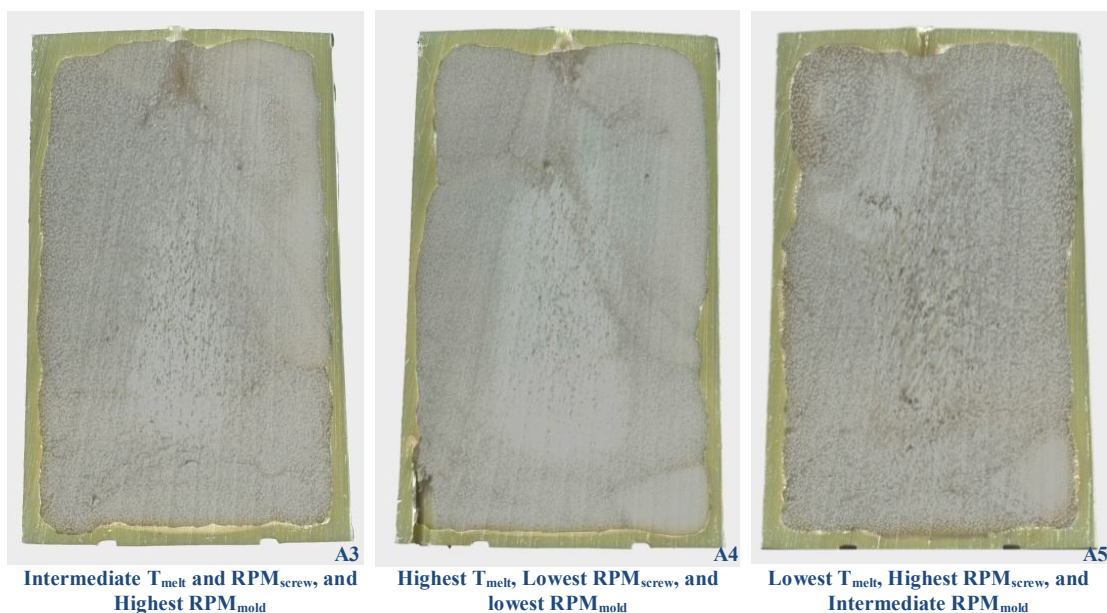
Figure 5-4: Cylindrical moldings associated with experimental scenarios A3-A5

When visually comparing the respective pictorials corresponding to each molding, it is apparent that experimental scenario A4 yielded the most uniform cell-sized foam core. Closer visual inspection of molding A4 revealed minimal cell coarsening present within the cellular community near the absolute center of the molding; this can be attributed to the incomplete evacuation of the processing gasses prior to the stabilization and recrystallization phase of the foam structure.

Processing scenario A5 created the coarsest cellular structure all about the molding's foam core. Evidence of incomplete CBA decomposition is present when inspecting the top left corner of the presented illustration (the actual bottom right corner of the molding and the furthest point from the extruder nozzle). The reasons behind the displayed phenomenon can be attributed to the relatively lower melt temperature endured by the foamable formulation during the foam filling segment of this experimental run (171-176 [^{o}C]), which was not high enough to decompose the CBA, even though the extruder's screw RPM was at its maximum value.

Molding A3 appears to demonstrate the finest skin thickness uniformity among the generated moldings. There is no evidence of significant cell coarsening or cell coalescence throughout the foam core of this sample. Altogether, moldings A3-A5 displayed a successful skin-foam bond at the insulated interface location associated with the filling gate.

Morphology Investigation

Random samples were obtained from moldings A3-A5 for inspection using SEM (Figure 5-5). For all three samples, SEM imaging revealed a strong bond between the distinct skin and foam layers; this is justified by the fact that the foaming extrudate is introduced

within the skin boundaries as the skin is still in a semi-molten/soft state, which allows the adherence of both layers together as the cooling process is commenced.
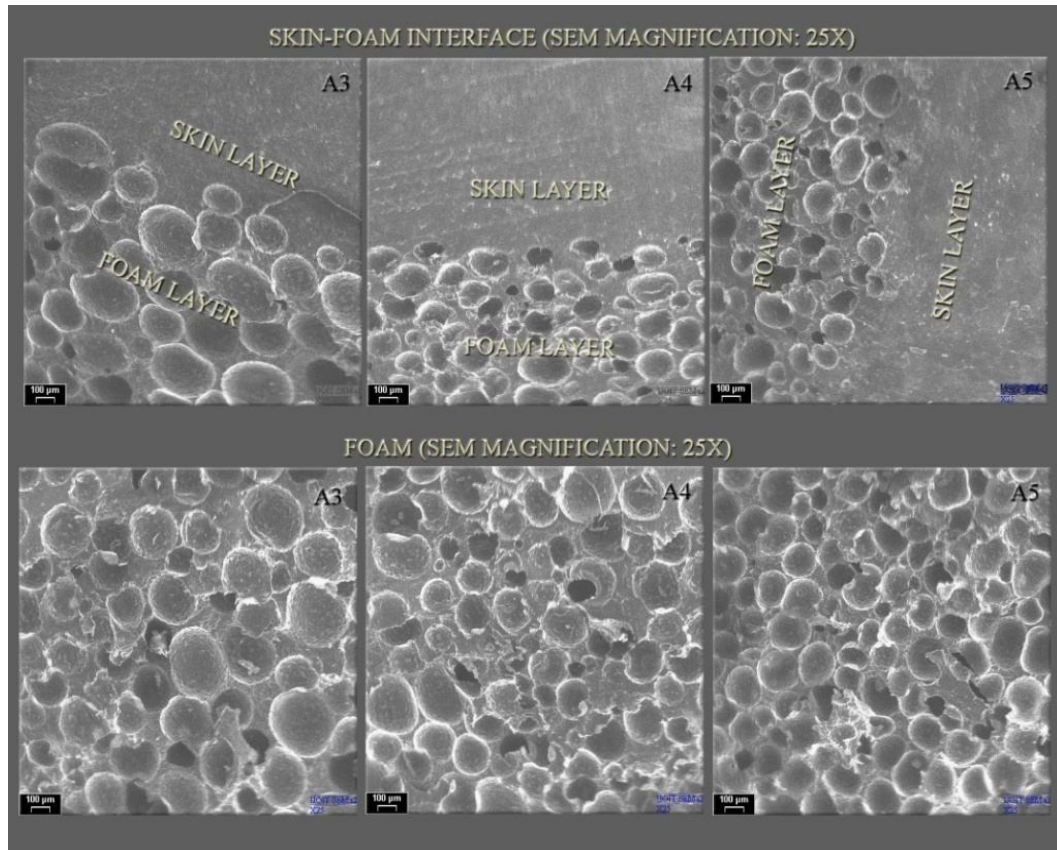
Figure 5-5: SEM imaging of Samples obtained from moldings A3-A5

Obtained foam morphologies were investigated with respect to their cell population, which is represented by Equation (5.1) [40]:

$$N = (n_{cells})^{3/2} \cdot VER$$

(5.1)

In equation (5-1), n_{cells} is the number of cells per unit area of 1 [cm^2], and is counted using a scaled SEM micrograph at a suitable location of the foamed article. Although the foam cells shown on the obtained micrographs were carefully counted and marked to avoid repeated, extra, or less counts, an uncertainty value of $\pm$ 20 [cells/cm^2]

was yet set throughout all the counting practices performed in this thesis; this is to account for the various errors in counting as well as the certainty that the counted object is a foam cell.

The value of n_{cells} for a selected sample within this series was found to be 1140 ± 20 [cells/cm^2] and the corresponding cell population density was determined to be 153963.3 ± 360 [cells/cm^3]. Subsequently, the computation of the average cell size ($D_{average}$) was conducted using Equation (5.2) [40]:

$$D_{average} = \sqrt[3]{\left[(VER-1) \cdot \frac{6}{\pi \cdot N} \right]}$$

(5.2)

The calculated average cell size for the presented case was 334 ± 25 [µm]. This indicates that the achieved foams within this series are particularly close to a fine-cell classification.

<u>Foam Density Analysis</u>

Samples A3-A5 were each cut further to extract cubes from the respective foam cores, exhibiting a minimum volume of 1 [in^3], in order to calculate and quantitatively assess the particular foam densities according to the standard approach (ASTM D1622 – 08). Based on this principle, four cubes were obtained from each sample, two of which were extracted from the top and bottom ends of the molding, and two from around the central volume of the molding.

A bar chart was then constructed as per Figure 5-6 in an attempt to evaluate the foam density distribution within each sample. Subsequent to a set of basic statistical calculations, it was concluded that sample A4 entailed the least deviation in foam density across its volume (standard deviation ≈10.3 [kg/m^3]), whereas sample A3 experienced the most divergence in foam density (standard deviation ≈39.2 [kg/m^3]) across its volume.

The obtained results confirmed the initial visual observations stated formerly; that is, the processing temperatures and screw RPM imposed by processing scenario A4 resulted in the most successful and uniform foam-core among all three samples. The maximum calculated standard deviation in foam densities across samples A3 to A5 was found at sample A3 to be ≈14% of the total average foam density calculated for that sample; although it conforms to an extreme case, this value is still considered acceptable and is significantly reduced as the processing entities reach their optimal levels.

Figure 5-6 displays the global average foam density associated with each sample, which was calculated based on averaging the previously-determined location-dependant individual foam densities. Using such entities, the deviation in average foam density between all three samples was analyzed to be 3.76 [kg/m^3].

Calculated Foam Densities for Moldings A3-A5

	top	middle1	middle2	bottom	σ (STD DEV)	Average Foam Density
A3	288.28	292.91	311.32	221.69	39.19	278.55
A4	289.19	275.98	279.66	298.98	10.32	285.95
A5	277.95	280.30	260.37	315.01	22.87	283.41
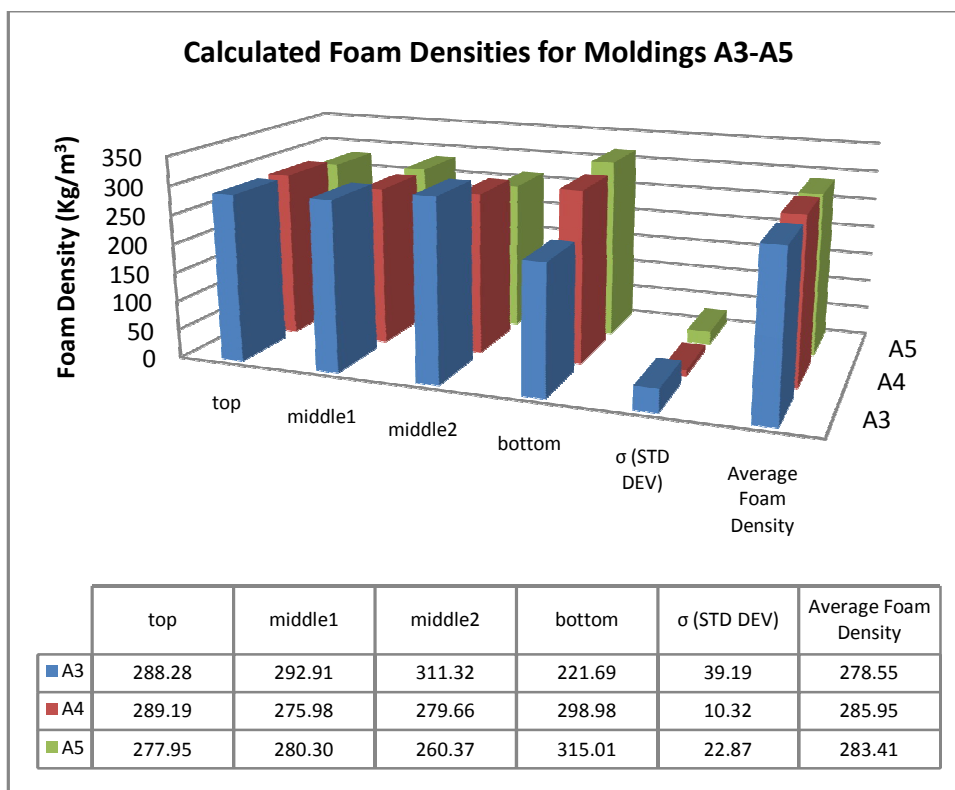
Figure 5-6: Calculated foam densities for moldings A3-A5

The relatively low variation in average foam density across the three samples verifies the consistency in generating comparatively accurate processing batch formulations in RRFM, furthermore, it implies that the implemented processing conditions for the PP grade used for foaming within this series produce foaming extrudate with reasonably uniform density along its length.

<u>Skin Thickness Uniformity Analysis</u>

The achieved moldings were also characterized in terms of skin thickness uniformity to investigate the effects of varying the processing parameters on the overall skin quality.

Thickness uniformity is commonly mathematically interpreted by calculating the statistical root mean square (RMS or R_q) for a preset theoretical thickness of 5.5 [mm] [40]:

$$R_q = \sqrt{\frac{1}{N}\sum(a-5.5)^2}$$
(5.3)

where N is the number of skin thickness measurements carried out at different locations throughout the part (set at 10), and "a" is the value obtained for each measurement in [mm]. The accuracy in determining the level of skin uniformity increases with the conducted amount of skin thickness measurements. The calculated R_q values pertaining to the solid-skin uniformity associated with samples A3-A5 are presented and compared in Figure 5-7.
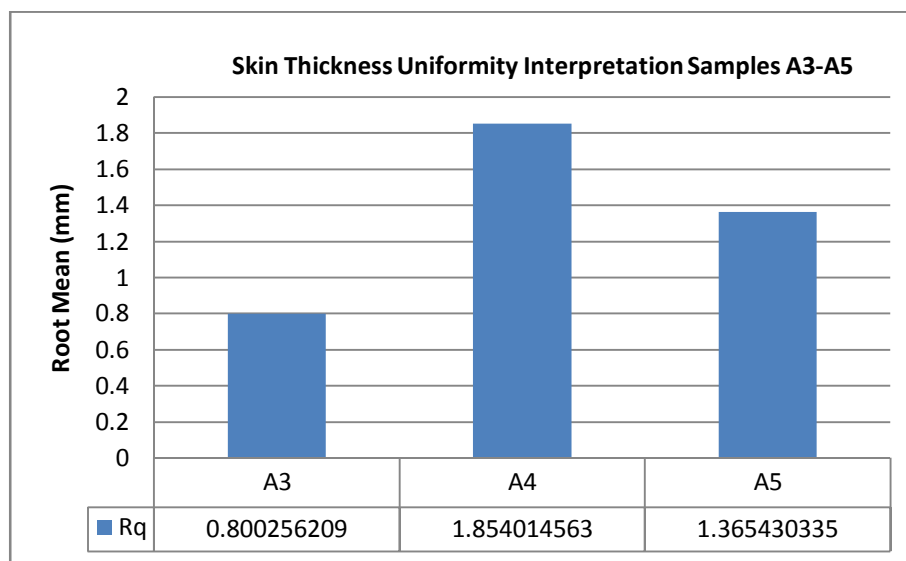
Figure 5-7: Skin thickness uniformity analysis of samples A3-A5

When observing the displayed results, it is evident that the solid-skin thickness was most uniform throughout sample A3, as only a variation of about 0.8 [mm] was demonstrated across the skin structure (≈14.5% variation). Additionally, sample A4 had the least uniform skin thickness throughout its cross-section (33.6% variation). This result essentially implies that the increased RPM of the mold during the foam filling segment enhanced the uniformity of the resulting skin.

5.3.1.4 VER Variation

Samples A6 and A7 were generated with an intention to test the applicability of processing integral-skin foam core articles of lighter weight, than the ones achieved during preliminary experimentation (i.e. 6-VER), by utilizing respective PP grades investigated within this series of experiments.

In terms of the used processing conditions, the processing temperatures employed throughout experiments A6 and A7 were similar to these used for experiments A3 and A4 respectively, while the mold RPM was set to that of experiment A3, in compliance with

the conclusions devised in the previous section. Figure 5-8 depicts the obtained samples associated with the aforementioned experimental runs.
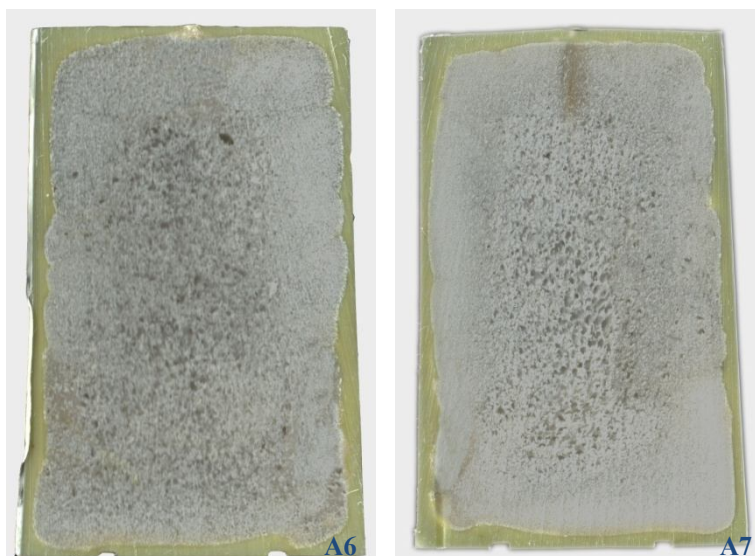
Figure 5-8: Resulting sample cut-outs, A6 and A7 (6-VER)

The resulting samples were investigated using SEM to analyze their overall morphologies with respect to the previously attained ones. Skin-foam interface and foam structures SEM images for samples A6 and A7 are depicted in Figure 5-10.
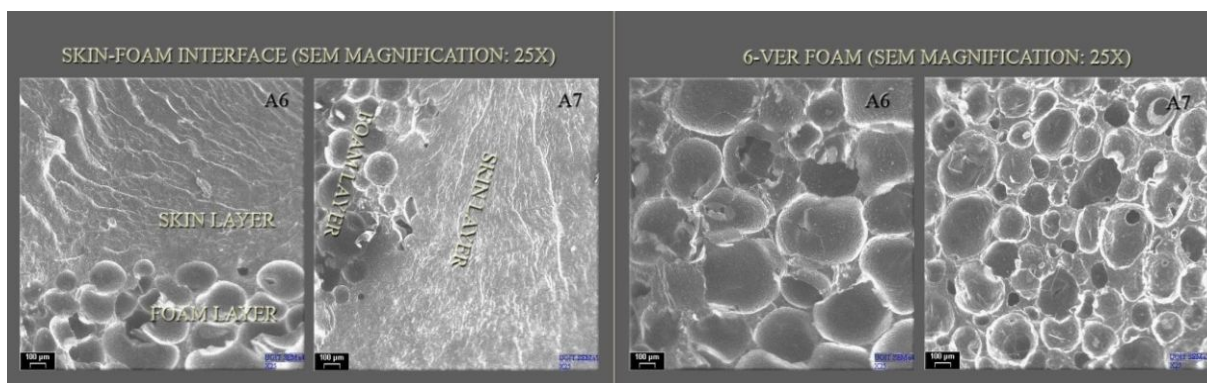
Figure 5-9: SEM imaging associated with samples A6 and A7

The analyzed skin-foam interface micrographs display a consistently strong bond between the skin and foam comprising entities for the respectively used material

formulation within this experimental series; the skin and foam layers are well integrated with no visible seams or parting marks present at the boundaries.

The acquired foam SEM images reveal that the respective distance between the cell boundaries achieved for experimental runs A6 and A7 is shorter than that observed for the ones linked to the 4-fold experimental runs; i.e. the percentage of voids is increased as the VER of the generated foam is increased; this is due to the increased amount of foam bubbles instigated by the larger percentage of CBA blended into the foamable formulation.

An average cell size value of 389 ± 25 [µm] was calculated for a selected sample within resulting from experiments A6 and A7, which allows concluding that the average cell size for a 6-fold expanded foam structure associated with the aforementioned materials formulation can yet achieve a fine-cell size by optimizing the experimental parameters.

The generated 6-fold samples, A6 and A7, were then subjected to the same foam density analysis performed on samples A3-A5. Figure 5-10 depicts the resulting bar charts representing the foam density distributions within each sample and comparing the global average foam densities of both samples.

The resulting graphical comparisons displayed that molding A7 attained higher divergence in foam density across its volume (standard deviation ≈ 20.47 [kg/m^3]), whereas molding A6 encompassed a more uniform density distribution (standard deviation ≈ 13.78 [kg/m^3]); this implies that the lower processing temperatures in this case resulted in a more uniform bubble stabilization and a better crystallization behavior. The deviation between the foam densities of both samples was calculated to be 16.78 [kg/m^3],

which essentially suggests that a larger variation in foam filling consistency for the 6-VER samples was experienced over the 4-VER samples.

6-VER Integral Skin PP Foams - Foam Density Analysis of Series A

	top	middle1	middle2	bottom	σ (STD DEV)	Average Foam Density
A6	155.35	145.66	139.15	170.86	13.78	152.75
A7	205.02	164.31	159.33	177.30	20.47	176.49
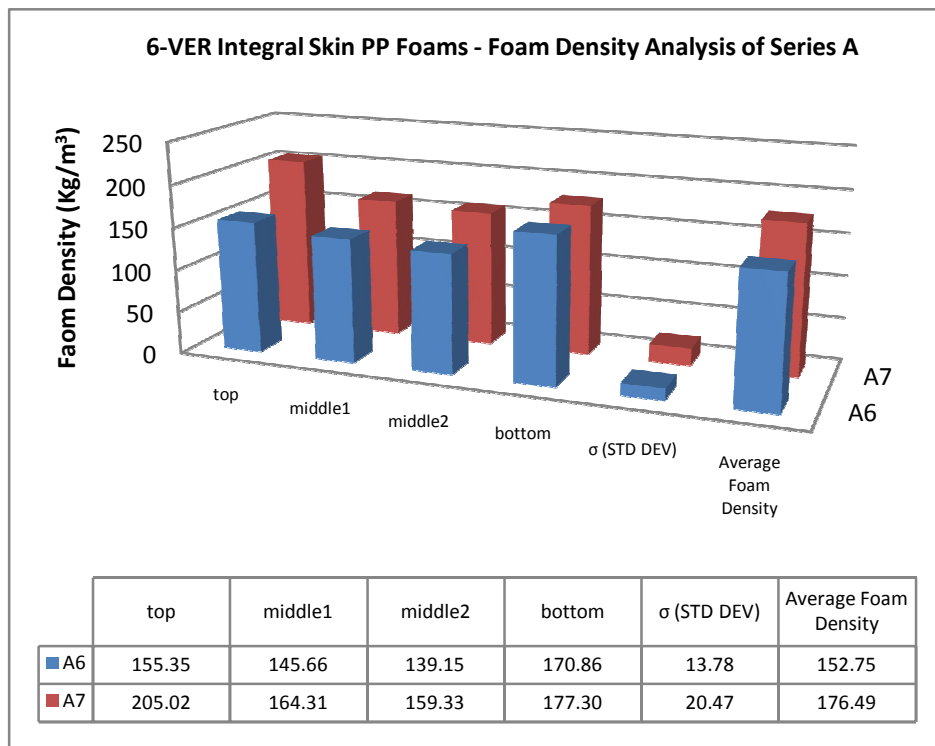
Figure 5-10: Foam density analysis of 6-VER integral-skin PP composites (Series A)

Average Foam Density Comparison PFHl451H (4-VER VS 6-VER)

	4-VER	6-VER
Average Foam Density	282.64	164.62
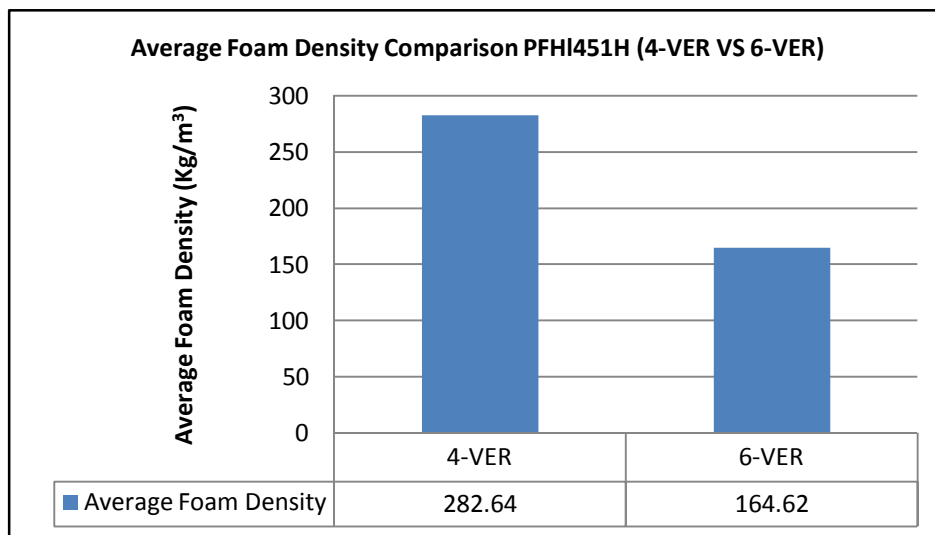
Figure 5-11: Average Foam Density Comparison (4-VER VS 6-VER)

Lastly, the average foam density values of all 4-VER and 6-VER cylindrical samples were respectively averaged and the results are displayed in Figure 5-11. The achieved weight reduction is evident when analyzing the results; this supported the success of RRFM in processing variant densities PP skin-surrounded foam composites.

5.3.1.5 Mold Shape and VER Variation

The final set of experiments within this series, namely A8 and A9, entailed using the most successful 6-fold and 4-fold foamable entities to generate a flat shaped molding resembling each. After conducting the pertinent experiments, the resulting articles were cut open and the achieved morphologies are illustrated in Figure 5-12.
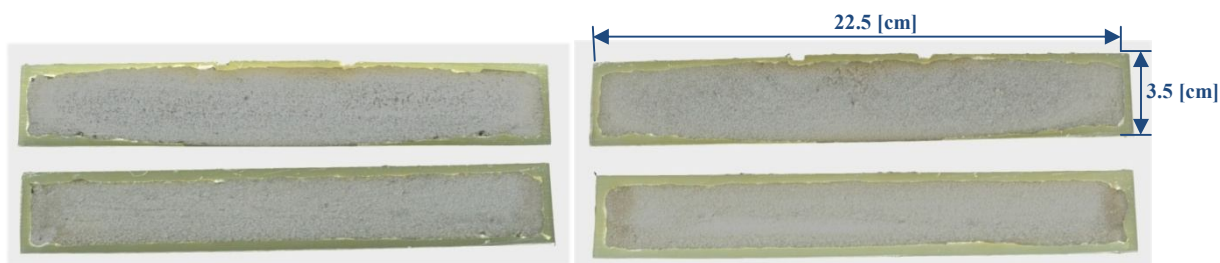
Figure 5-12: Molding A6 (6-VER) and Molding A7 (4-VER) - flat shaped samples

The displayed scans in Figure 5-12 illustrate the successful accomplishment of the task deployed for this respective set of experiments. Both, moldings A6 and A7, display excellent foam filling extents, the respective skin-foam interface areas are seamless, and the skin thickness is highly uniform along the volume of the molding, except for the filling location, where slight skin thinning occurred, due to the mold's vertical position during filling and the extensional forces employed by the foam on the skin in that area while in molten state.

The SEM micrographs associated with each of samples A6 and A7 are presented in Figure 5-13, where the orderliness and uniformity within the obtained cellular structure is emphasized.
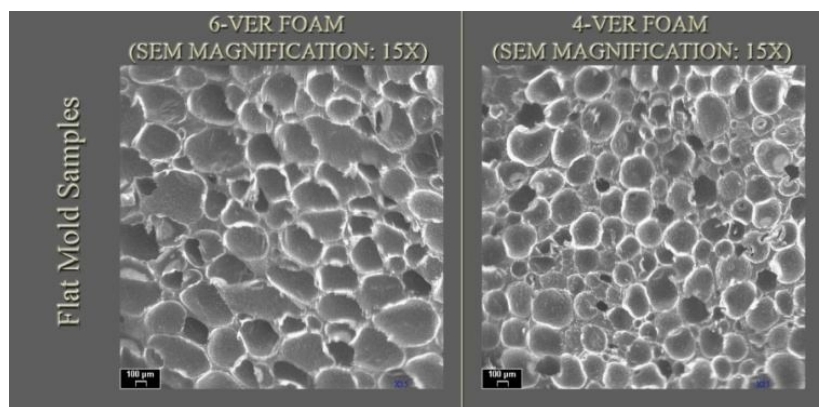
Figure 5-13: SEM micrographs attained for flat mold samples A6 and A7

Likewise, a foam density chart was constructed with respect to the conducted experimental runs and subsequently presented in Figure 5-14.

	Far End 1	Center 1	Center 2	Far End 2	σ (STD DEV)	Average Density
■ A6 (6-VER)	211.93	160.92	149.51	207.86	31.96	182.55
■ A7 (4-VER)	207.14	219.29	219.36	211.53	6.04	214.33
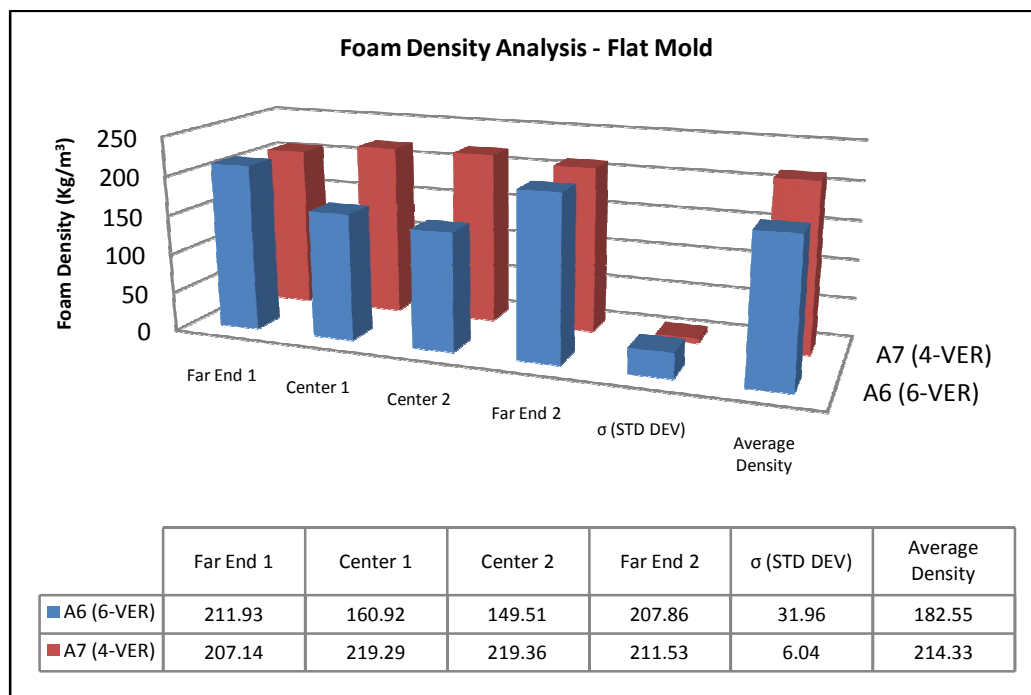
Figure 5-14: Foam Density Analysis - Flat Mold

The main conclusions drawn from the chart were that the 4-fold expanded core exhibited a more uniform cellular density distribution among its volume when compared to the 6-fold analog. However, the achieved overall average foam density of the 6-fold article complied more consistently with the previous average foam density results associated with the cylindrical mold experiments.

5.3.2 Experimental Series B

The second experimental series involved processing articles exhibiting a PFSB786 solid integral skin ($\approx$5.5 [mm] thickness) binding a PF6523 completely foamed core.

Figure 5-15: Typical cylindrical molding generated throughout experimental Series B

The implemented experimental procedure within this series was performed with a global objective of investigating the effects associated with varying the MFI of the foam-comprising PP grade on the overall morphology of the generated article; Figure 5-15

depicts a 3-dimensional photographic representation of a typical molding achieved using the employed materials formulations and parameters within this series.

5.3.2.1 Recorded Experimental Values

Similarly, a variety of entities were documented along the course of the conducted experiments; these include: the processing melt temperatures, the melt pressures, and the final weight of the generated samples. Table 5-2 displays the respective log associated with each of the conducted processing runs with regards to the engineered plan of experimental series B.

Table 5-2: Measured parameters throughout the experimental Series B

Experiment Code	Constituents	Processing T_{melt} [^{0}C]	Processing Melt Pressure [PSI]	Skin Weight [g]	Overall Part Weight [g]
B1	Skin: PFSB786 (MFI 8g/10 min) Foam: PF6523 (MFI 4 g/10 min)	169 - 178	180 - 0	280	650
B2		165 - 173	200 - 0	280	635
B3		165 - 177	180 - 0	280	630
B4		170 - 183	150 - 0	280	629
B5		169 - 174	150 - 0	280	611
B6		165 - 173	200 - 0	280	480
B7		166 - 175	220 - 0	280	475
B8		177 - 184	230 - 0	280	517
B9		175 - 185	200 - 0	280	560

5.3.2.2 Validation through Repeatability

Three consecutive successful moldings were achieved as a result of conducting processing scenarios B1, B2, and B3; these are depicted in Figure 5-16.
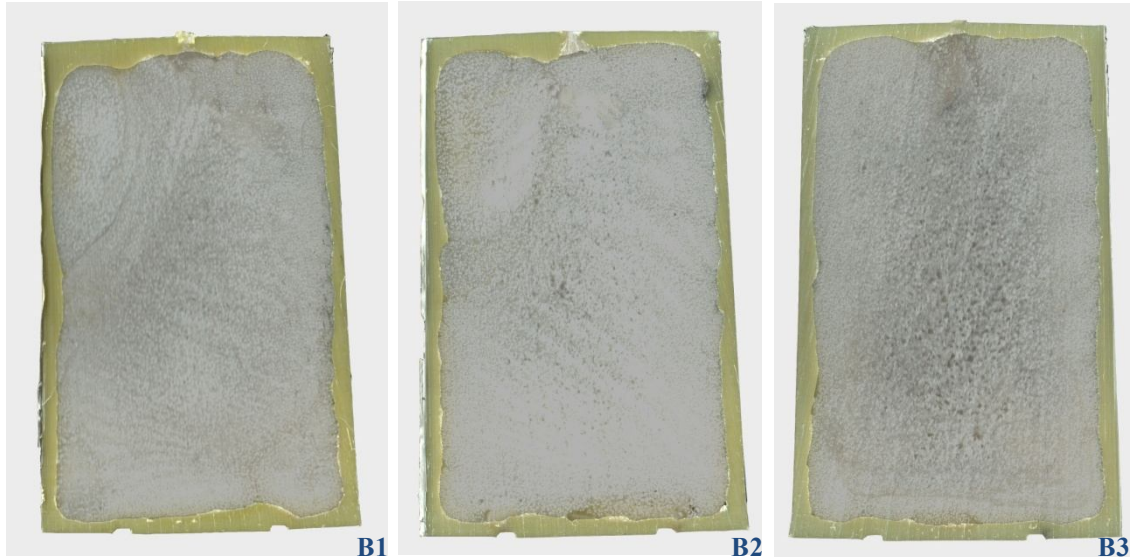
Figure 5-16: Scanned moldings associated with experimental scenarios B1, B2, and B3

The preliminary visual inspection of the obtained moldings revealed that, yet again, a high degree of control over the fundamental processing environment and critical parameters binding RRFM was accomplished. The resulting samples, B1-B3, bared no significant filling gaps or perforations at any location throughout the skin-foam boundary or within the distinct skin and/or foam layers. Thus, the success of PF6523 as a foam-core comprising PP grade in RRFM, which is compatible with skin material PFSB786, was also validated through the conducted process repeatability assessment experiments.

5.3.2.3 Processing Parameters Variation

Prior to conducting this experimental series, a decision was made to adapt the screw and mold RPM values that proved to produce the best results, in terms of skin thickness uniformity and foam distribution, throughout the entirety of the series. Thus, a screw and mold RPM of 85 and 16 were correspondingly set fixed for each of experimental trials to follow.

Visual Analysis

Figure 5-17 depicts the cylindrical moldings associated with experimental scenarios B3-B5, where a variation in processing temperatures was executed.

Close visual inspection of all moldings revealed incidents of cell coarsening particularly present within the cellular community near the absolute center of the obtained structures; this can be attributed to the incomplete evacuation of the processing gases prior to the stabilization and recrystallization phase of the foamed core. Also, incidents of solidified plastic residue were located across the central top position within all moldings (B3-B5). The reasons behind the displayed phenomenon can be attributed either to the incomplete evacuation of the purging PP grade from the extruder prior to instigating the foaming segment, or the presence of an undesired bond between the purge material and the foaming polymer in the extruder barrel.
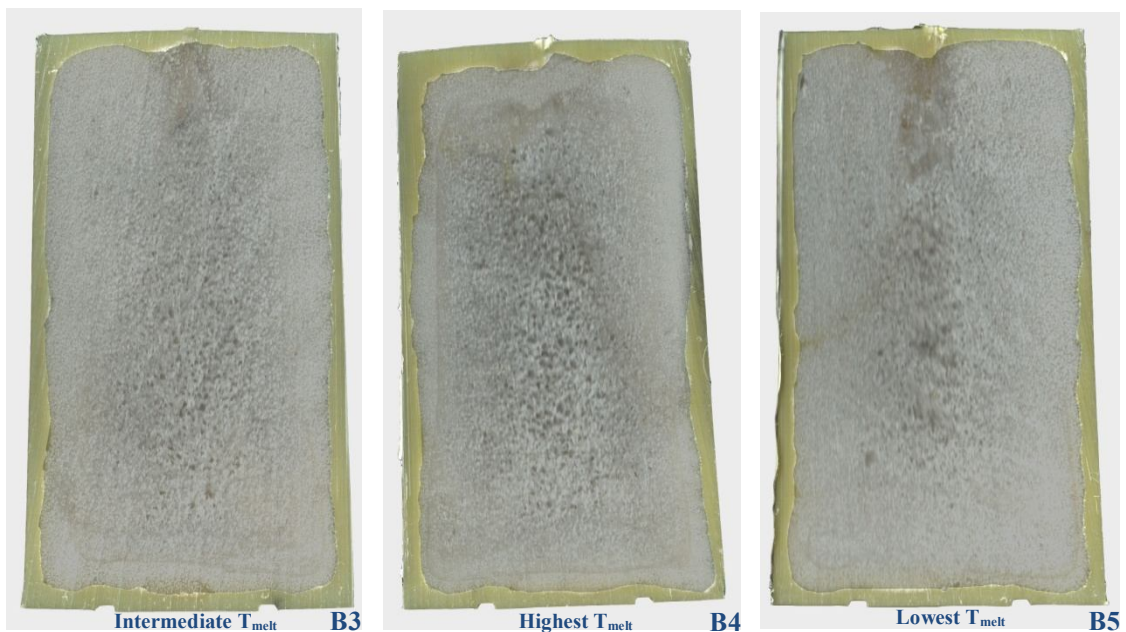
Figure 5-17: Cylindrical moldings associated with experimental scenarios B3-B5

Another reason that can cause this phenomenon is perhaps the lower extrudate melt temperature when initiating the foam pumping segment, which can be a cause of generating non-foamed PP extrudate at the top of the achieved moldings since this, is a location where the pumped extrudate is prompted to dwell first.

When comparing the respective pictorials corresponding to each sample cutout, it is apparent that experimental scenario B5 yielded the most uniform cell-sized foam core, this claim is valid since no extreme variations in visible cell density were discovered. It is also evident that sample B5 was followed by sample B3 and lastly sample B4 in the mentioned respect.

Furthermore, closer visual inspection revealed that moldings B3 and B4 demonstrate the finest skin thickness uniformity within the compared batch. This was confirmed by evaluating and comparing the RMS of 10 skin thickness measurements across all three moldings, yielding the results in Figure 5-18.

Skin Thickness Uniformity Interpretation

	B3	B4	B5
Rq	0.491660452	1.14093821	0.879073376
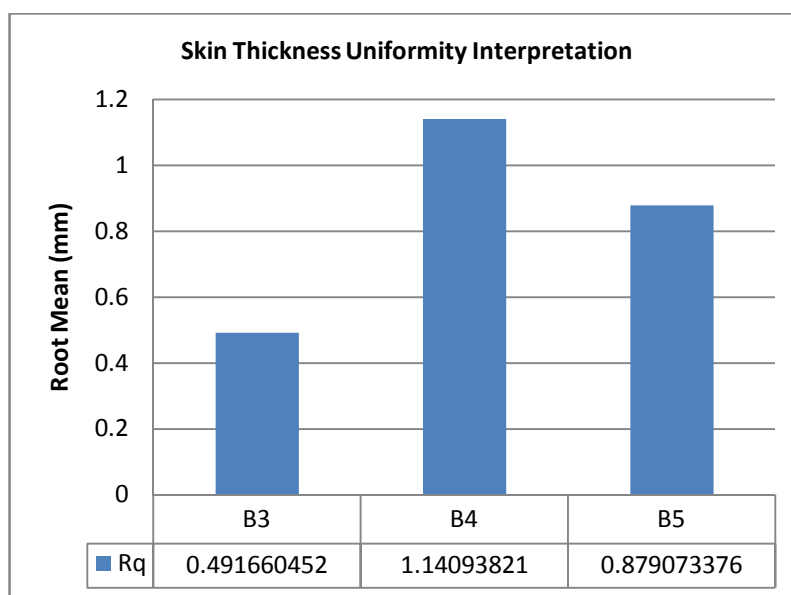
Figure 5-18: Skin thickness uniformity analysis (PFSB786 skin + PF6523 foam)

It is also noteworthy that all moldings within this series exhibited improved skin uniformity over their corresponding rivals in experimental Series A. This justifies the fact that increased mold RPM during the foam filling course improves the obtained skin morphology.

Lastly, moldings B3-B5 altogether display more aesthetically pleasant foam cores than these obtained for their analogs pertaining to Series A. This is possibly attributed to the lower die zone temperature imposed for the formulations within this series, which allows avoiding color change at the extrudate surface. Also, the higher MFI associated with the used foaming resin can contribute to the better core aesthetics, since the extrudate in this case flows more smoothly within the mold when pumped by the extruder and rotated for distribution.

<u>Morphology Investigation</u>

SEM was used to inspect a random set of samples obtained from moldings B3-B5 with the resulting micrographs illustrated in Figure 5-19.

When visually analyzing the outcomes, it can be concluded that a strong bond exists between the distinct skin and foam layers. The integration between both phases is apparent due to the absence of seams, parting lines, or dislocations close to or at the inspected boundaries.

The value of n_{cells} for a selected sample within this series was found to be 960 ± 20 [cells/cm^2], and the corresponding cell population density was determined to be 118978.1 ± 360 [cells/cm^3]. It then follows that the calculated average cell size value, associated with a random set of foam samples generated by means of experiments B3-B5, is 389 ± 25 [μm].
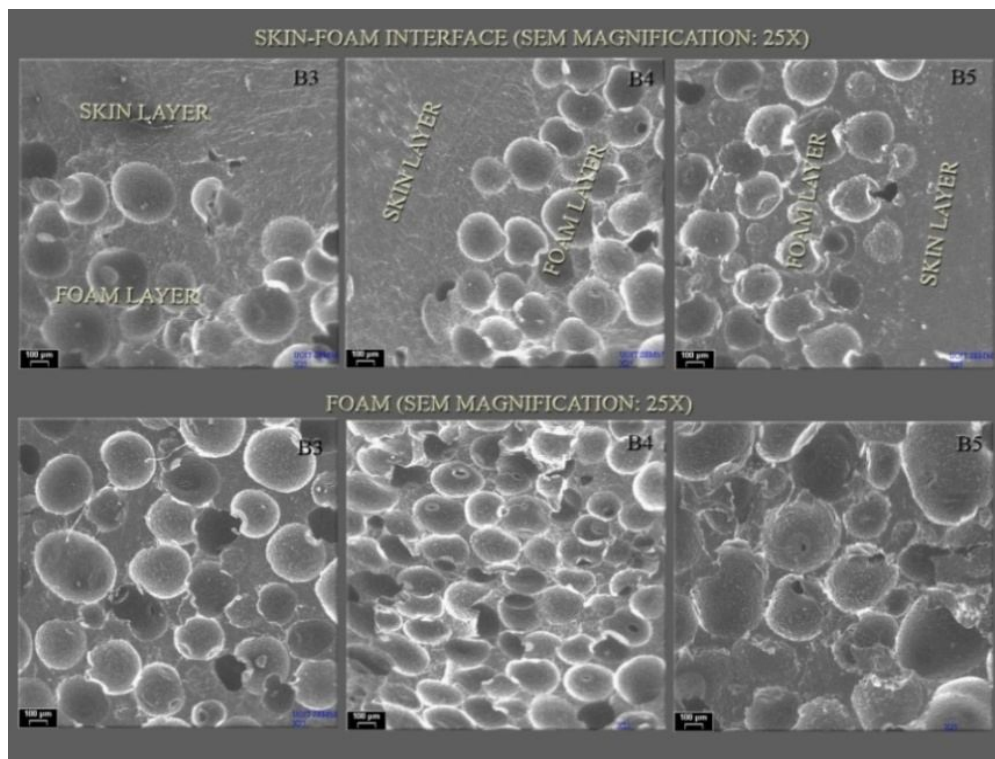
Figure 5-19: SEM imaging of Samples obtained from moldings B3-B5

Foam Density Analysis

Foam density samples were then extracted from moldings B3-B5 as per the method described during presenting the analyses pertaining to experimental Series A at an earlier section of this thesis; this to investigate overall foam density distribution within each sample and then compare the average foam densities of all samples.

A bar chart exhibiting the same structure as the one formerly presented in Figure 5-6 was then constructed in Figure 5-20 with the purpose of evaluating the foam density distribution within each sample. Observing the chart, it is apparent that throughout all samples, the top section has a higher foam density than that of the other sections; this is explained by the previously emphasized presence of non-foamed solid plastic residue at each of the samples in this area.

Basic statistical analysis then allowed concluding that sample B5, which corresponds to the lowest employed processing temperatures, entailed the least deviation in foam density across its volume (standard deviation ≈ 26.7 [kg/m^3]), whereas sample B3 experienced the most divergence in foam density (standard deviation ≈ 41.38 [kg/m^3]) across its volume. The obtained results confirmed that the processing temperatures and screw RPM imposed during processing scenario B5 resulted in the most uniform foam-core among all three samples.

Foam Density Measured at Selected Locations of Moldings B3-B5

	top	middle1	middle2	bottom	σ (STD DEV)	Average Density
B3	310.34	283.67	288.72	351.30	30.79	308.51
B4	322.89	253.98	260.46	333.77	41.38	292.78
B5	276.69	263.58	234.72	298.62	26.70	268.40
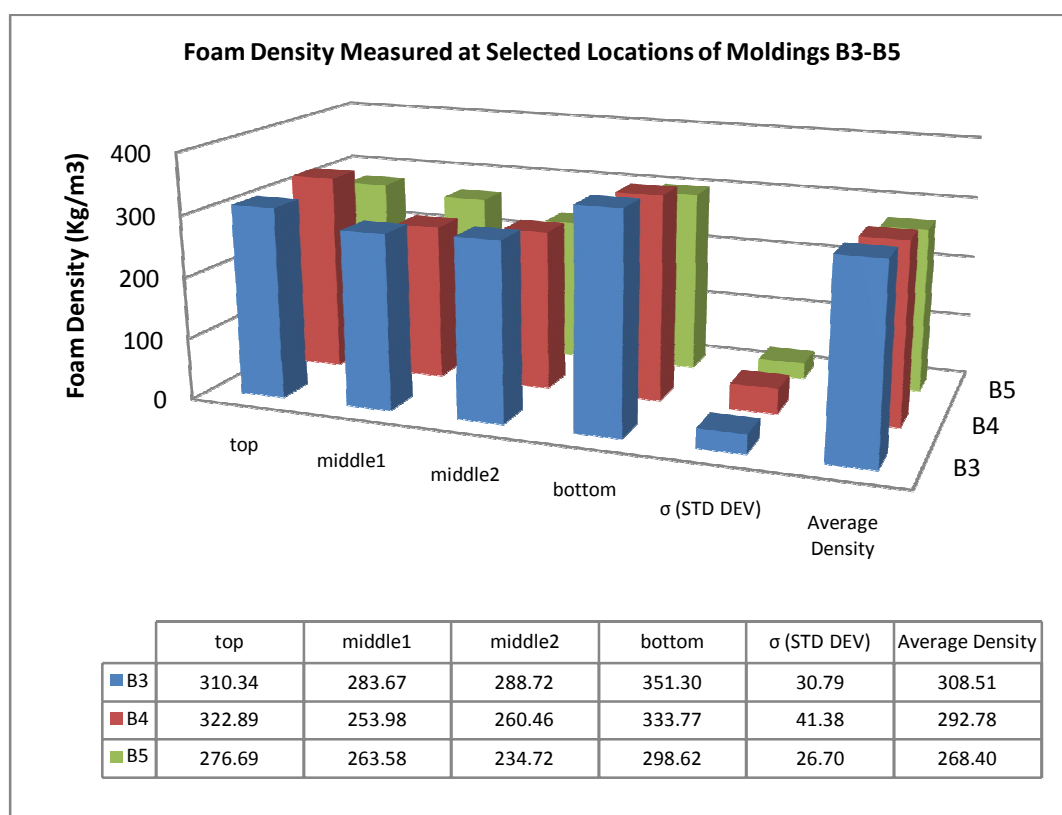
Figure 5-20: Calculated foam densities for moldings B3-B5

Furthermore, sample B5 was analyzed to have the lowest average foam density among the ones obtained through all 3 processing scenarios. When mathematically dividing the density of the bulk solid plastic PP resin PF6523 (900 [kg/m^3]) by the

average foam density of sample B5 (268.41 [kg/m^3]), a VER of $\approx$3.35 is obtained; which is certainly the closest VER value, obtained by far, to the theoretical value of 4 used in calculating the initial formulation constituents.

The errors generated within the experimentally achieved foam density values can be attributed to the losses in the blowing gases experienced within the foaming extrudate at the extrusion port, during the cooling and foam stabilization segments of the RRFM cycle, and due to the generally weak melt strength of PP.

The determination of the correction factor corresponding to the CBA-resin formulation expression is to be investigated as an opportunity; however, the aspects of such opportunity are beyond the scope of the material presented in this thesis.

5.3.2.4 Foam Density Variation

Samples B6 and B7 explore the applicability of processing integral-skin foam core cylindrical moldings, with a 6-fold based foam core, using PF6523 as the foam-comprising PP grade.

In terms of the used processing conditions, the processing parameters employed throughout experiments B6 and B7 mimic the ones used for experiments B5 and B3 respectively. Figure 5-21 depicts the obtained samples linked to the presented experimental runs. The relatively larger foam bubbles viewed at the center of sample B7 are attributed to the higher melt temperature during foaming at this VER.

Figure 5-21: Resulting sample cut-outs B6 and B7 (6-VER)

The respective figures show that complete core filling was achieved in both cases, and the skin and foam layers are well integrated, with no visible seams or parting marks present at the boundaries. This conclusion is also evidently supported by the SEM micrographs shown in Figure 5-22.
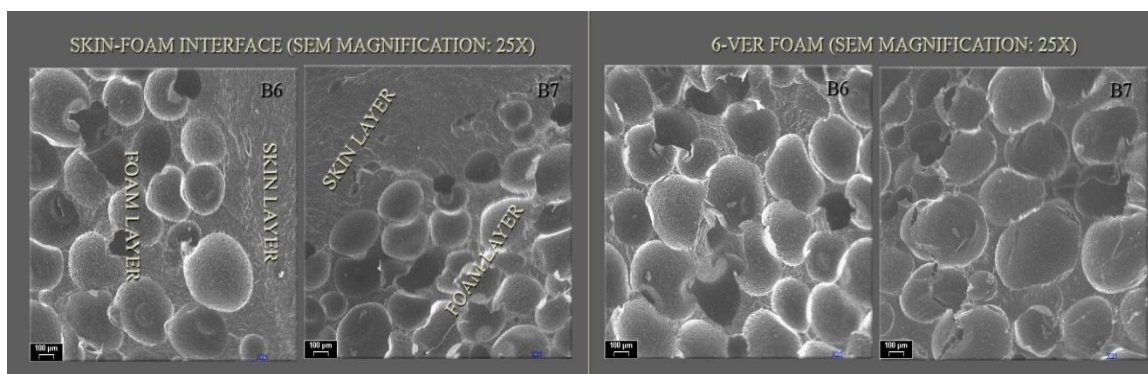
Figure 5-22: SEM micrographs associated with samples B6 and B7

The obtained average foam densities for samples B6 and B7 were plotted in Figure 5-23 against their analogs, which were calculated earlier for the 4-VER samples pertaining to the same foam-comprising PP grade.

Average Foam Density Comparison PF6523 (4-VER VS 6-VER)

	4-VER (PF6523)	6-VER (PF6523)
■ Foam Density (Kg/m3)	289.90	171.76
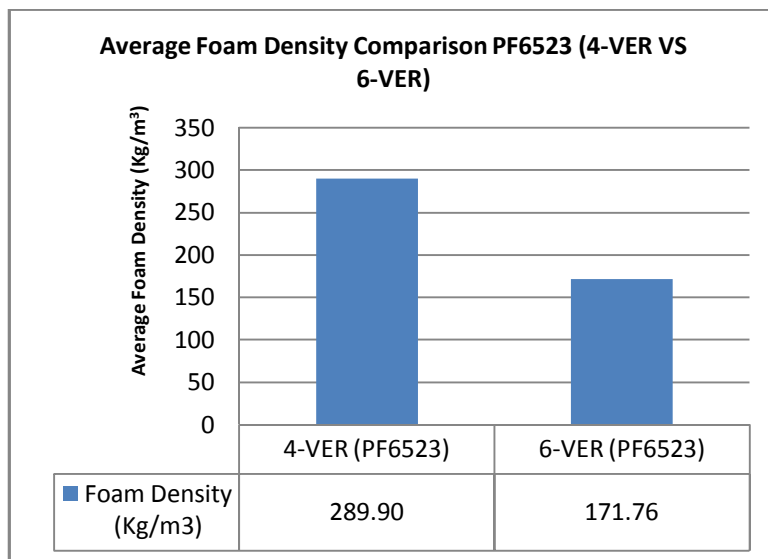
Figure 5-23: Average foam density comparison PF6523 (4-VER VS 6-VER)

It was observed that the displayed proportion relating the foam densities attained at both expansion ratios ($\rho_{4\text{-VER}}/\ \rho_{6\text{-VER}} = 1.68$) is comparable to the one displayed in experimental Series A, when PFHL451H when used for the foam layer ($\rho_{4\text{-VER}}/\ \rho_{6\text{-VER}} = 1.72$). The stated findings allow concluding that there is a steadily experienced inaccuracy between the theoretical VER prescribed to generate a particular foamable formulation in RRFM and the practical VER achieved by using the respective formulation.

5.3.2.5 Mold Shape and VER Variation

Experiments B8 and B9 were conducted to conclude this series of experiments that entailed PF6523 as the foam comprising resin grade. The most successful processing conditions were adapted to generate a flat shaped integral-skin foamed core molding. After conducting the pertinent experiments, the resulting articles were cut open and the achieved morphologies along with the generated SEM micrographs associated with samples B8 and B9 were illustrated in Figure 5-24.

(a)

(b)
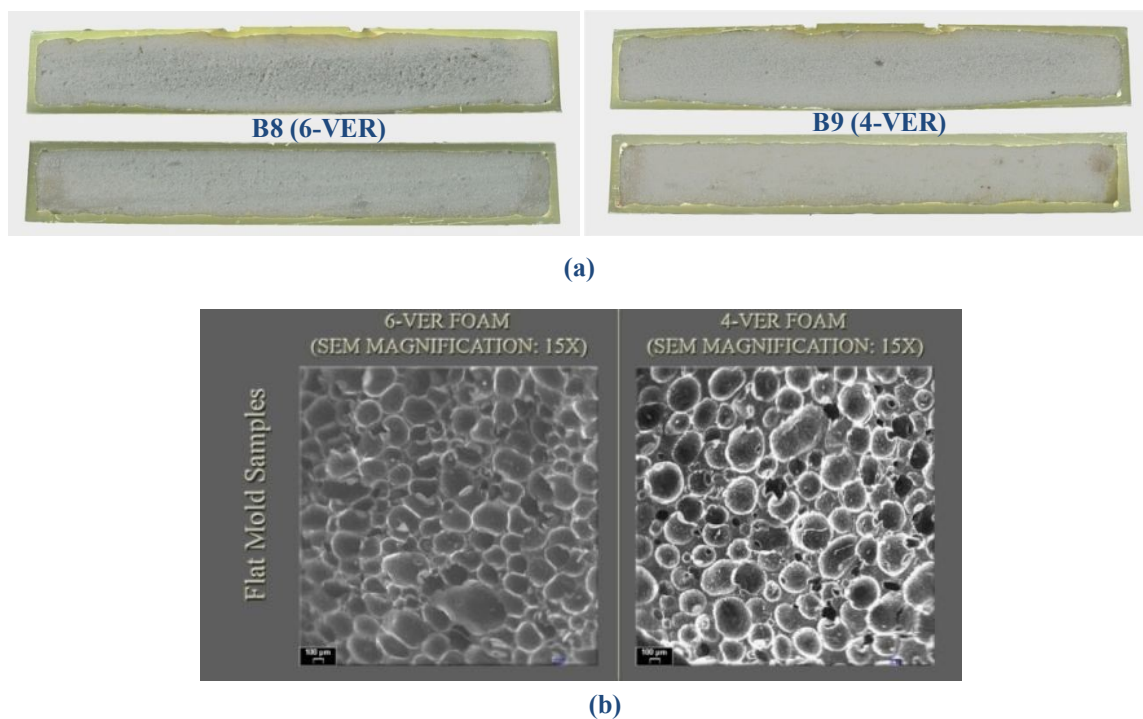
Figure 5-24: (a) Scanned samples B8 and B9 (b) The corresponding SEM micrographs

5.3.3 Experimental Series C

The last battery of experiments was conducted to investigate the opportunity of processing integral-skin PP composites exhibiting a solid-skin comprised of a PP copolymer (PFSB786, MFI 8 [g/10 min]) and a foam core comprised of another compatible PP copolymer (PFSR257M, MFI 2 [g/10 min]). The nature of such skin-foam blend is especially significant for applications that require the respective end-use articles to demonstrate improved impact properties.

As mentioned in Section 4.4.6, the devised experimental work within this series is solely focused on developing a processing strategy, through investigating a variety of tactics, which will allow achieving cylindrical and flat shaped moldings comprising the aforementioned constituents.

5.3.3.1 Recorded Experimental Parameters

Similarly, a variety of entities were documented along the course of the conducted runs; these include: the processing melt temperatures, the melt pressures, and the final weight of the generated samples. Table 5-3 displays the respective log associated with each of the conducted processing runs with regards to the experimental plan of Series C.

Table 5-3: Measured parameters throughout the experimental Series C

Experiment Code	Constituents	Processing T_{melt} [^{o}C]	Processing Melt Pressure [PSI]	Skin Weight [g]	Overall Part Weight [g]
C11	Skin: PFSB786 (MFI 8g/10 min) Foam: PFSR2587M (MFI 2 g/10 min)	170 - 178	100 – 0	280	463
C22		161 - 165	250 - 0	280	635
C33		135 - 142	1300 - 0	280	630
C44		158 - 161	150 - 0	280	629
C55		150 - 152	330 - 0	280	622
C66		148 - 152	350 - 0	280	634
C77		165 - 171	400 - 0	280	570

5.3.3.2 Analysis of the Obtained Moldings C11-C44

Experimental run C11 entailed foaming resin C by setting the extruder barrel temperatures at a high enough level to promptly trigger the decomposition of the CBA and consequently the foaming process by imposing minimal heating/frictional action by the extruder screw (i.e. low RPM). The recorded processing melt temperature during the course of this experiment dwelled in the range of 170-178 [^{o}C] (Table 5-3); nevertheless, the characterized melting peak of PFSR257M was approximately 150 [^{o}C]. Accordingly, the relatively high processing melt temperature experienced by the molten polymer promoted the weakening of its melt strength, which deteriorated the polymer's ability to resist bubble growth during foaming. Thus, severe cell coalescence was displayed throughout the resulting molding; the observed deficiency in foam structure was

especially aggravated around the absolute center of the article, where the polymer's temperature is at its highest level for the longest period of time, as a result of the relatively low heat transfer rate at this location due to the insulative properties of the foam. The resulting structure, C11, can be observed in Figure 5-25.

The second attempt entailed commencing a method to allow the polymer to preserve the blowing bubbles by maintaining its melt strength; in view of that, a 10 [^{o}C] reduction in the temperatures of each of the extruder barrel zones was employed in addition to decreasing the residence time of the foamable blend in the barrel by increasing the screw RPM from 60 to 85 [RPM]. The resulting structure, C22, is shown in Figure 5-25. When visually inspecting the overall morphology, it is evident that a significant improvement in the integrity of the resulting foam core was attained. Nonetheless, signs of cell coalescence and degradation were still experienced, on a smaller scale, around the center of the molding. Moreover, a large gap was present in the top right corner of the molding due to what was analyzed to be an excessive cooling incident of the skin and/or foaming melt during and/or before the foam introduction step.

The third experimental run, C33, involved an attempt to further conserve the melt strength of PFSR257M for foaming, which involved using Celogen OT as a foaming agent, while correcting the foamable formulation accordingly. Due to the relatively lower decomposition temperature of Celogen OT ($\approx$159 [^{o}C]) when compared to Celogen AZ ($\approx$203-209 [^{o}C]), it was possible to hypothesize that PFSR257M could be foamed at temperatures compatible with its melting range. Upon employing a full 15 [^{o}C] temperature reduction across the barrel zones and starting the foaming process, on the contrary, it was apparent that the achieved extrudate entailed an excessively rough

texture, indicating the incompatibility of the foamable formulation and/or environment. The resulting molding is illustrated in Figure 5-25.
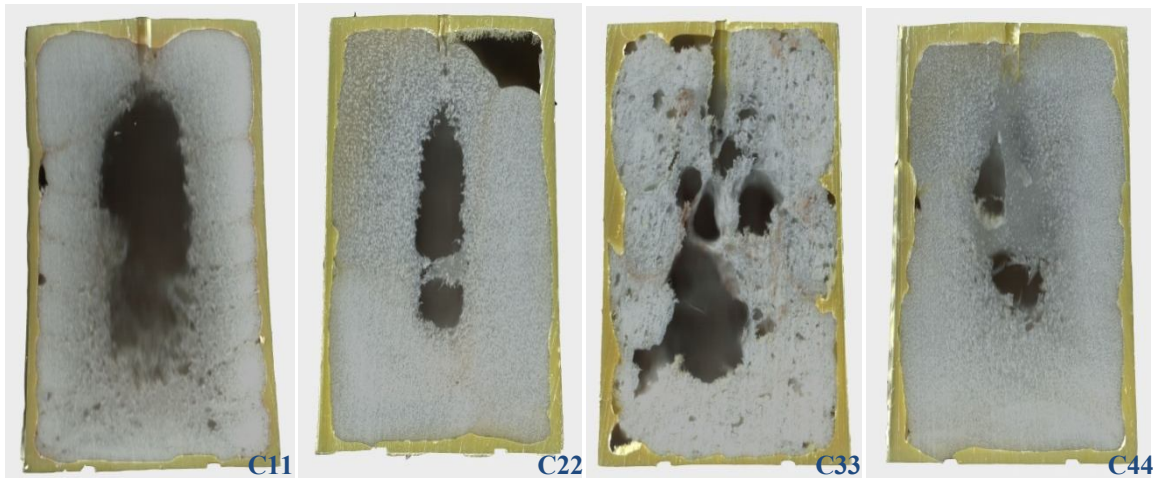
Figure 5-25: Resulting moldings associated with experiments C11-C44

Upon visual inspection, it was observed that an extreme divergence in skin thickness uniformity was present besides the poor integrity of the resulting foam core, rendering the concept of using Celogen OT ineffective.

Further efforts were then focused on devising a method to foam PFSR257M using Celogen AZ-120. Experimental trial C44 involved increasing the extruder screw RPM to 95 and reducing the processing melt temperature to a range of 158-161 [^{o}C], while reducing the variation between barrel zones' temperatures to 5 [^{o}C] between zone 1 and zone 2 and 10 [^{o}C] between zone 2 and zone 3. This devised processing methodology displayed significant improvements to the morphology of the resulting foam core (Figure 5-25). The deterioration experienced in the center of the molding was reduced and the achieved skin-foam interface and skin thickness uniformity were better than the ones obtained for runs C11-C33.

5.3.3.3 Analysis of the Obtained Moldings C55 and C66

Methodology C44 was then modified further by reducing the processing melt temperature to a range of 148-153 [^{o}C], setting the temperatures of the barrel zones only 5 [^{o}C] apart, and fixing the screw RPM at the maximum value (100 [RPM]). The resulting moldings, pertaining to trials C55 and C66, demonstrated the highest level of success among the ones obtained across experimental Series C; Figure 5-26 depicts the resulting morphologies associated with the mentioned experimental trials.

Visual inspection of the generated samples revealed voids at different locations of the skin-foam boundary, which are primarily present due to the rapid cooling and solidification of the foaming melt prior to adhering to the skin, since foaming of the PP grade PFSR257M was set to take place at a temperature that is close to its characterized melt temperature, causing it to freeze faster than the other PP grades used for foaming throughout the conducted experiments.
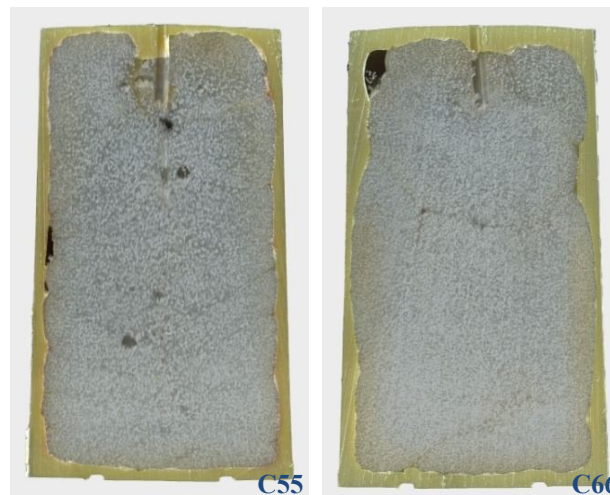
Figure 5-26: Resulting morphologies of experiments C55 and C66

5.3.3.4 Flat Shaped Molding

Finally, the devised experimental entities were slightly modified, as per the experimental plan presented in Table 4-9, to accommodate the processing environment of the flat plate mold, which requires the rapid expansion of the polymer in order to reach the far corners of the mold prior to the excess cooling of the skin layer. Subsequently, the experimental cycle was accomplished and the resulting sample is depicted in Figure 5-27.

Figure 5-27: Flat shaped molding corresponding to experiment C77

Samples were acquired from molding C77 for inspection using SEM. The obtained morphologies are illustrated in Figure 5-28.
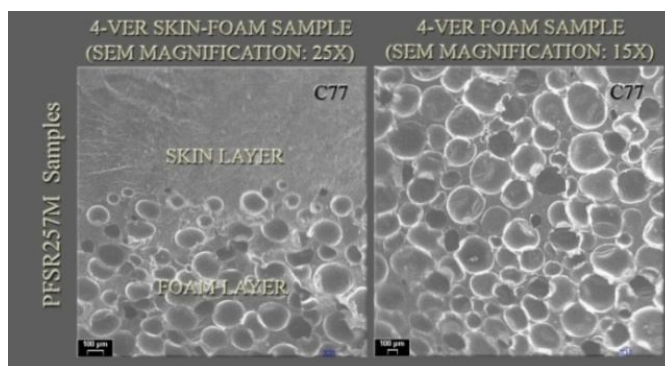
Figure 5-28: SEM micrograph of sample C77

Close examination of the generated SEM micrographs yet confirm the strong interface characteristics at the skin-foam boundary demonstrated by the respective

material blend used within this series. Cell population density for a selected 4-VER foam sample was calculated to be 108000 ± 360 [cells/cm^3]. This value was utilized to directly calculate an average cell size of 413 ± 25 [μm].

5.3.4 Global Remarks

Three unique PP-PP skin-foam blends, used in the processing of integral-skin foamed core cylindrical and flat shaped moldings in RRFM, were closely investigated throughout this chapter.

5.3.4.1 Effects of MFI Variation

Two PP homopolymers, PFHL451H (MFI 2 [g/10 min]) and PF6523 (MFI 4 [g/10 min]), with the second sustaining a MFI that is twice as high as the first, were proved to achieve successful moldings through the experimental runs. The achieved average cell densities, when utilizing both resins for foaming purposes, were rather comparable as indicated by the comparative bar chart shown in Figure 5-29 (a), with PF6523 exhibiting a slightly higher average foam density when foamed with respect to both, the 4-fold and a 6-fold formulation. The distribution of the foam structure associated with PFHL451H appeared to be more uniform than that of PF6523. Also, the lowest average cell size calculated for the foam obtained using PFHL451H proved to be smaller than the one obtained for PF65234, particularly at the higher VER. This result allowed concluding that the PP grade with the lower MFI preserved its melt strength over the one with higher MFI during foaming in RRFM. However, it is worth noting that the average cell size calculation methodology is based on particularly selected locations within each of the

moldings; hence, the presented results can considerably vary or prove to be different throughout future ventures.
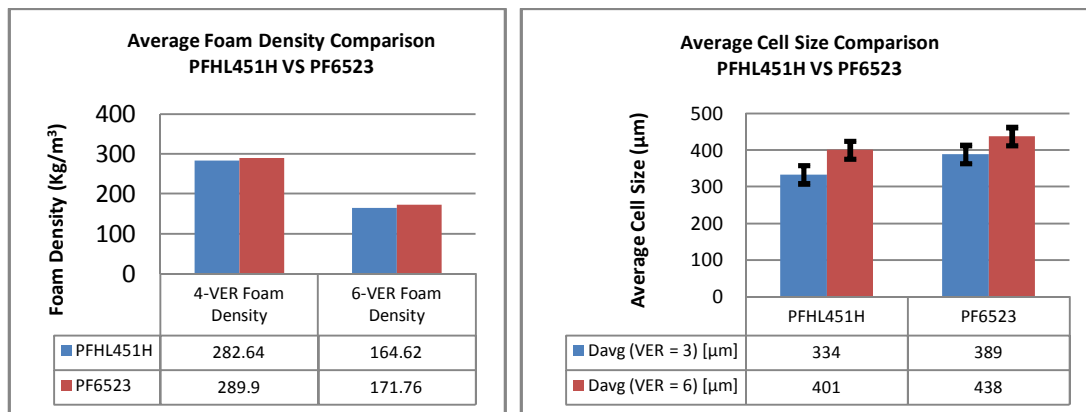
Figure 5-29: Foam characteristics comparison between PFHL451H and PF6523

5.3.4.2 Effects of Extruder Die Temperature

The temperature at the die zone of the is an essential parameter for controlling the nucleation and growth of foam cells in RRFM as well as the preservation of the blowing gasses within the foaming extrudate.

It was observed through preliminary experiments that the melt strength of the PP grades studied in this thesis improved significantly with decreasing the die zone temperature, while the cell size and the degree of cell rupture associated with the foamed extrudate increased gradually with increasing the die temperature. At instants when the temperature of the die is too high (polymer dependant), the extrudate experiences a cavity, pertaining to extreme cell coalescence, throughout its absolute center in the direction of extrudate flow.

5.3.4.3 Performance Evaluation of the Insulated Interface

A selection of SEM micrographs was generated to investigate the performance of the insulated interface design with respect to all three material blends presented in this thesis; this is depicted in Figure 5-30. The illustrated micrographs reveal a strong bond between the respective skin and foam layers at the insulated interface location for all three material blends. The satisfactory morphologies prove that the design of the insulated interface is applicable to a wide materials and processing window with respect to the RRFM processing technology.
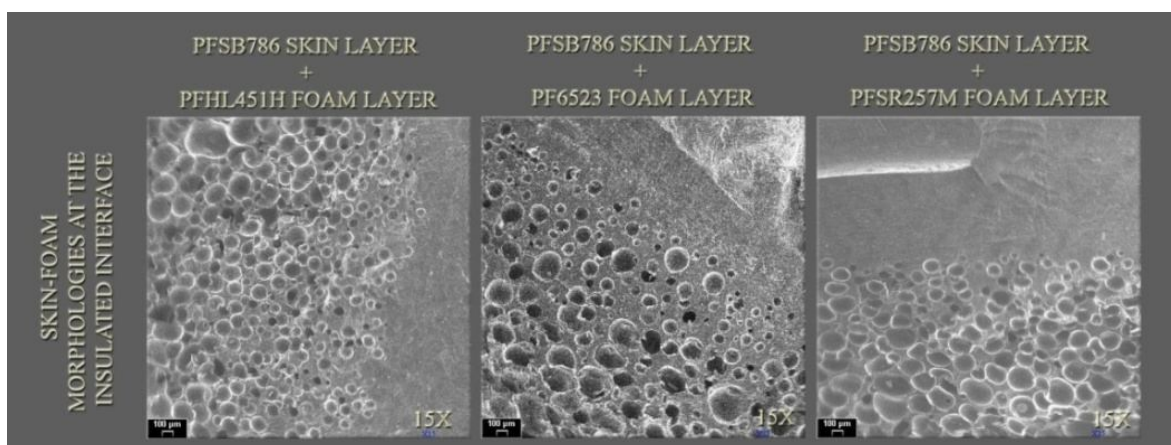
Figure 5-30: Skin-foam behavior at the insulated interface location

5.3.5 Summary

Three unique PP-PP skin-foam blends, used in the processing of integral-skin foamed core cylindrical and flat shaped moldings in RRFM, were successfully processed and thoroughly analyzed throughout this chapter. The presented conclusions and devised processing methodologies and strategies are applicable to a wide variety of PP grades that can be used to serve an extended range of end-use applications.

Chapter 6: Conclusions and Future Work

This chapter provides a conclusive discussion of the most important accomplishments presented throughout this thesis and suggests aspects of future research endeavors.

6.1 Concluding Remarks

The fundamental drawbacks of the conventional rotational foam molding process in manufacturing skinless or integral-skin plastic parts entailing partially or completely foamed cores include its intrinsically lengthy processing cycle times in addition to the variable quality of the respectively manufactured parts.

6.1.1 RRFM: A Remedial Solution

In response to the indicated problem, a remedial process, namely Rapid Rotational Foam Molding, was designed, developed, and evaluated. This novel processing technology treats the aforementioned drawbacks by decoupling the foam fabrication segment from the entirety of the conventional practice and achieving it through the most efficient continuous plastic fabrication process; extrusion. The devised practice accomplishes up to 35% savings in processing cycle times by eliminating the need to utilize extensive and delicate compounding, palletizing, then heating procedures to achieve skin and foam layers with the desired attributes. Additionally, RRFM demonstrated improvements in the overall quality of manufactured articles compared to their analogs achieved using the conventional process.

6.1.2 Design of an Experimental Setup

The introduced time and energy savings in addition to the predicted improvements in the produced moldings' quality exploited through employing RRFM were assessed and experimentally verified using an in-house custom-made industrial-grade lab-scale semi-automatic experimental setup.

The experimental setup was carefully designed, built, and developed, through a systematic design engineering methodology, to accommodate the RRFM processing concept. Disciplined concept generation, concept evaluation and selection, engineering target specification, quality function deployment, and finite element and engineering analyses models were concurrently pursued throughout the design process of the experimental setup. Factors like operator safety, design for manufacturing, design for assembly, design for maintainability, and user friendliness were simultaneously considered at all design stages. Moreover, preventive maintenance procedures were regularly performed to preserve the consistent functionality of the experimental setup during the conducted experimental batteries.

6.1.3 Experimental Evaluation and Feasibility Analysis

A preliminary set of planned experimental trials was employed along with DSC and TGA materials characterization methods to investigate the most important entities that govern the manufacture of integral-skin foamed core PP composites using the RRFM process. Subsequent to achieving a working range of processing parameters, a final set of experiments was designed and implemented in order to validate and examine the reliability and repeatability of the process, the effects of varying the processing

parameters within the predetermined successful ranges on the manufactured parts, and the ability of RRFM to produce articles of different volume expansion ratios and shapes.

In total, three distinct PP-based materials formulations, of different morphological, compositional, and rheological natures, were investigated throughout the concluding experimental work. The thoroughly analyzed results proved the success of the RRFM concept in processing integral-skin foamed core PP moldings for all three formulations. In terms of integral-skin quality, a bubble-free non-degraded solid integral skin was achieved all along the accomplished experimental series with calculated variability in skin thickness uniformity as low as 8.9% and as high as 33.7 %.

In terms of foam characteristics, complete foam filling has been achieved in all cases, with no significant gaps, venting issues, or foam quality deterioration due to poor processing melt strength. An average foam density of as low as 152.75 $[kg/m^3]$ and as high as 308.51 $[kg/m^3]$ was achieved for the 6-VER and the 4-VER moldings, respectively. The SEM analysis performed to examine the morphologies pertaining to the achieved moldings revealed that an average cell size of as low as 334 $\pm$ 25 $[\mu m]$ was achieved, this indicates that with further refinement of the processing parameters it would be feasible to produce fine-celled PP foams with a more uniform cell-size distribution in RRFM.

RRFM proved to provide a viable solution to the challenges faced in processing PP foams exhibiting an integral-solid-PP-skin by imposing a large degree of control over the entities of (i) the foam processing segment, by utilizing the astutely regulated extrusion process and (ii) the skin processing segment, by enforcing successful conventional rotational molding parameters.

6.2 Future Work

Future work performed in the capacity of developing the RRFM processing technology can be simultaneously conducted in a multiplicity of areas.

The capabilities of the RRFM processing concept are to be validated further through a wide variety of PP grades as well as other polyolefins, which suite a selection of useful applications. Moreover, additional experimental work in the field should investigate the ability of the process to produce larger and more complex geometries while preserving the same repeatability and efficiency rates that are currently achievable.

The derivation of the process-specific optimal process-governing analytical methodologies is yet to be accomplished through further planned experimental batteries. Such task will allow an accurate determination of the desired material formulations leading to a more controlled process.

Further time and energy savings can also be achieved by investigating methods that allow reducing the processing cooling time, which is considered long due to the insulative effects imposed by the foam layer. Moreover, automating the interface removal method, using a manipulator or a similar system, should be considered to enhance the consistency, efficiency, and safety of the RRFM experimental setup.

6.3 Thesis Concluding Statement

Concisely, a novel, efficient, capable, reliable, repeatable, and greener processing concept has been established the realm of manufacturing skinless/integral-skin cellular composites in rotational molding. The evolution of RRFM has promoted the broadening of the currently achievable materials/processing/applications window.

REFERENCES

[1]. R.J. Crawford. *Plastics Engineering, Third Edition*. Department of Mechanical, Aeronautical and Manufacturing Engineering, The Queen's University of Belfast. Published by Butterworth-Heinmann. (1998)

[2]. D.V. Rosato. *Plastics Engineering, Manufacturing & Data Handbook*. Published by Springer. (2001)

[3]. Callister W. *Fundamentals of Materials Science and Engineering 7th Edition*. Wiley United States. ISBN 0-471-39551-X. (1986)

[4]. S. Merryweather. *Machinery FYI Charts*. Plastics News Staff. Plastics News Magazine. Grand Rapids, Michigan, USA. (2009)

[5]. D. Klempner and K.C. Frisch. *Handbook of Polymeric Foams and Foam Technology*. University of Detroit, Polymer Institute, Detroit. Hanser Publishers (Oxford University Press in USA). (1991)

[6]. D. Eaves. *Handbook of Polymer Foams*. University of Birmingham. Rapra Technology Publishing. (2004)

[7]. S.T. Lee, C.B. Park, and N.S. Ramesh. *Polymeric foams: technology and science of polymeric foams*. Published by CRC Press. (2006)

[8]. J. Frados. *Plastics Engineering Handbook, 4th Ed*. Society of the Plastics Industry. Van Nostrand Reinhold. New York. (1976)

[9]. M. Chanda and S. K. Roy. *Plastics Technology Handbook 3rd Ed*. Publisher: Marcel Dekker. (1998)

[10]. A.K. Mohanty, M. Misra, and L. Drzal. *Natural fibers, biopolymers, and biocomposites*. Published by CRC Press. (2005)

[11]. J.L. Throne. *Thermoplastic Foam Extrusion: An Introduction*. Published by Hanser Verlag. (2004)

[12]. C. Maier and T. Calafut. *Polypropylene: the definitive user's guide and databook.* Published by William Andrew. (1998)

[13]. M .B. Bradley and E.M. Phillips. *SPE ANTEC Technical Papers*, p. 717-720 (1990).

[14]. C.B. Park and L.K. Cheung. Polymer Engineering. Science. 37:1,p. 1-10 (1997).

164

[15]. R. Heinz and W. Michaeli. *SPE ANTEC Technical Papers*. p. 1661-1665 (2001).

[16]. H.E. Naguib, J.X. Xu, C.B.Park, A. Hesse, U. Panzer, and N. Reichelt. *SPE ANTEC Technical Papers*. p.1623-1630 (2001).

[17]. J.L. Throne, *Thermoplastic Foams, Sherwood Technologies, Inc*., Sherwood Publ., Ohio (1996)

[18]. G.L. Beall, *Rotational Molding: Design, Materials, Tooling, and Processing*. Hanser/Gardner Publications, Inc., Cincinnati (1998)

[19]. R.J. Crawford. *Rotational Moulding of Plastics, 2nd Edition*. John Wiley and Sons Inc. (1996)

[20]. S.-J. Liu and C.-H. Tsai, Polym. Eng. Sci., 39, 1776 (1999)

[21]. S.-J. Liu and C.-H. Yang. *SPE ANTEC Technical Papers*. 46, 1309, (2000)

[22]. F. Voelke. *Hollow-Pattern Forming Machine*. U.S. Patent No. 803,799. (1905)

[23]. P.F. Bruins. *Basic Principles of Rotational Molding*. Polytechnic Institute of Brooklyn. CRC Press. pp3-15 (1971)

[24]. R. Pop-Iliev. *Generating Alternative Time-and-Energy-Saving Processing Concepts for Rotational Foam Molding*. . *SPE ANTEC Technical Papers.* Paper # 304017, pp. 2732-2736 (2007)

[25]. R. Pop-Iliev, K. Christian, and E. Abdalla, *"Rapid Rotational Foam Molding of Integral Skin Cellular Composites"*, The 25th Annual Meeting of the Polymer Processing Society 2009 (PPS 25), March 1-5, 2009, Goa, India, Reference number: GS-XI-OP6, pp. 182 (2009)

[26]. R. Pop-Iliev, *"Extrusion-assisted Rotational Foam Molding"*, Book of abstracts of the 24th Annual Meeting of the Polymer Processing Society 2008 (PPS 24), pp. II.65, Paper reference number: S04-391, Keynote Presentation, June 15-19, 2008, Salerno, Italy (2008)

[27]. G.S. Baker and W. Perks. *Machine for Molding Chocolate and the Like*. U.S. Patent No. 947,405. (1910)

[28]. J. Clewell and R. Fields. *Cast Resins Having Integral Sheen*. U.S. Patent No. 2,265,226. (1941)

[29]. Unknown Author. *Rankings and Lists: North American Rotomolders*. Plastics News Magazine. Global Group. (2008)

[30]. S. Merryweather. *FYI: North American Rotomolders Survey*. Plastics News Magazine. Global Group. (2005)

[31]. R.J. Crawford and M.P. Kearns. *Practical Guide to Rotational Moulding*. Rapra Technology Limited. (2003)

[32]. C.A. Harper. *Handbook of Plastic Processes*. John Wiley and Sons. (2006)

[33]. R. Pop-Iliev and C.B. Park, *"Processing of Polypropylene Foams in Compounding-based Rotational Foam Molding,"* SPE, ANTEC, Technical Papers, Vol. 46, pp. 1314-1325 (2000)

[34]. (Invited) R. Pop-Iliev, G. Liu, F. Liu, C.B. Park, S. D'Uva, and J.A. Lefas, *"Rotational Foam Molding of Polyethylene and Polypropylene,"* SPE, RETEC, Innovations in Rotational Molding in the Year 2000 and Beyond, pp. 95-104, Strongsville, Ohio (1999)

[35]. R. Pop-Iliev, G. Liu, F. Liu, C.B. Park, S. D'Uva, and J.A. Lefas, *"Comparison of Dry Blending Based and Melt Compounding Based Rotomolding Techniques for LLDPE Foams,"* SPE, ANTEC, Technical Papers, Vol. 45, pp. 1457-1467 (1999)

[36]. S. Lee and S.N. Ramesh. *Polymeric Foams: Mechanisms and Materials.* CRC Press. (2004)

[37]. H.R. Kricheldorf et al. *Handbook of Polymer Synthesis*. CRC Press. (2004)

[38]. R. Pop-Iliev, N. Dong, D. Xu, and C.B. Park, *"Visualization of the Foaming Mechanism of Polyethylene Blown by Chemical Blowing Agents under Ambient Pressure,"* Advances in Polymer Technology, Vol. 26, Issue 4, pp. 213-222, DOI 10.1002/adv.20102 (2008)

[39]. G.Liu, C. Park, and J. Lefas. Polymer Engineering and Science, 38, pp.1997 (1998)

[40]. R. Pop-Iliev, D. Xu, and C.B. Park, *"Manufacturability of Fine-Celled Cellular Structures in Rotational Foam Molding,"* Journal of Cellular Plastics, Vol. 40, No. 1, pp. 13-25 (2004)

[41]. R. Pop-Iliev and C.B. Park, *"Single-step Rotational Foam Molding of Skin-surrounded Polyethylene Foams,"* Journal of Cellular Plastics, Vol. 39, No. 1, pp. 49-58 (2003)

[42]. R. Pop-Iliev and C.B. Park, *"Melt Compounding Based Rotational Foam Molding Technology for Processing Polypropylene Foams,"* Journal of Reinforced Plastics

and Composites, Vol. 21, No. 2, pp. 101-120, (2002) and Vol. 21, No. 12, pp. 1079-1100 (2002)

[43]. R. Pop-Iliev. *Processing of Fine-Cell Polypropylene Foams in Compounding Based Rotational Foam Molding*. M.A.Sc. Thesis. University of Toronto. (1999)

[44]. R. Pop-Iliev, G.M. Rizvi, C.B. Park. *Formulating Foamable Resins for Achieving a Given VER in Rotational Foam Molding*. SPE ANTEC. Paper 0908. (2001)

[45]. R. Pop-Iliev, G.M. Rizvi, C.B. Park. *The Importance of Timely Polymer Sintering While Processing Polypropylene Foams in Rotational Molding*, Polymer Engineering and Science, Vol. 43, No. 1, pp. 40-54. (2003)

[46]. F. Jacob. *"Method of Molding a Plastic Article having a Cellular Body and Protective Skin"*. U.S. Patent No. 2,950,505. (1956)

[47]. R. I. Kleine. *"Process for Producing Hollow Bodies Reinforced with a Foamed Structure"*. U.S. Patent No. 3,505,137. (1970)

[48]. J. Lemelson. *Method for Molding Composite Bodies.* U.S. Patent No. 3,875,275. (1975)

[49]. H. Mori, E. Adachi, and Y. Noguchi. *"Method of Producing Composite Shaped Articles from Thermoplastic Resins"*. U.S. Patent No. 3,962,390. (1976)

[50]. Wheeler Boyce Mold Company Catalogue. URL:<www.boyce.com>

[51]. D.R. Ekserova and P.M. Krugliakov. *Foam and Foam Films: Theory, Experiment, Application*. Published by Elsevier. Pp. 10-20. (1998)

[52]. C.A. Harper. *Modern Plastics Handbook*. McGraw-Hill Professional. (2000)

[53]. C. Rauwendaal. *Polymer Extrusion*. Hanser Verlag. (2002)

[54]. P. Troester. *Extruder Invention*. U.S. Patent No. 2,092,015. (1935)

[55]. R. Colombo. *Extrusion head for molding synthetic resins*. U.S. Patent No. 2,592,658 (1952).

[56]. R. Pasqueti. *Machine for mixing and extruding*. U.S. Patent No. 2749571. (1953)

[57]. http://www.dow.com/about/aboutdow/history/1890s.htm

[58]. J.M.G. Cowie. *Polymers: Chemistry and Physics of Modern Materials*. CRC press. Pp1-20. (1991).

[59]. G.S. Misra. *Introductory Polymer Chemistry*. New Age International. (1993)

[60]. R. Young and P. Lovell. *Introduction to Polymers*. CRC Press. (1991)

[61]. A. Calhoun, A.J. Peacock. *Polymer Chemistry: Properties and Applications.* Published by Hanser Verlag. (2006)

[62]. TA Instruments. *Differential Scanning Calirometry. User's Manual*. TA Instruments (2007).

[63]. Bhadeshia H. *Thermal Analysis Techniques: Differential Thermal Analysis*. University of Cambridge, Materials Science and Metallurgy Department. Cambridge, United Kingdom (2002)

[64]. S. Hunt, "*Determination of Structure and Stability with Thermal Analysis and Calorimetry",* TA Instruments Inc. Seminar, Mississauga, September 27, 2007. (2007)

[65]. M. Kelsey and J. Foreman, *Temperature Measurements in TGA, Limitations of Test Methods for Plastics, ASTM STP 1369, J. S. Peraro, Ed*., American Society for Testing and Materials, West Conshohocken, PA. (2000)

[66]. TA Instruments. Thermogravimetric Analysis. TA Instruments Homepage. (2007) http://www.tainstruments.com

[67]. Intertek Homepage. Thermogravimetric Analysis. Intertek Analytical Services. United States (2007) http://www.itscb.com/

[68]. C. Maier and T. Calafut. *Polypropylene: the definitive user's guide and databook.* Published by William Andrew. (1998)

[69]. N. Pasquini and A. Addeo. *Polypropylene handbook 2nd edition*. Hanser Verlag. (2005)

[70]. IUPAC. *Compendium of Chemical Terminology, 2nd ed. (the "Gold Book")*. Compiled by A.D. McNaught and A.Wilkinson. Blackwell Scientific Publications, Oxford. (1997).

[71]. M. Orchin, R.S. Macomber, F. Kaplan. *The vocabulary and concepts of organic chemistry*. John Wiley and Sons. (2005)

[72]. S.H. Hamid. *Handbook of polymer degradation*. CRC Press. (2000)

[73]. T. Whelan. *Polymer Technology Dictionary*. Published by Springer. (1994)

[74]. R.G. Parrish. *Microcellular Foam Sheet*. U.S. Patent No. 3,637,458. (1972)

[75]. T. Harada. *Polypropylene composition and Foamed Polypropylene Sheet There-from*. U.S. Patent No. 3,846,349. (1973)

[76]. T. Ueno and K. Nakamura. *Foams prepared from polypropylene resin composition and process for producing same*. U.S. Patent No. 4,298,706. (1981)

[77]. N. Fukushima, Y. Kitagawa, T. Okumura, and K. Sakakura. *Highly foamed polypropylene product and an extrusion process for forming the product*. U.S. Patent No. 4,522,955. (1985)

[78]. C.B. Park, G. Liu, F. Liu, R. Pop-Iliev, S. D'Uva, and B. Zhang. *Production of foamed low-density polypropylene by rotational molding.* U.S. Patent No. 6,103,153. (2000)

[79]. D.G. Ullman. *The Mechanical Design Process, 3rd Edition*. McGraw Hill. Corvallis OR. (2003)

[80]. Husky. *Single Cavity Valve Gate Homepage.* (2006)
URL: <http://www.husky.ca/hotrunners/content-62-41.html>

[81]. Wayne Machine and Die Company, *Homepage*
URL: <http://www.waynemachine.com> (2006)

[82]. K. Christian and R. Pop-Iliev. *Extrusion-Assisted Rotational Molding of Fine-Celled Polyethylene Foams*. SPE, FOAMS 2008. (2008)

[83]. E. Abdalla and R. Pop-Iliev, *"Processing Integral-skin Polypropylene Foams Utilizing Extrusion-Assisted Direct-Foaming Rotational Molding"* SPE, ANTEC 2009, June 22-24, 2009, Chicago, IL, USA, Manuscript ID: ANTEC-0115-2009, Accepted (2009)